Deregulation of Host Gene Expression and Control of Wart Formation by Papillomavirus E8^E2

Dissertation

der Mathematisch-Naturwissenschaftlichen Fakultät
der Eberhard Karls Universität Tübingen
zur Erlangung des Grades eines
Doktors der Naturwissenschaften
(Dr. rer. nat.)

vorgelegt von
Franziska Kühner
aus Sinsheim

Tübingen
2023

Gedruckt mit Genehmigung der Mathematisch-Naturwissenschaftlichen Fakultät der Eberhard Karls Universität Tübingen.

Tag der mündlichen Qualifikation: 10.07.2023

Dekan:	Prof. Dr. Thilo Stehle
1. Berichterstatter:	Prof. Dr. Alexander Weber
2. Berichterstatter:	Prof. Dr. Frank Stubenrauch

1 Zusammenfassung

Persistierende Infektionen mit humanen Papillomviren (HPV) der Hochrisiko-Typen wie HPV16 können anogenitalen und oropharyngealen Krebs verursachen. HPV infizieren Keratinozyten in der Basalschicht von kutanen und mukosalen Epithelien. Das virale E8^E2 Protein ist ein hochkonservierter Repressor der PV-Replikation und der Genexpression, der Vorteil der Expression von E8^E2 für PV bleibt jedoch unklar. HPV16 Genome ohne Expression von E8^E2 (E8-), zeigen ebenfalls eine verstärkte Genomreplikation und virale späte Proteinexpression in differenzierten Zellen. Durch eine globale Transkriptomanalyse von differenzierten HPV16 Wildtyp und E8- Zelllinien wurde eine geringe Anzahl von unterschiedlich exprimierten Genen identifiziert. Die Analyse ausgewählter Gene deutete darauf hin, dass ihre Deregulierung die Differenzierung von Keratinozyten erfordert und mit der späten viralen Transkription korreliert. In Übereinstimmung damit wurde die Deregulierung dieser Wirtszellgene durch das zusätzliche Ausschalten der viralen *E4* und *E5* Gene, von denen bekannt ist, dass sie die produktive Replikation fördern, gemildert. Diese Daten zeigen zum ersten Mal, dass die produktive HPV16-Replikation die Transkription der Wirtszellen moduliert.

Durch die Expression und Aufreinigung des HPV16 E2 Proteins für die anschließende Produktion polyklonaler Antikörper in Kaninchen konnte ich die Expression von E2 und E8^E2 Proteinen in HPV16-positiven Zelllinien charakterisieren. Eine geringere Anzahl von wt im Vergleich zu E8- Zellen weist nukleäre E2 Foci auf, die mit dem Replikationsprotein RPA32 kolokalisiert sind und somit höchstwahrscheinlich virale Replikationszentren darstellen. Zellen mit E2 Foci exprimierten auch das späte virale E4 Protein, was darauf hindeutet, dass diese Zellen den produktiven Replikationszyklus erreicht haben. Dies bestätigt, dass HPV16 E8^E2 die produktive Replikation reguliert und ermöglichen es, die Rolle von E2 und E8^E2 im Lebenszyklus von HPV16 weiter zu untersuchen.

Da PV sehr speziesspezifisch sind, ist das *Mus musculus* (Mmu) PV1-Maus-Modell ein geeignetes Modell, um die Funktion von E8^E2 *in vivo* zu untersuchen. Kürzlich durchgeführte Studien haben gezeigt, dass MmuPV1 E8^E2 Knock-out-Genome eine erhöhte virale Genexpression in kultivierten Keratinozyten aufweisen, aber in T-Zell-defizienten Foxn1$^{nu/nu}$ Mäusen keine Warzen bilden. Ich konnte zeigen, dass das MmuPV1 E8^E2 Protein mit Komponenten des NCoR/SMRT Co-Repressor-Komplexes in Abhängigkeit von der E8 Domäne interagiert, um die Transkription und Replikation zu unterdrücken, was darauf hindeutet, dass diese Interaktion zwischen MmuPV1 und HPV konserviert ist. Interessanterweise zeigen MmuPV1 E8^E2 mt Genome eine stark erhöhte Expression des viralen späten E4 Proteins in undifferenzierten murinen Keratinozyten. MmuPV1 E4 verursachte einen Arrest in der G2-Phase des Zellzyklus, ähnlich wie seine HPV-Gegenstücke. Dies verhindert höchstwahrscheinlich die Ausbreitung virusinfizierter Keratinozyten in der Basalschicht des Epithels, was das Ausbleiben der Warzenbildung *in vivo* erklärt. Zusammenfassend deuten diese Daten darauf hin, dass die Hauptfunktion von E8^E2 darin besteht, die unvorgesehene Induktion des produktiven Replikationszyklus in basalen Keratinozyten zu verhindern.

2 Abstract

Persistent infections with high-risk human papillomaviruses such as HPV16 can cause anogenital and oropharyngeal cancers. HPV infect keratinocytes in the basal layer of cutaneous or mucosal epithelia. The viral E8^E2 protein is a highly conserved repressor of PV replication and gene expression, but the advantage of the expression of E8^E2 for PV remains unclear. HPV16 genomes lacking E8^E2 expression (E8-) show also enhanced genome replication and viral late protein expression in differentiated cells. A small number of differentially expressed genes were identified by global transcriptome analysis of differentiated HPV16 wild-type (wt) and E8- cell lines. The analysis of selected genes suggested that their deregulation requires keratinocyte differentiation and correlated with viral late transcription. Consistent with this, the additional knock-out of the viral *E4* and *E5* genes, which are known to enhance productive replication, alleviated the deregulation of these host cell genes. These data reveal for the first time that productive HPV16 replication modulates host cell transcription.

Through the expression and purification of the HPV16 E2 protein for subsequent polyclonal antibody production in rabbits, I was able to characterize the expression of E2 and E8^E2 proteins in HPV16 positive cell lines. A smaller number of wt compared to E8- cells display nuclear E2 foci and these colocalize with the replication protein RPA32 and thus represent most likely viral replication centers. E2 foci-positive cells also expressed the viral late E4 protein indicating that these cells have entered the productive replication cycle. This confirms that HPV16 E8^E2 regulates productive replication and makes it possible to further explore the roles of E2 and E8^E2 in the life cycle of HPV16.

Since PV are highly species-specific, a suitable model to investigate E8^E2 function *in vivo* is the *Mus musculus* (Mmu) PV1-mouse model. Recent studies revealed that a MmuPV1 E8^E2 knock-out genome displays increased viral gene expression in cultured keratinocytes, but failed to form warts in T-cell deficient Foxn1$^{nu/nu}$ mice. I was able to show that the MmuPV1 E8^E2 protein interacts with NCoR/SMRT co-repressor complex components in an E8-domain dependent manner in order to repress transcription and replication, indicating that this interaction is conserved between MmuPV1 and HPV. Interestingly, MmuPV1 E8^E2 mt genomes display greatly increased expression of the viral late E4 protein in undifferentiated murine keratinocytes. MmuPV1 E4 caused an arrest in the G2 phase of the cell cycle, similar to its HPV counterparts, and this most likely prevents the expansion of virus-infected keratinocytes in the basal layer of the epithelium which explains the lack of wart formation *in vivo*. In summary, these data indicate that the main function of E8^E2 is to prevent the unscheduled induction of the productive replication cycle in basal-like keratinocytes.

Contents

3 Introduction

3.1 Papillomaviruses

Papillomaviruses (PV) are non-enveloped, double-stranded DNA viruses. Of the more than 440 different sequenced genotypes 220 infect humans (Doorslaer et al., 2016). Papillomaviruses infect keratinocytes in the basal layer of cutaneous or mucosal skin in a species specific manner. HPV infection can cause a number of diseases in women as well as men, including genital warts and different types of cancers (Schiffman et al., 2007).

3.2 Classification of human papillomaviruses and clinical relevance

Human papillomaviruses can be phylogenetically allocated to five different genera: alpha-, beta-, gamma-, mu- and nu-HPV (Figure 1).

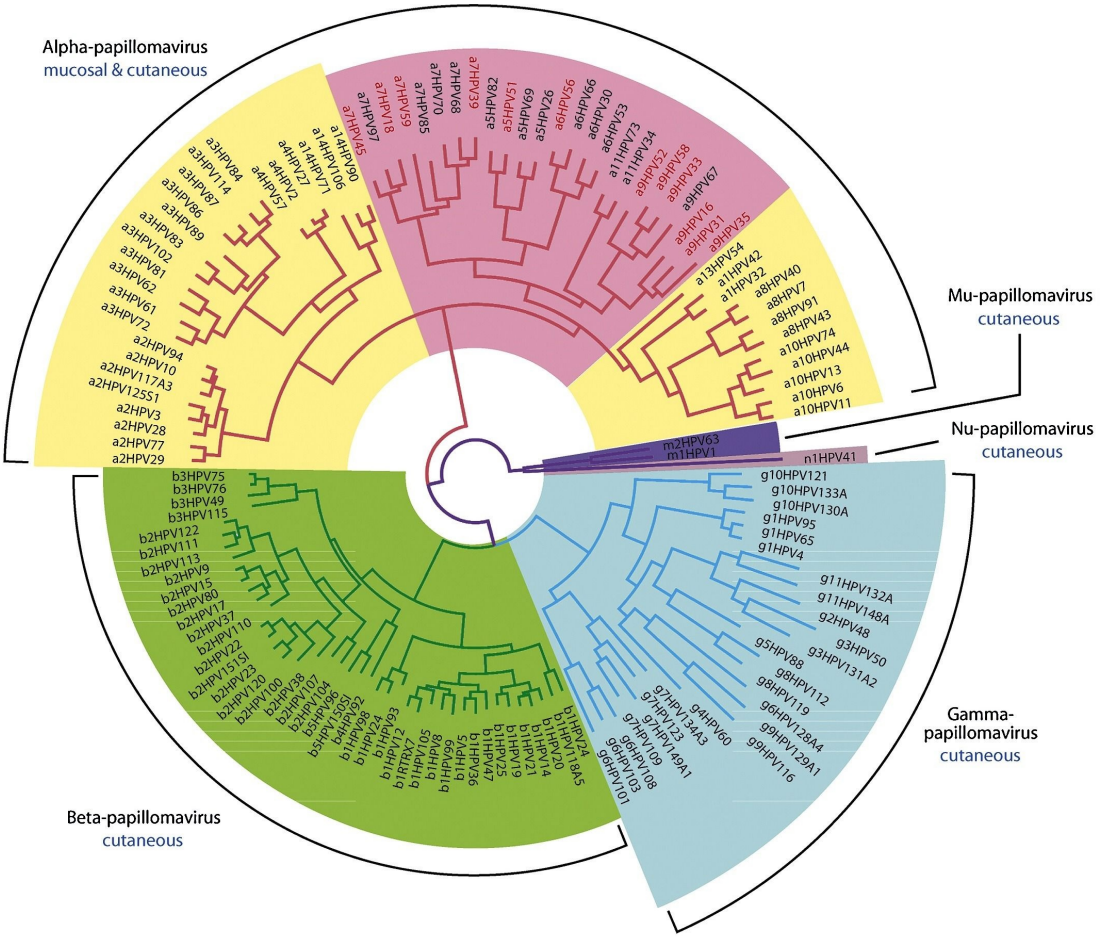

Figure 1: Classification of human papillomaviruses. Human papillomaviruses are classified into five genera: alpha-, beta-, gamma-, mu- and nu-HPV. The evolutionary tree is based on alignment of the E1, E2, L1, and L2 genes. Alpha- (yellow for low-risk and pink for high-risk), beta- (blue) and gammapapillomavirus (green) represent the largest groups. The high-risk types written in red are confirmed human carcinogens. Figure from Egawa and Doorbar, 2017.

Papillomaviruses are divided into low-risk (LR) and high-risk (HR) types, only the latter can cause cancer (zur Hausen, 2009). The major risk factor for the development of cervical, other anogenital cancers as well as a percentage of cancers of the oropharynx is persistent infection with the HR HPV types 16, 18, 31, 33, 35, 39, 45, 51, 52, 56, 58, and 59 (De Martel et al., 2017). Cervical cancer is the fourth most common cancer among women globally. In 2020 about 90% of the new cases and deaths worldwide occurred in low- and middle-income countries, due to limited access to prevention and late diagnosis (Sung et al., 2021; Stelzle et al., 2021). Oropharynx cancer is now the most common cancer caused by HPV in the US, surpassing cervical cancer (Chaturvedi et al., 2011; Tota et al., 2019; Van Dyne et al., 2018).
Beta HPV have been linked to the development of cutaneous squamous cell cancer (cSCC) in patients with epidermodysplasia verruciformis (EV) and in organ transplant recipients (Howley and Pfister, 2015; Orth, 2006). EV is a rare genodermatosis caused by mutations in the *CIB1*, *EVER1* and *EVER2* genes (De Jong et al., 2018).

3.3 Structure of the HPV genome

Human papillomaviruses have a circular double-stranded DNA genome of about 8 kb. High risk HPV genomes contain reading frames for early (E1, E2, E4, E5, E6, E7) and late proteins (L1, L2), as well as a non-coding region of about 1 kb (upstream regulatory region, URR).
Beta-HPV do not encode a *E5* gene (Howley and Pfister, 2015). Complete wt beta-HPV genomes are not able to immortalize normal human keratinocytes, in contrast to high risk alpha HPV genomes (Dürst et al., 1987; Woodworth et al., 1989; Rehm et al., 2022b; Rehm et al., 2022a). Many papillomaviruses encode the highly conserved E8 reading frame, which is transcribed as spliced E8^E2 mRNA (Kuehner and Stubenrauch, 2022). Interestingly, immortalization of keratinocytes by the beta HPV49 genome requires the inactivation of the viral E8^E2 repressor protein, whereas HPV8 and HPV38 E8- genomes are unable to immortalize NHK (Rehm et al., 2022b; Rehm et al., 2022a).
There are two main promotors in HR-HPV. The major early promoter is located in front of the *E6* gene and is highly active in both undifferentiated and differentiated keratinocytes. The major late promoter, located in the *E7* gene, is only highly active in differentiated keratinocytes (Grassmann et al., 1996; Hummel et al., 1992; Wang et al., 2011).
The early viral transcripts are processed at the early polyadenylation signal downstream of the *E5* gene, late transcripts can be processed at either the early or the late polyadenylation signal downstream of L1 (Graham, 2008; Jia and Zheng, 2009; Johansson and Schwartz, 2013; Wu et al., 2017). A high risk HPV genome is shown in Figure 2.

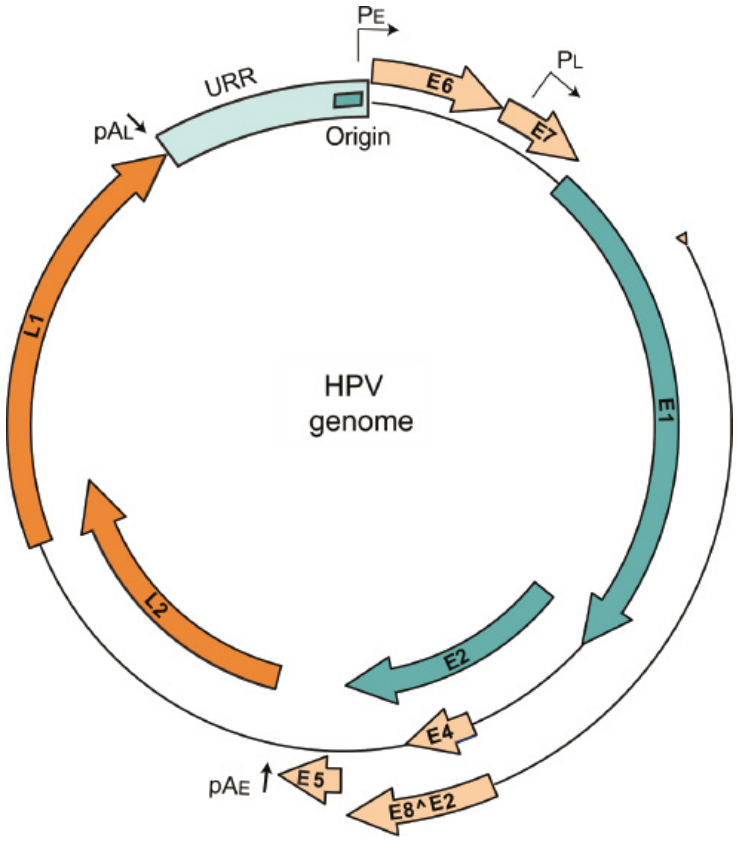

Figure 2: Alpha HPV genome organization. The circular dsDNA genome of an alpha-HPV is pictured here. The replication proteins, E1 and E2, are shown in dark cyan, the structural proteins are shown in orange. URR= upstream regulatory region (light cyan), P_E= early promotor, P_L= late promoter, pA_E= early polyadenylation site and pA_L= late polyadenylation site. The replication origin is indicated. From McBride, 2017.

3.4 Viral life cycle

The HPV replication cycle is linked to the differentiation state of the infected keratinocytes of mucosal and cutaneous epithelia (Figure 3). The viral life cycle starts after mitosis and the entry of the virus into the nucleus (Calton et al., 2017). The ubiquitous transcription factors SP1 (specificity protein 1) and AP1 (activator protein 1) are involved in HPV transcription (Gloss and Bernard, 1990; Hoppe-Seyler and Butz, 1992; Thierry et al., 1992; Thierry, 2009). Amplification of the viral genome can activate the DNA damage response (DDR) due to torsional stress on the viral genome caused by clashing replication forks (Bristol et al., 2017). Furthermore, high-risk HPV E1, E6 and E7 can activate the DDR when expressed on their own (James et al., 2020). Activation of DDR is required for the amplification stage of the viral life cycle (Beglin et al., 2009; Hong and Laimins, 2013; Moody and Laimins, 2009; Spriggs and Laimins, 2017).

The viral genome is maintained at a low copy number after initiation of replication and in the proliferating infected cell moving through the epithelium. The copy number increases in the upper layers of the epithelium through amplification (James et al., 2020). Expression of early viral proteins, which modulate genome replication (E1, E2, E8^E2), viral gene expression

(E2, E8^E2) and host cell pathways (E5, E6, E7) takes place after initial transcription. Infected cells in the suprabasal layer express S-phase markers upon cell division and activate cellular DNA replication, which is due to the activities of the HPV E6 and E7 oncoproteins (Moody and Laimins, 2010). In the middle layer of the epithelium, infected cells activate the differentiation-dependent viral late promoter located in *E7*, amplify their genomes and begin to express the viral E4 protein (Doorbar, 2013; Moody and Laimins, 2010). Furthermore, changes in viral late promoter activation, polyadenylation site usage and splicing patterns of viral transcripts result in the differentiation-dependent expression of the late L1 and L2 proteins, which leads to the synthesis of infectious virions in the uppermost layers of the epithelium. The mechanisms controlling the switch to the productive phase remain uncertain (Doorbar, 2013; Kuehner and Stubenrauch, 2022).

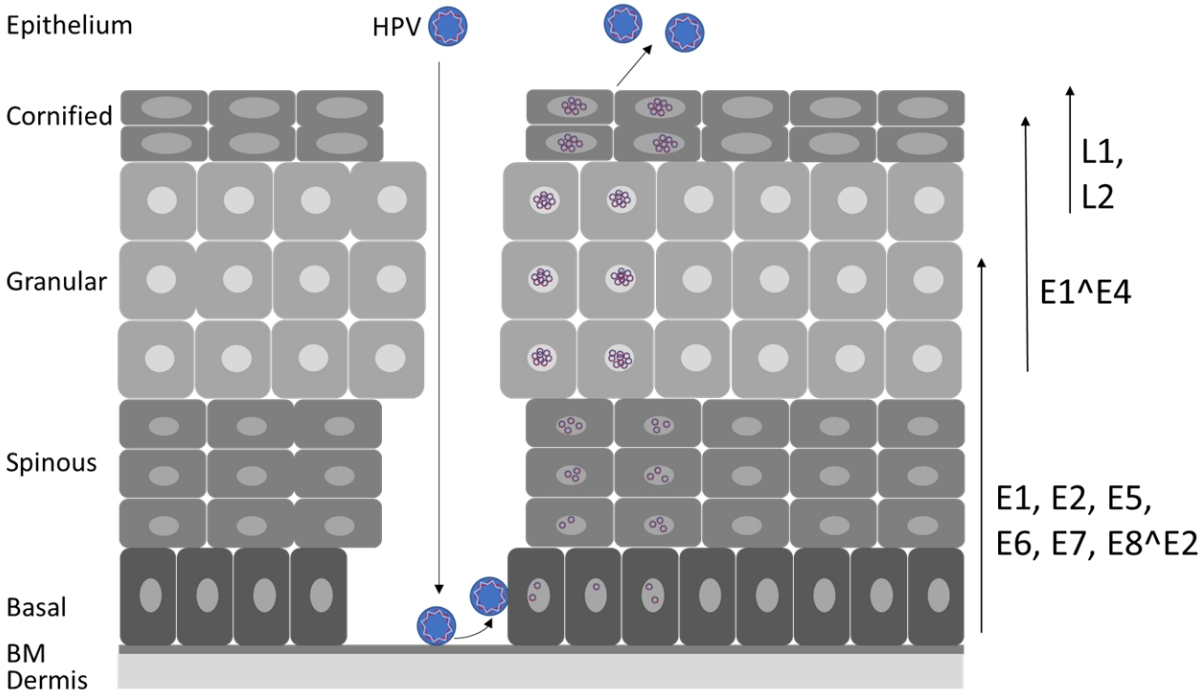

Figure 3: HPV life cycle. Schematic representation of the stratified epithelium and the HPV life cycle. Differentiation dependent expression of viral proteins is indicated with arrows on the right. Basal cells are infected via microlesions in the epithelial barrier. The viral E5, E6, and E7 oncoproteins as well as the replication modulatory E1, E2, and E8^E2 proteins are expressed after introduction of viral genomes into undifferentiated keratinocytes. Expression of *E1^E4* coincides with viral genome amplification. Expression of L1 and L2 in terminally differentiated cells leads to the packaging of viral genomes, virion synthesis, and the release of virions. Figure from Kuehner and Stubenrauch, 2022

3.5 Papillomavirus proteins

3.5.1 The E1 and E2 replication proteins

E1 and E2 are highly conserved, sequence-specific DNA binding proteins. The viral origin of replication, located in the URR, is recognized by the E1 protein. DNA is unwound by E1's helicase activity and then replicated by the recruitment of the cellular DNA replication machinery. Even though DNA damage signaling and genomic stress can reduce the quality of E1-E2-mediated DNA replication leading to a higher mutation frequency, the quantity is not changed (Bristol et al., 2016). E1 consists of an N-terminal regulatory domain, a DNA-binding domain (DBD) that is also responsible for dimerization, and a C-terminal oligomerization domain (Bergvall et al., 2013). The E2 protein consists of a transactivation domain (TAD), a C-terminal DNA binding and dimerization domain (DBD), connected by an unstructured hinge domain. The conserved N-terminal domain (200 aa) of E2 mediates the binding of E1 to the viral origin (Bergvall et al., 2013; McBride, 2013). The E2 DBD is responsible for the specific recognition of E2 binding sites (E2BS) and also for the dimerization of E2 proteins (McBride, 2013). The integration of the virus usually disrupts the E1 and/or E2 open reading frames (ORFs), leading to transcriptional activation of the viral oncogenes E6 and E7 (Akagi et al., 2014; Kadaja et al., 2009; Tsakogiannis et al., 2015;Wentzensen et al., 2004; Xu et al., 2013).

3.5.2 The E8^E2 repressor protein

HPV16 E8^E2 is translated from a spliced mRNA that initiates at a promoter within the E1 gene and uses a splice donor site at nucleotide (nt) 1302 linked to the main splice acceptor (SA) site in *E4* at nt 3358 (Straub et al., 2015). E8^E2 shares the hinge and the DBD with E2 and can therefore bind to viral genomes via E2 binding sites in the URR (Kuehner and Stubenrauch, 2022). The E2 N-terminal domain is replaced by the E8 domain and binds to cellular NCoR/SMRT-HDAC3 corepressor complexes (Dreer et al., 2016; Powell et al., 2010). The E8^E2 -NCoR/SMRT interaction represses both gene expression from viral promoters and the E1- and E2-dependent replication of the viral origin (Dreer et al., 2016; Powell et al., 2010). The exon structure of the E8^E2 mRNA as well as the E8 peptide sequence is conserved among PV, emphasizing the importance of E8^E2 expression during the viral life cycle (Puustusmaa and Abroi, 2016). Short-term phenotypes of PV E8^E2 knock-out (E8-) genomes are highly conserved, including increased genome replication and viral gene expression. Interestingly, there are differences in the long term: HR-HPV16 E8- and beta-HPV49 E8-, but not HR-HPV31 E8- genomes can be stably maintained extrachromosomally in high copy numbers in keratinocytes (Lace et al., 2008; Rehm et al., 2022b; Straub et al., 2014; Stubenrauch et al., 2000). The change of the HPV16 E8 residues K5/W6/K7 to A5/A6/A7 in HPV16 KWK mt genomes also resulted in an increase in copy numbers and amounts of early and late viral transcripts compared to wt genomes in undifferentiated keratinocytes. Furthermore, E2 RNA levels were increased 4-fold in E8- cell lines and 3.8-fold in E8 KWK mt cell lines (Straub et al., 2014). One possible

explanation for the function of E8^E2 is the evasion of the innate immune response to avoid downregulation of cellular proliferation and the induction of senescence (Bristol et al., 2017; James et al., 2020). Intriguingly, MmuPV1 E8- genomes did not induce warts in T cell-deficient mice in contrast to wt genomes, indicating that E8^E2 limiting viral protein expression is not to prevent T cell-mediated elimination of infected cells and its function is not primary an immune-evasive mechanism (Stubenrauch et al., 2021). The change of E8^E2 and E2 amounts or activities in differentiated cells could also be part of the switch from the non-productive to the productive replication phase of papillomaviruses (Straub et al., 2014).

3.5.3 The E4 protein

The start of productive replication in suprabasal keratinocytes is marked by by the activation of the viral late promoter in *E7* and genome amplification leading to the abundant expression of the viral E4 protein (Grassmann et al., 1996; Hummel et al., 1992; Pray and Laimins, 1995; Sterling et al., 1993). The non-structural late protein E4 is expressed form the spliced E1^E4 RNA, and is localized in the cytoplasm (Doorbar, 2013; Moody and Laimins, 2010). The function of E4 during the early life cycle of HPV is not completely understood, but several studies suggest that it is involved in productive genome amplification, the induction of a G2-arrest, the modulation of kinase activity, and virus assembly (Doorbar, 2013). The E4 protein can associate with and reorganize the cytokeratin network of the host cell, which might contribute to efficient virus release (Doorbar et al., 1991; Roberts et al., 1997; Roberts et al., 1994; Wang et al., 2004). Interestingly, the role of E4 varies greatly between different HPV types and cell backgrounds. For HPV16 different effects depending on the length of the E4 protein expressed in a spontaneously immortalised human keratinocyte cell line were described (Nakahara et al., 2005). For HPV18 and 31, loss of full length E4 protein can result in impaired genome amplification in human primary foreskin keratinocytes (Wilson et al., 2005; Wilson et al., 2007). Truncated HPV11 E4 has been reported not to compromise life cycle completion in a human foreskin keratinocyte cell line immortalized by transduction with the telomerse reverse transcriptase (TERT) gene (Fang et al., 2006). This great variability suggests that E4 may have different functions in papillomaviruses (Egawa et al., 2017).

3.5.4 The E5, E6 and E7 oncoproteins

The early oncoproteins E5, E6 and E7 contribute to tumour progression. Of the five genera of HPV, only the alpha HPV encode and express E5 (Basukala and Banks, 2021). HPV E5 have weak transforming activity *in vitro* in comparison to BPV E5, which is BPV1s major transforming protein (DiMaio et al., 1986), but HPV E5 can still transform mammalian cells (Genther Williams et al., 2005; Maufort et al., 2010; Stöppler et al., 1996). The E5 protein contributes to genome amplification in differentiated cells (Egawa and Doorbar, 2017; Fehrmann et al., 2003; Genther et al., 2003; Nakahara et al., 2005; Wilson et al., 2005). E5 increases growth factor signalling,

in particular epidermal growth factor receptor (EGFR), to promote exit from G0-G1 (Ilahi and Bhatti, 2020; Roden and Stern, 2018). Upon integration of high-risk HPV genomes, E5 is often disrupted, but sometimes expression of E5 is still detectable in HPV16 positive cervical and oropharyngeal cancers, indicating that E5 may contribute to malignant progression of the cancer (Chang et al., 2001; Kell et al., 1994; Sahab et al., 2012; Taberna et al., 2018; Um et al., 2014). Differentiation-dependent replication of HPV genomes requires the activities of the E6 and E7 proteins, which induce cell cycle entry and a DNA damage response in suprabasal cells (Moody, 2017). E6 binds and triggers proteasomal degradation of p53 and other pro-apoptotic factors to promote cell survival. E7 binds to multiple targets, notably RB, to overcome its restriction (Roden and Stern, 2018). Beta HPV oncoproteins share some targets, but act somewhat differently (Tommasino, 2017). Ectopic expression of high-risk E6 and E7, but not low-risk HPV, can immortalize primary keratinocytes and induce genomic instability (zur Hausen, 2002). DDR can activate the innate immune response, HPV have to suppress that to avoid downregulation of cellular proliferation and the induction of senescence disrupting the viral life cycle (Bristol et al., 2017; James et al., 2020). The transcription of interferon-stimulated genes (ISGs) through ISGF3 (interferon stimulated gene factor 3) is activated by class 1 interferons (Ivashkiv and Donlin, 2014; Schoggins, 2014; Schoggins et al., 2014). HPV E7 binds to STING preventing the production of interferon (Lau et al., 2015), HPV E6 can inhibit IRF3's transcription (Ronco et al., 1998). Figure 4 illustrates how high-risk HPV E5, E6 and E7 regulate pathways that promote the hallmarks of cancer (Hanahan and Weinberg, 2011; zur Hausen, 2002).

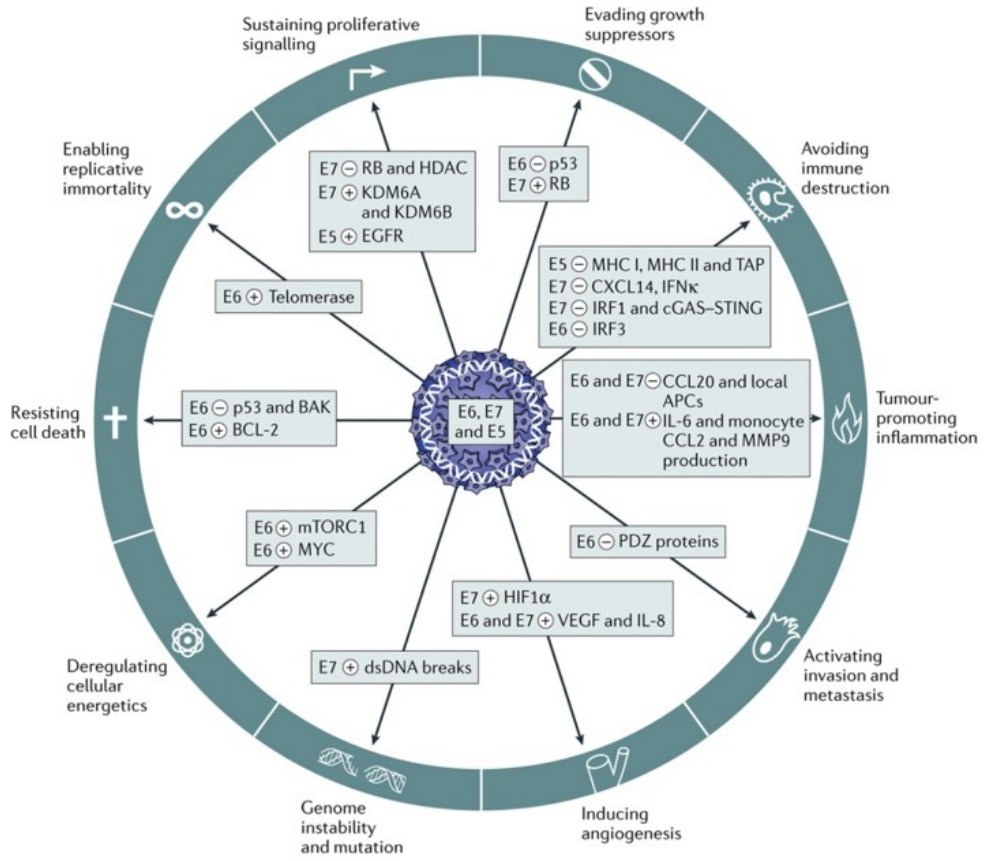

Figure 4: Hallmarks of cancer affected by high-risk HPV oncoproteins. High-risk HPV E5, E6 and E7 regulate pathways that promote the hallmarks of cancer (Hanahan and Weinberg, 2011; zur Hausen, 2002). Through deregulation of pathways, proliferative signaling is sustained (E7 and E5), replicative immortality is enabled (E6), invasion and metastasis is activated, cellular energetics are deregulates (E6) and local angiogenesis is induced (E6 and E7). Growth suppressors that promote cell death are then supressed by E6 (via degradation of p53 among other things), which can result in dsDNA breaks, genomic instability and mutations. Furthermore, immune evasion mechanisms have been evolved by high-risk HPV. EGFR (epidermal growth factor receptor); HDAC (histone deacetylase); HIF1 alpha (hypoxia-inducible factor 1 alpha); KDM6A (lysine-specific demethylase 6A); VEGF (vascular endothelial growth factor). From Roden and Stern, 2018.

3.5.5 The capsid proteins L1 and L2

The viral genome is packaged into capsids which consist of the major capsid protein L1 and the minor capsid protein L2 only in the most superficial cell layers. While L1 can self-assemble into empty virus-like particles (VLPs), L2 lacks this capacity. The icosahedral capsid is composed of 360 copies of L1 and 12–72 copies of the L2 protein. (Buck et al., 2013; Chen et al., 2000; Buck et al., 2008; Goetschius et al., 2021; Mikuličić et al., 2021; Modis et al., 2002). L1 interacts with heparan sulfate proteoglycans of the basement membrane, and is necessary for entry into the target cell (Buck et al., 2013). Even though L2 alone does not form capsids, it is involved in packaging, capsid assembly, and endosomal release of the virus (Wang and Roden, 2013).

3.6 HPV vaccination

Since 2007, HPV vaccination has been recommended and reimbursed for girls in Germany (STIKO, 2007). In June 2018 the German Standing Committee on Vaccination (STIKO) recommended the additional vaccination of adolescent boys due to the high burden of disease of HPV-associated cancers in men (STIKO, 2018a; STIKO, 2018b; Wähner et al., 2023). Virus-like particles (VLPs), which lack the oncogenic viral genome and are immunologically similar to native virions, can be produced through the recombinant expression of L1 and are the basis for HPV vaccines licensed today (Kirnbauer et al., 1992; Roden and Stern, 2018). Since the protection by L1 VLP is type-restricted, it is necessary to include several HPV types to ensure a broad neutralization and high and durable titers of neutralizing antibodies (Breitburd et al., 1995; Deschuyteneer et al., 2010; Suzich et al., 1995). Table 1 compares the bivalent, quadrivalent and nonavalent HPV vaccines (De Oliveira et al., 2019; Brotherton, 2018).

Table 1: HPV vaccine types

	Bivalent vaccine	**Quadrivalent vaccine**	**Nonavalent vaccine**
Company	GlaxoSmithKline	Merck	Merck
Brand name	Cervarix	Gardasil, silgard	Gardasil 9
L1 virus like particle types	HPV16/18	HPV6/11/16/18	HPV-6/11/16/18/ 31/33/45/52/58
Cross protection	HPV31/33/45	HPV31	Unknown
Expression system	Baculovirus-insect cell	Yeast	Yeast
Licensed in Germany	2007	2006	2016

Although the vaccines mentioned before are very effective in prophylaxis of HPV associated malignancies, they do not have therapeutic effects, suggesting a need for therapeutic reagents (Roden and Stern, 2018).

3.7 *Mus musculus* papillomavirus (MmuPV1)

The species-specificity of papillomaviruses makes it necessary to address phenotypes of PV mutant genomes in *in vivo* models. The *mus musculus* papillomavirus 1 (MmuPV1), first described in 2011 (Ingle et al., 2011), belongs to the PV genus pi and allows investigating the effects of viral mutants on tumor formation in mice. Its genomic organization is comparable to other PV and it lacks a *E5* ORF (Figure 5).

MmuPV1 encodes and transcribes E8^E2. The MmuPV1 (m)E8^E2 protein inhibits MmuPV1 promoter activity and the E1 and E2-dependent activation of the viral origin of replication. The mutation of the E8 start codon (E8-) in the MmuPV1 genome results in greatly increased viral gene expression in cultured murine tail keratinocytes (Stubenrauch et al., 2021). Surprisingly, MmuPV1 E8- genomes did not induce warts in Foxn1$^{nu/nu}$ mice suggesting that E8^E2 is necessary for tumor formation *in vivo* (Stubenrauch et al., 2021). Foxn1$^{nu/nu}$ mice, first described by Flanagan in the 60s (Flanagan, 1966), are nude and athymic. These mice are T cell-deficient due to agenesis of the thymus and are severely immunocompromised (Pantelouris, 1968).

MmuPV1 E6 interacts with MAML1 (Mastermind-like protein 1), similarly to cutaneous low-risk HPV E6 proteins that bind MAML1 and inhibit NOTCH signaling (Meyers et al., 2017). Saunders-Wood and colleagues suggested that the interaction between MAML1 and E6 was necessary for the basal-layer persistence of MmuPV1 E6-expressing cells (Saunders-Wood et al., 2022). MmuPV1 E7 can bind the C terminal domain of RB1 through its C terminus (Grace and Munger, 2017; Wang et al., 2010; Wei et al., 2021), independently of a canonical LXCXE (L, leucine; C, cysteine; E, glutamic acid; X, any amino acid) binding motif.

MmuPV1 has a differentiation-dependent life cycle similar to HPV. Epithelial lesions are induced and the viral late proteins E4 and L1 are expressed in suprabasal layers of such lesions (Brendle et al., 2021; Handisurya et al., 2014; Uberoi et al., 2016; Saunders-Wood et al., 2022). Preclinical models for papillomavirus-mediated disease and cancer of the anal tract (Blaine-Sauer et al., 2021), head and neck cancer (Wei et al., 2020) and disease of the female reproductive tract (Spurgeon et al., 2019) were described in the last years.

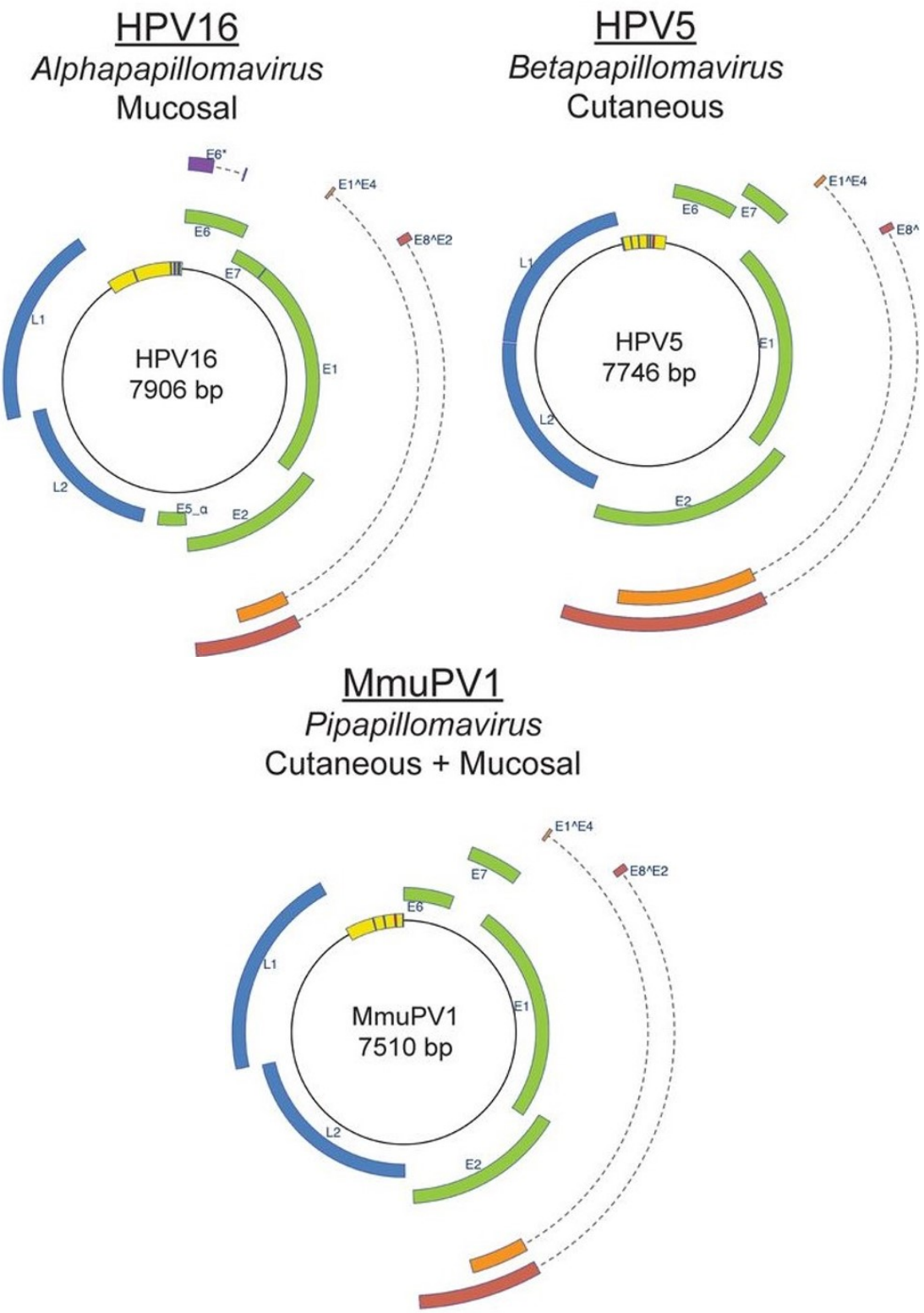

Figure 5: Comparison of MmuPV1 genome with alpha and beta HPV. MmuPV1 genomic organization, classification, and tissue tropism compared to an alphapapillomavirus (HPV16) and a betapapillomavirus (HPV5). Figure from Spurgeon and Lambert, 2020

3.8 NCoR/SMRT corepressor complex

Gene expression is controlled by a cascade of transcription factors and coactivators or corepressors, which modify specific residues of histones and thereby regulate the accessibility of chromatin to the basal transcription machinery (Glass and Rosenfeld, 2000).

Histones can be modified through (de)acetylation of lysine residues in N-terminal histone tails (Allfrey et al., 1964; Grunstein, 1997; Verdin and Ott, 2015), coactivators have histone acetyltransferase (HAT) activity, while corepressors possess histone deacetylase (HDAC) activity (Brownell et al., 1996; Ng and Bird, 2000; Sterner and Berger, 2000; Taunton et al., 1996). Furthermore, methylation, phosphorylation, ubiquitylation and glycosylation of histones are involved in transcriptional control (Dall'Olio and Trinchera, 2017; Lawrence et al., 2016).

Nuclear hormone receptors (NRs) are responsible for the regulation of transcription of target genes in a ligand-dependent manner (Ishii, 2021). Through the integration and delivery of developmental, hormonal and environmental cues to the genome, they act as genetic switches of gene transcription (Emmett and Lazar, 2019). The main corepressors responsible for gene suppression mediated by NRs are NCoR1 (nuclear receptor corepressor 1) and the closely related SMRT (silencing mediator of retinoic acid and thyroid hormone receptor, also NCoR2), which have been first identified in the mid 1990s (Chen and Evans, 1995; Hörlein et al., 1995; Ordentlich et al., 1999; Park et al., 1999). NCoR1 and SMRT proteins form core complexes with HDAC3 (histone deacetylase 3), TBL1 (transducin-beta like 1), TBLR1 (TBL-related 1) and GPS2 (G protein pathway suppressor 2) (Guenther et al., 2000; Li et al., 2000; Yoon et al., 2003; Zhang et al., 2002). The conserved interaction between HPV E8^E2 and the cellular NCoR/SMRT corepressor complexes (Figure 6) is important for the mediation of repression of transcription and DNA replication (Dreer et al., 2016).

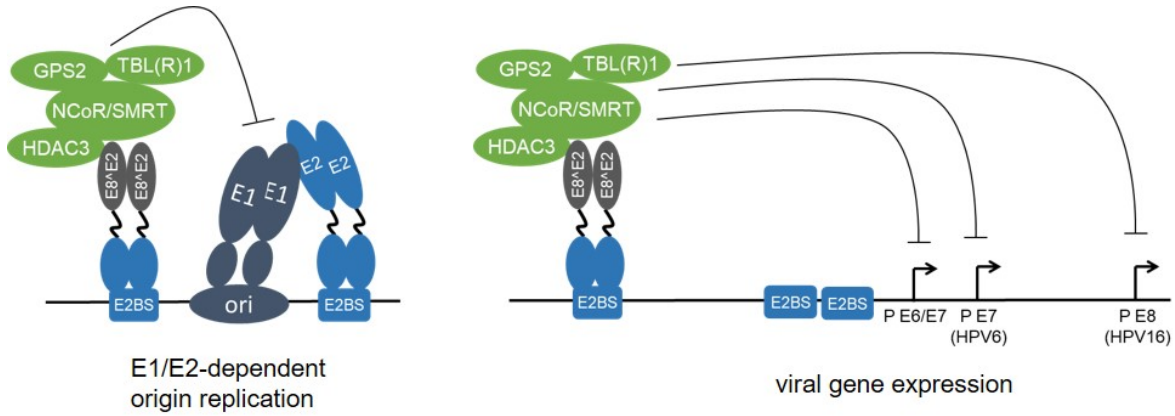

Figure 6: HPV E8^E2 proteins repress viral replication and transcription. HPV E8^E2 proteins bind to E2BS via the C-terminal DNA binding domain. The E8 domain recruits NCoR/SMRT corepressor complexes consisting of of GPS2, HDAC3, NCoR1, SMRT (NCoR2), TBL1, and TBLR1. This inhibits the transcription from different viral promoters and E1/E2-dependent replication of the viral origin. Figure from Kuehner and Stubenrauch, 2022

3.9 Objectives

It is known that cell lines that stably express HPV16 E8- genomes maintain higher copy numbers and express higher levels of early and late transcripts than wt genomes under both undifferentiated and differentiated conditions (Lace et al., 2008; Straub et al., 2014). An increased viral transcription in undifferentiated normal mouse tail keratinocytes (NMTK) was also described for MmuPV1 E8- genomes. In contrast, MmuPV1 E8- genomes did not induce warts in T cell-deficient Foxn1$^{nu/nu}$ mice suggesting that E8^E2 is necessary for tumor formation *in vivo* (Stubenrauch et al., 2021).
The advantage of the expression of E8^E2 for PV remains unclear, as well as the amount of E2 and E8^E2 protein during the PV replication cycle. To explore this, the cellular transcriptome of HPV16 wt and E8- cell lines were compared to identify deregulated cellular genes. Furthermore, HPV16 E2 was purified for antibody production to characterize the expression of E2 and E8^E2 on a protein level in HPV positive cell lines. To provide further evidence that the lack of wart formation *in vivo* is due to the lack of E8^E2 and not cis-elements overlapping with the E8 start codon, additional mutations in E8 were generated. Furthermore, the interaction of mE8^E2 with NCoR/SMRT components and its importance on E8^E2's repression activity were analyzed.

4 Material and Methods

4.1 Material

4.1.1 Antibodies

4.1.1.1 Primary antibodies

Table 2: Primary antibodies

Epitope	Host	Supplier (Order number)	Application	Dilution
ATF3	rb	cell signaling (#18665)	WB/IF	1/100-1/1,000
Cytokeratin 10	ms	DAKO (#M7002)	IF	1/200
Cytokeratin 10	rb	Novus (#NBP2-75765)	IF	1/200
Cytokeratin 14	ch	Biolegend (#906004)	IF	1/300
HA Tag	ms	cell signaling (#2367)	WB/IF	1/1,000
HA Tag	rb	cell signaling (#3724)	WB/IF	1/1,000
HDAC3	ms	cell signaling (#3949)	WB	1/1,000
HPV16 E1^E4	ms	Santa Cruz (#53324)	WB/IF	1/200-1/500
HPV16 E2	rb	self-made	WB/IF	1/200-1/1,500
HPV16 E2 B9	ms	Wieland et al., 2020	WB/IF	1/200-1/1,500
HSP90	ms	Santa Cruz (#69703)	WB	1/2,000
MmuPV1 E4	rb	Egawa et al., 2021	WB/IF	1/200-1/3,000
RPA32	rat	cell signaling (#2208)	IF	1/200
TBL1	ms	Santa Cruz (#137006)	WB	1/1,000
YFP	ms	Clontech (# 632381)	WB	1/1,000

4.1.1.2 Secondary antibodies

Table 3: Secondary antibodies

Epitope	Host	Conjugate	Supplier	Dilution	Application
Mouse IgG	goat	Alexa Fluor 488	Invitrogen	1/1,000	IF
Rabbit IgG	goat	Alexa Fluor 555	Invitrogen	1/1,000	IF
Chicken IgG	goat	Alexa Fluor 555	Invitrogen	1/1,000	IF
Mouse IgG	donkey	Alexa Fluor 555	Invitrogen	1/1,000	IF
Rabbit IgG	donkey	Alexa Fluor 488	Invitrogen	1/1,000	IF
Rabbit IgG	goat	Alexa Fluor 405	Invitrogen	1/1,000	FCA
Mouse IgG	goat	IRDye® 680RD	Li-Cor	1/15,000	WB
Mouse IgG	goat	IRDye® 800CW	Li-Cor	1/15,000	WB
Rabbit IgG	goat	IRDye® 680RD	Li-Cor	1/15,000	WB
Rabbit IgG	goat	IRDye® 800CW	Li-Cor	1/15,000	WB

4.1.2 Bacterial culture

4.1.2.1 Antibiotics

Table 4: Antibiotics

Antibiotic	Supplier	Final Concentration
Ampicillin	Thermo Fisher	100 µg/ml
Kanamycin	Thermo Fisher	30 µg/ml
Zeocin	Thermo Fisher	25 µg/ml

4.1.2.2 Competent bacterial strains

Table 5: Competent bacterial strains

Strain	Supplier
E. coli DH5 alpha	Clontech Laboratories Inc.
E. coli BL21(DE3)	New England BioLabs

4.1.2.3 Media for bacterial culture

Table 6: Media for bacterial culture

Media	**Ingredients**
Freezing medium	65% glycerol 0.1 M $MgSO_4$ 0.025 M Tris [pH 8.0]
LB medium (for growth of liquid cultures)	2.5% [w/v] LB broth powder dissolved in H_2O 100 µg/ml ampicillin or 30 µg/ml kanamycin
LB agar	2.5% [w/v] LB broth powder 1.2% [w/v] select agar dissolved in H_2O 100 µg/ml ampicillin or 30 µg/ml kanamycin
SOC medium	2% [w/v] bacto-trypton 0.5% [w/v] bacto-yeast extract 10 mM NaCl 2.5 mM KCl 10 mM $MgCl_2$ 10 mM $MgSO_4$ 20 mM glucose
TB medium	24 g/L yeast extract 12 g/L peptone 0.4% [v/v] glycerol 5 g/L NaCl 17 mM KH_2PO_4 72 mM K_2HPO_4 2 mM $MgSO_4$ 0.05% [w/v] glucose 100 µg/ml ampicillin or 30 µg/ml kanamycin

4.1.3 Buffers and solutions

Table 7: Buffers and solutions

Buffer/Solution	Ingredients
Antibody dilution buffer (IF)	1x PBS 1% [w/v] BSA fraction V 0.3% [v/v] triton-X 100
Annealing buffer (oligonucleotides)	200 mM potassium acetate 60 mM HEPES-KOH [pH 7.5] 4 mM magnesium acetate
Blocking buffer (IF)	1x PBS 5% [v/v] normal goat/donkey serum 0.3% [v/v] triton-X 100
Blocking buffer (WB)	1x PBS 5% [w/v] nonfat dried milk powder
CAPS transfer buffer (WB)	10 mM CAPS 10% [v/v] methanol pH 10.3
Coomassie staining solution	0.05% [w/v] coomassie brilliant blue R-250 10% [v/v] acetic acid 25% [v/v] isopropanol
CoIP elution buffer	50 mM Tris-HCl [pH 6.8] 50 mM DTT 1% SDS 1 mM EDTA 0.005% bromphenol blue 10% glycerol
DNA-loading buffer (10x)	20% [w/v] ficoll 400 0.1 M Na_2-EDTA pH 8.0 1% [w/v] SDS 0.25% [w/v] bromphenol blue 0.25% [w/v] xylene cyanol

Table 7: Buffers and solutions (continued)

Buffer/Solution	**Ingredients**
Elution buffer	20 mM maltose 20 mM Tris-HCl [pH 8 @ 8 °C] 600 mM NaCl 5% [v/v] glycerol 1 mM TCEP
FCA buffer	1% FCS in 1x PBS
FCA blocking buffer	10% FCS in 1x PBS
FCA PI-staining solution	50 µg/ml PI 0.33 mg/ml RNAse A
FCA permeabilization buffer	1% FCS in 1x PBS 0.1% triton-X-100
Firefly luciferase buffer	100 mM KPO_4 [pH 7.8] 15 mM $MgSO_4$ 5 mM ATP 1 mM D-luciferin
Lysis buffer (Luciferase assay)	100 mM potassium phosphate buffer [pH 7.8] 1% [v/v] triton-X 100 1 mM DTT
Lysis buffer (Low molecular weight DNA)	400 mM NaCl 20 mM Tris-HCl [pH 7.5] 5 mM EDTA [pH 8]
Lysis buffer (Protein test expression)	50 mM Tris-HCl [pH 8 @ 8 °C] 200 mM NaCl 5% [v/v] glycerol 1 mM EDTA

Table 7: Buffers and solutions (continued)

Buffer/Solution	**Ingredients**
Lysis buffer (Protein expression)	40 mM Tris-HCl [pH 8 @ 8 °C] 50 mM NaCl 3 mM $MgCl_2$ 5% [v/v] glycerol 1 mM TCEP 1250 U benzonase (Merck) 3.5 mg/ml lysozyme EDTA-free protease inhibitor cocktail
Mounting media (IF)	25% [v/v] glycerol 10% [w/v] mowiol 4-88 100 mM Tris-HCl [pH 8.5]
PBS (10x)	137 mM NaCl 2.7 mM KCl 1.5 mM KH_2PO_4 [pH 7.2]
PBS-T	0.05% [v/v] tween-20 in 1x PBS
Renilla luciferase buffer	Gaussia-juice 1 mM coelenterazine
RIPA buffer (WB)	1% [v/v] igepal CA 630 1% [w/v] sodium deoxycholate 0.1% SDS [v/v] 150 mM NaCl 10 mM sodium phosphate [pH 7.2] 2 mM EDTA 50 mM sodium fluoride 1x cOmplete protease inhibitor (EDTA free) 1x PhosStop phosphatase inhibitor
Running buffer (SEC)	20 mM HEPES pH 7.5 600 mM NaCl 5% [v/v] glycerol 1 mM TCEP

Table 7: Buffers and solutions (continued)

Buffer/Solution	**Ingredients**
Running buffer (MBP trap)	40 mM Tris-HCl [pH 8 @ 8 °C] 50 mM NaCl 5% [v/v] glycerol 3 mM $MgCl_2$ 1 mM TCEP
SDS-PAGE running buffer (5x)	125 mM Tris-HCl 0.96 M glycine 17.3 mM SDS
TAE buffer (50x, DNA electrophoresis)	2 M Tris 1 M acetic acid 0.1 M EDTA pH 8.5

4.1.4 Chemicals and reagents

Table 8: Chemicals and reagents

Chemical/Reagent	**Supplier**
Acetic acid	Merck
Agar	Carl Roth
Agarose LE	VWR
Bromophenol blue	Thermo Fisher
BSA (Albumin Bovine Fraction V)	Carl Roth
Bovine collagen I	Thermo Fisher
Chloroform	Carl Roth
cOmplete protease inhibitor cocktail	Roche
Coomassie brilliant blue R-250	Thermo Fisher
Collagen type 1 from rat tails	Corning
Coelenterazine (CTZ)	PJK
D-luciferin	PJK
DAPI	Fluka Honeywell
DEPC	Carl Roth
Dithiothreitol (DTT)	Thermo Fisher
dNTPs	Thermo Fisher
EDTA	Carl Roth

Table 8: Chemicals and reagents (continued)

Chemical/Reagent	**Supplier**
Ethanol	Honeywell
Formaldehyde	Carl Roth
FuGENE® HD transfection reagent	Promega
G418/ geneticin	Thermo Fisher
Gaussia juice fluid	PJK
Gene ruler 1 kb Plus DNA ladder	Thermo Fisher
Gene ruler 100 bp DNA ladder	Thermo Fisher
Glycerine	Carl Roth
Isopropanol	Honeywell
LightCycler® SYBR Green I master	Roche
Lipofectamine RNAiMAX reagent	Thermo Fisher
Lysozyme	Merck
Magnesium chloride	Carl Roth
Maltose	Carl Roth
Manganese chloride	Merck
Methanol	Honeywell
Monopotassium phosphate	Carl Roth
Mowiol 4-88	Carl Roth
Paraformaldehyde	Thermo Fisher
PageRuler prestained protein ladder	Thermo Fisher
Penicillin-Streptomycin	Thermo Fisher
Peptone	Carl Roth
PhosSTOP	Roche
Potassium chloride	Carl Roth
Potassium dihydrogen phosphate	Carl Roth
Roti®-Load 4x	Carl Roth
Rotiphorese® Gel 30	Carl Roth
Rubidium chloride	Merck
Sodium chloride	Carl Roth
Sodium dodecyl sulfate (SDS)	Carl Roth
Sodium hydroxide	Carl Roth
TCEP	Thermo Fisher
Tris	Carl Roth
Tween-20	Signa Aldrich
Xylene cyanol	Merck
Yeast extract	Carl Roth

4.1.5 Consumables

Table 9: Consumables

Consumable	Supplier
10 µl pipette tips	Biozym
200 µl and 1000 µl pipette tips	Greiner Bio-One GmbH
10ml serological pipets	Corning
25ml serological pipets	Corning
50 ml centrifuge tubes	Greiner Bio-One GmbH
5ml serological pipets	Corning
C-Chip counting chamber	NanoEnTek
Cell Culture Plates (Nunc, 6 well, 12 well, 24 well)	Thermo Fisher
Cell lifter (Corning, Costar®)	Thermo Fisher
Coated cell culture dishes (100 mm)	Thermo Fisher
µColumns	Miltenyi Biotec
Conical centrifuge tubes (CELLSTAR®, 15+50 ml)	Greiner Bio-One
Cover slips	Carl Roth
Cryo tubes bacterial stocks (3.6 ml)	Thermo Fisher
Cryo tubes cell culture (Cryo.s, 2 ml)	Greiner Bio-One
Filter pipette tips (10, 20, 200, 1000 µl)	Thermo Fisher
High precision microscope cover glasses	Paul Marienfeld GmbH Co. KG
HiLoad® 16/600 Superdex® 200 prep grade S200	GE Healthcare Life Sciences
HiLoad® 16/600 Superdex® 75 prep grade S75	GE Healthcare Life Sciences
LightCycler® 480 multiwell plate 96, white	Roche
MBPTrap™HP (1 and 5ml)	Cytiva Life Sciences
Nitrocellulose membrane (0.22 µm)	Whatman plc
Pierce™ protein concentrator PES (10K MWCO)	Thermo Scientific
Reaction tubes (1.5 ml, 2.0 ml)	Eppendorf
Scalpel, disposable	B. Braun Melsungen AG
Sterile filters 0.22 µm, 0.45 µm (Millex-GP)	Merck KGaA
SuperFrost plus adhesion slides	Thermo Scientific
Syringe	B. Braun
Transfection tubes (3.5 ml)	Sarstedt AG + Co. KG
Tubes for bacterial culture (14 ml, sterile)	Greiner Bio-One
Whatman paper	Whatman plc

4.1.6 Enzymes

Restriction enzymes and respective buffers from New England Biolabs or Thermo Fisher have been used, in addition to the following enzymes:

Table 10: Enzymes

Enzyme	Supplier
Exonuclease V (RecBCD)	NEB
Dispase II (neutral protease, grade II)	Roche
FastAP Thermosensitive Alkaline Phosphatase	Thermo Fisher
GoTaq G2 DNA Polymerase	Promega
Pyrobest DNA Polymerase	Takara Bio Inc.
T4 DNA Ligase	Thermo Fisher

4.1.7 Eukaryotic cell culture

4.1.7.1 Eukaryotic cell lines generated for this thesis

Table 11: Eukaryotic cell lines generated for this thesis

Cell line	Mutation
HPV16 wt NHK (normal human keratinocyte)	HPV16 114b wt genome, was kindly provided by M. Dürst (Kirnbauer et al., 1993)
HPV16 E8- NHK	The E8- mutation replaces the codon for W6 with a stop codon in the E8 ORF (TGG to TAG) (Lace et al., 2008, Straub et al., 2014)
HPV16 E8-E4- NHK	E4 mutation st15 (Nakahara et al., 2005) was introduced into the HPV16 E8- genome to prevent E4 expression
HPV16 E8-E5- NHK	Stop codon at residue 3 of E5 was introduced into the HPV16 E8- genome to prevent E5 expression

4.1.7.2 Eukaryotic cell lines used

Table 12: Eukaryotic cell lines used

Cells	Origin
C33A	HPV-negative cervical carcinoma cell line, carrying mutations in TP53 and RB1 (Auersperg, 1964, Scheffner et al., 1991, Yee et al., 1985).

Table 12: Eukaryotic cell lines used (continued)

Cells	Origin
HeLa	HPV18 positive cervical carcinoma cell line (Gey, 1952).
HPV16-positive human keratinocyte cell lines	Generated in our laboratory by stably transfecting NHK derived from different donors with HPV16 wt or mutant genomes.
NIH-3T3-J2 (J2)	Murine fibroblast cell line, used as feeder cell layer for keratinocytes (Jainchill et al., 1969).
Normal human keratinocytes (NHK)	NHK were isolated from human foreskin after routine circumcision upon informed consent of patients which was approved by the ethics committee of the medical faculty of the university Tübingen (6199/2018BO2) and performed according to the principles of the declaration of Helsinki.
Normal mouse tail keratinocytes (NMTK)	Isolation from mouse tails as described previously (Stubenrauch et al., 2021).

4.1.7.3 Media for eukaryotic cell culture

Table 13: Media for eukaryotic cell culture

Media	Ingredients
DMEM-CS	Dulbecco's Modified Eagle Medium (Thermo Fisher) 50 mg/l gentamycin 10% [v/v] CS (Calf serum)
DMEM-FCS	DMEM (Thermo Fisher) 50 mg/l gentamycin 10% [v/v] FCS (Fetal calf serum)
E-media	three parts DMEM (Thermo Fisher) one part Ham's F12 (Thermo Fisher) 5% [v/v] FCS Hyclone 24 µg/l adenine 0.4 ng/l hydrocortisone

Table 13: Media for eukaryotic cell culture (continued)

Media	Ingredients
E-media (continued)	10 ng/l cholera toxin 5 µg/l transferrin 20 pM 3,30-5-triodo-L-thyronine 5 ng/l epidermal growth factor 5 µg/l insulin 100 U/ml penicillin and 100 µg/ml streptomycin
KSFM	Keratinocyte Serum-Free Medium (Thermo Fisher) 0.05 mg/ml bovine pituitary gland extract 0.005 µg/ml recombinant human EGF 50 mg/l gentamycin
KSFM without Ca_2Cl	KSFM without calcium chloride (Thermo Fisher) 0.05 mg/ml bovine pituitary gland extract 0.005 µg/ml recombinant human EGF 100 U/ml penicillin and 100 µg/ml streptomycin supplemented with 50 µM Ca^{2+}

4.1.8 Kits

Table 14: Kits

Kit	Supplier	Application
EZ1 DNA Tissue Kit	Qiagen	DNA extraction
µMACS HA Isolation Kit	Miltenyi Biotec	CoIP and IP
QIAgen®Plasmid Plus Maxi Kit	Qiagen	plasmid DNA isolation
QIAgen® Plasmid Plus Midi Kit	Qiagen	plasmid DNA isolation
QIAprep® Spin Miniprep Kit	Qiagen	plasmid DNA isolation
QIAquick® Gel Extraction Kit	Qiagen	DNA extraction agarose gels
QIAshredder® Kit	Qiagen	homogenizing cell lysates
QuantiTect Reverse Transcription Kit	Qiagen	cDNA synthesis
QIAquick PCR Purification Kit	Qiagen	PCR purification
Rapid DNA Ligation Kit	Thermo Fisher	DNA ligation
RNeasy® Mini Kit	Qiagen	RNA isolation

4.1.9 Laboratory equipment

Table 15: Laboratory equipment

Equipment	Supplier
Autoclave	ZIRBUS technology GmbH
ÄKTA pure protein purification system	Cytiva
BioPhotometer spectrophotometer	Eppendorf AG
BioRobot EZ1® DSP workstation	Qiagen
Certomat IS shaking incubator	B. Braun Biotech International GmbH
CO_2 incubator C200	LaboTect
French Pressure Cell FA-078	Thermo Scientific
Fluorescence microscope Axio Observer.Z1	Zeiss
Herasafe sterile workbench	Thermo Fisher
Intas Gel iX20 Imager	Intas Science Imaging Instruments GmbH
Kelvitron® T incubator	Heraeus
LI-COR Odyssey® Fc Imaging System	LI-COR Biosciences
LightCycler® 480 Instrument	Roche
µMACS Seperator	Miltenyi Biotec
MACS Quant Analyzer VYB Flow Cytometer	Miltenyi Biotec
Milli-Q UF Plus	Merck KGaA
Mini-, Wide-, Sub Cell GT chambers	Bio-Rad Laboratories, Inc.
Mr. Frosty freezing container	Thermo Fisher
Multipette plus	Eppendorf AG
NanoDrop 2000 spectrophotometer	Thermo Fisher
Neubauer Chamber 0.100 mm	Glaswarenfabrik Karl Hecht GmbH Co. KG
PCT 200 Peltier Thermal Cycler	Bio-Rad Laboratories, Inc.
pH-meter WTW pH 526	Xylem Inc.
PIPETMAN Classic TM P10/20/200/1000	Gilson Inc.
Pipettor pipetus	Hirschmann Laborgeräte GmbH Co. KG
PowerPac 200	Bio-Rad Laboratories, Inc.
Precision scales GJ and 770	KERN + SOHN GmbH
Reax top vortexer	Heidolph Instruments GmbH Co. KG
Research® Pro electronic pipette 5 - 100 µl	Eppendorf AG
SonoPuls Sonifier UW 2200	Bandelin electronic GmbH Co. KG
Sprout mini centrifuge	Heathrow Scientific
Tabletop centrifuges 5804R, 5810R	Eppendorf AG
Tabletop centrifuges 5417R, 5424R	Eppendorf AG
Thermomixer comfort	Eppendorf AG
ThermoStat plus	Eppendorf AG

Table 15: Laboratory equipment (continued)

Equipment	Supplier
Trans-Blot Cell chamber	Bio-Rad Laboratories, Inc.
Transmitted light microscope DM IRB	Leica Camera AG
TriStar2S	Berthold Technologies GmbH Co. KG
UV transilluminator NU-72 KL	Konrad Benda Laborgeräte
VacuSafe scavenge pump	INTEGRA Biosciences AG
Water bath WB10	Memmert GmbH Co. KG

4.1.10 Plasmids

All inserts were verified by DNA sequencing and mutant PV genomes were completely sequenced to ensure that no additional changes were introduced during the cloning procedure.

Table 16: Plasmids

Plasmid	Properties
GPS2-sYFP	coding sequence of human GPS2 inserted into pSYFP2-C1
pCI-Neo-Rluc	based on pCI-neo (Promega), expresses a codon-optimized version of the renilla luciferase amplified from plasmid pGL4.72 (Promega)
pC18-Sp1-luc	four synthetic E2 binding sites and two synthetic SP1 binding sites upstream of a minimal adenovirus major late promoter composed of the TATA box and the initiator element inserted into the luciferase reporter plasmid pALuc (a kind gift of G. Steger, Institute of Virology, Cologne, Germany)
pGL mURR/E1-luc	MmuPV1 nt 6899 to 7510/ 1 to 741 were inserted between the NheI and NcoI sites of pGL3-basic (Stubenrauch et al., 2021)
pSV2 neo	Provides selectable marker for resistance to antibiotic G418 in mammalian cell lines
pAsylum MmuPV1 E8- genome	MmuPV1 genome with E8 ATG (nt 1094 to 1096) exchanged to ACG (Stubenrauch et al., 2021)

Table 16: Plasmids (continued)

Plasmid	Properties
pAsylum MmuPV1 E8 SD mt genome	MmuPV1 genome with mutation in the E8 splice donor (AG|GT to AA|GT)
pAsylum MmuPV1 E8 Stop mt genome	MmuPV1 genome with G9X mutation
pAsylum MmuPV1 E8^E2 RPR mt genome	MmuPV1 genome with K2/L3/K4 exchange to R2/P3/R4
pAsylum MmuPV1 wt genome	MmuPV1 genome in pAsylum as previously described by Wang et al., 2015
pBS HPV16 114b:1 genome	HPV16 114/b wt genome, was kindly provided by M. Dürst (Kirnbauer et al., 1993)
pBS HPV16 E8- genome	HPV16 genome with E8- mutation that replaces the codon for W6 with a stop codon in the E8 ORF (TGG to TAG) and is silent in the overlapping E1 gene
pBS HPV16 E8 KWK mt genome	HPV16 genome with E8 residues K5/W6/K7 changed to AAA (Straub et al., 2014)
pBS HPV16 E8- E4- genome	HPV16 genome with E4 L15 stop (TTA to TAA) and E8 W6 stop (TGG to TAG)
pBS HPV16 E8- E5- genome	HPV16 genome with E5 N3 stop (AAT to TAA) and E8 W6 stop (TGG to TAG)
PEF-IRES-P hPGK1	encoding the cDNA for human phosphoglycerate kinase 1 (PGK1) as standard for qPCR
pETm41	Expression plasmid with sequences for 6xHis tag, MBP tag (maltose binding protein) and tobacco etch virus (TEV) cleavage site (all N terminal on backbone)

Table 16: Plasmids (continued)

Plasmid	Properties
pETm41-HPV16 E2C co	Expression plasmid for the codon optimized HPV16 E2 fragment as a His_6-MBP-TEV-HPV16 E2C co fusion protein (E2 hinge aa202-286, DBD/Dimerization aa286-365) cloned in pETm41
pSG5	Expression plasmid with SV40 early promoter and polyadenylation signal, T7 bacteriophage promoter, beta-globin intron II, with different PV protein genes insterted: pSG HPV16 E2 pSG5 HPV16 E2-HA pSG HPV16 E8^E2 pSG5 HPV16 E8^E2 -HA pSG5 HPV16 E8 KWK pSG5 HPV16 E8 KWK-HA pSG5 mE8^E2 RPR pSG mE8^E2 d9-11 pSG mE1 G126V pSG5 mE8^E2 wt pSG 3xHA-mE1^E4
pSYFP2-C1	pSYFP2-C1 was a gift from Dorus Gadella (Addgene plasmid 22878, Kremers et al., 2006)
psYFP-HDAC3	coding sequence of human HDAC3 inserted into pSYFP2-C1
pUC57 HPV16 E1^E4^L1	HPV16 nt 865 to 880/ 3358 to 3632/ 5639 to 5696, concentration determination (dilution series) in HPV16 qPCR, ordered from genscript
pUC57 MmuPV1 E1^E4^L1	MmuPV1 nt 662 to 757/ 3139 to 3431/ 5372 to 5496, concentration determination (dilution series) MmuPV1 qPCR, ordered from genscript

Table 16: Plasmids (continued)

Plasmid	Properties
pUC57 MmuPV1 URR^E4	MmuPV1 nt 7108 to 7243/ 3139 to 3318, Concentration determination (dilution series) qPCR MmuPV1, ordered from genscript
sYFP-TBLR1	coding sequence of human TBLR1 inserted into pSYFP2-C1

4.1.11 Software

Table 17: Software

Software	Version
FlowLogic	8.3
GraphPad Prism	9.1.2
ICE	1.0.9.8
Image Studio software	2.0
ImageJ	1.53e
Intas Gel Doc	0.2.14
Snap Gene	4.1.9
ZEN 2 (blue edition)	2.0.0.0

4.1.12 Synthetic oligonucleotides

4.1.12.1 siRNAs

Table 18: siRNAs

siRNA	Supplier	Order number	Sequence
AllStar neg. control	Qiagen	SI03650318	proprietary
ON-TARGETplus HDAC3 (human)	Dharmacon	J-003496-09	AAAGCGAUGUGGAGAUUUA
ON-TARGETplus SMARTpool GPS2 (human)	Dharmacon	M-004329-01	UGACAGAGCCAAACAAAUG GCGCUGCACCGGCACAUUA GCGAUUCUACCACAAGUGA UGGAUAAGAUGAUGGAACA
ON-TARGETplus SMARTpool NCoR1 (human)	Dharmacon	L-003518-00	GCACACGGCCGAUAAUUGA GCACUUAUUUGACUUCUCA GGAAAGUCCUCCAUACGA GCUGAGGGCUUCUGCAAGAU
ON-TARGETplus SMARTpool NCoR2 (human)	Dharmacon	L-020145-01	GCGAUGCGGAAGAAGCUAA GGCAGUAUCAUGAGAACAU AGGCAUCCCAGGACCGAAA CAGCCAGGGAAGACGCAAA
ON-TARGETplus SMARTpool Ncor1 (mouse)	Dharmacon	L-058556-00	GCAGUGGAAGGAAGUAUAA GAAAUCCCACGGCAAGAUA CAACAACUCAGGUAAUCA CCAGGUCGAUGACAAGUGA
ON-TARGETplus SMARTpool Ncor2 (mouse)	Dharmacon	L-045364-00	GGCAAAGCCCACUGACUUA GCAUGAGGUUUCUGAGAUC GAAUGAGGUUCCCAGAGUU GUACCCACCUUACCUCAUC
TBL1XR1 FlexiTube siRNA (human)	Qiagen	SI03025925	TTGTTTGATGGTCGACCAATA

4.1.12.2 Primers

Table 19: Primers

Primer	Sequence 5'-3'
HPV16 E1^E4 3440 R	AGGCGACGGCTTTGGTATG
HPV16 E1^E4 880/3358 F	TGGCTGATCCTGCAGCAGC
HPV16 E4^L1 3503 F	CCCTGCCACACCACTAAGTT
HPV16 E4^L1 5690 R	CTGGGACAGGAGGCAAGTAG
HPV16 E6Star 226/409 F	ACAGTTACTGCGACGTGAGATG
HPV16 E6Star 445 R	TTCTTCAGGACACAGTGG
hsATF3 F	GTGCCGAAACAAGAAGAAGG
hsATF3 R	TGGAGTCCTCCCATTCTGAG
hsCYR61 F	CAACCCTTTACAAGGCCAGA
hsCYR61 R	TGGTCTTGCTGCATTTCTTG
hsHDAC3 E1 F	ACGTGGGCAACTTCCACTAC
hsHDAC3 E3 R	GACTCTTGGTGAAGCCTTGC
hsKRT10 F	CGCCTGGCTTCCTACTTGG
hsKRT10 R	CTGGCGCAGAGCTACCTCA
hsNCOR 1715 F	GAAAGACTGCCAACAGTCAGG
hsNCOR 1883R	CATCGAGAGGTCTCCACAGG
hsPDL1 1F	GTGCCGAAACAAGAAGAAGG
hsPDL1 1R	TGGAGTCCTCCCATTCTGAG
hsPGK1 F	CTGTGGGGGTATTTGAATGG
hsPGK1 R	CTTCCAGGAGCTCCAAACTG
hsSMRT 1428 F	GCACGAGGTGTCAGAGATCA
hsSMRT 1653 R	GAACTTCTCCCGGAAGGTCT
hsTBLR1 E11 F	CCAGCATTGGATGTTGATTG
hsTBLR1 E13 R	ATGTGCTTGCAAATCATGGA
hsULBP1 F	CAACCCTTTACAAGGCCAGA
hsULBP1 R	TGGTCTTGCTGCATTTCTTG
mE1^E4 3312 R	ATGCAGGTTTGTCGTTCTCC
mE1^E4 721 F	CGTCGTACGTGAACCTCAGA
mE4^L1 3295 F	AGAACGACAAACCTGCATCC
mE4^L1 5451 R	TCGTCTGTGCTCTGCACTTT
mE6 7 F	ATCGGCAAAGGCTACACTCTC
mE6 194 R	CTGCGGCACACAATACAAGC
mE7 491 F	GTGAGCCTGACCTACCCGAT
mE7 622 R	GTCGCAGCAAAAGCAGGTTG
mE8E2 1055 F	GAAAGAGCAGGAGACGGTTG

Table 19: Primers (continued)

Primer	**Sequence 5'-3'**
mE8^E2 3169 R	TTTTTGATGCCCTTCTTTGG
mE8^E2 3312 R	ATGCAGGTTTGTCGTTCTCC
mNcor1 F	CTGGTCTTTCAGCCACCATT
mNcor1 R	CCTTCATTGGATCCTCCATC
mPGK1 F	GAAGGGAAGGGAAAAGATGC
mPGK1 R	TCAAAAATCCACCAGCCTTC
mSmrt F	GGGTAAATATGACCAGTGGGAAGAG
mSmrt R	TGGCATTCAGAGGGTTAAAAGC
mURR^E4 3169 R	TTTTTGATGCCCTTCTTTGG
mURR^E4 7138 F	TCTGTTGGCTGTGTGCTCTC
Mycoplasma PCR F	CCAGACTCCTACGGGAGGCA
Mycoplasma PCR R	TGCGAGCATACTACTCAGGC

4.2 Methods

4.2.1 DNA methods

4.2.1.1 Agarose gel electrophoresis

To separate nucleic acids according to their size, agarose gels were prepared with 0.7 % to 2 % of agarose in TAE buffer and ethidium bromide, and placed in TAE buffer for electrophoresis. In order to determine fragment size, an Invitrogen 1 Kb Plus DNA ladder was used as standard. Samples were loaded with DNA loading buffer and gels were run at 90 V for 30-60 min followed by analysis with the Intas Gel iX20 Imager imaging system.

4.2.1.2 Restriction digest

For restriction digest, nucleic acids were incubated with a mixture of enzyme, buffer and additives according to the manufacturer's instructions and incubated for 1 hour or 15 min for fast digest enzymes. The reaction was stopped by incubation at 65 $^{\circ}\mathrm{C}$ or 80 $^{\circ}\mathrm{C}$ for 20 min, depending on the applied enzyme. Agarose gel electrophoresis was performed to confirm successful digestion.

4.2.1.3 Isolation of DNA after electrophoretic separation

Purification of DNA after digestion of plasmid DNA with restriction enzymes or after amplification of DNA via PCR was done by electrophoretic separation followed by recovery of the nucleic acid from the agarose gel with the QIAquick® Gel Extraction Kit (Qiagen) according to the manufacturer's instructions.

4.2.1.4 Quantification of nucleic acids

Concentration of nucleic acids was measured with the NanoDrop reader, using the respective dissolvent for blanking. Purity was determined by the ratio of absorbance at 260 nm and 280 nm with 1.8 for pure DNA and 2.0 for pure RNA. If necessary, samples were diluted to obtain reliable results.

4.2.1.5 Hybridization of oligonucleotides

The oligonucleotide pairs were diluted to a final concentration of 1 µg/ µl. 12.5 µl of each oligonucleotide were mixed with 25 µl 2x annealing buffer. The following hybridization protocol was used by default (Table 20).

Table 20: Hybridization steps of oligonucleotides

Temperature	Time
95 °C	5 min
70 °C	10 min
0.1 °C/s	to 60 °C
60 °C	10 min
0.1 °C/s	to 50 °C
50 °C	10 min
0.1 °C/s	to 40 °C
40 °C	10 min
0.1 °C/s	to 25 °C
25 °C	10 min
0.1 °C/s	to 4 °C
4 °C	∞

4.2.1.6 Polymerase chain reaction (PCR)

To amplify DNA, PCR was performed in a 50 µl mix containing the following reagents:

Table 21: PCR reagents and amounts

Reagent	Amount
10 x PCR-buffer	5 µl
dNTPs	4 µl
Forward Primer (1µM)	2.5 µl
Reverse Primer (1µM)	2.5 µl
Template	2 µl
Polymerase	0.25 µl
USF-H_2O	33.75 µl

The following amplification program was used by default:

Table 22: PCR cycler program

Step	Temp. (in °C)	Duration (in min)	Cycles
Initial denaturation	95	5	1
Denaturation	95	1	
Annealing	55	1	35
Elongation	72	1	
Terminal elongation	72	10	1

4.2.1.7 Sequencing

All newly generated plasmid DNAs were sequenced before being used for the first time. This was done by sanger sequencing performed by the Eurofins Scientific SE/ GATC Biotech AG (Luxemburg).

4.2.1.8 Molecular cloning

Ligation of DNA fragments, eluted from agarose gels, with linearized vectors was performed using the rapid DNA ligation kit (Fermentas) according to the manufacturer's instructions. The circular plasmids generated were subsequently transformed into competent E.coli.

4.2.1.9 Isolation of low molecular weight DNA from mammalian cells

Cells were washed with PBS, then scarped of the 100 mm dish and centrifuged for 20s at 4 °C and 14,000 rpm. The pellet was resuspended in 1ml lysis buffer (400 mM NaCl, 20 mM Tris-HCl [pH 7.5], 5 mM EDTA pH 8) and proteinase K and SDS was added to a final concentration of 50 µg/ml and 0,2% respectively. After shaking for several hours at 55 °C, NaCl was added to a final concentration of 1M and incubation overnight at 4 °C. The next morning samples were centrifuged for 1h at 4 °C and 1,4000 rpm. Next, a phenol–chloroform extraction was performed. RNase A (50 µg/ml) was added to the aqueous phase and incubated at 55 °C for one hour. The second phenol-chloroform extraction was then performed, and 250% sample volume of ethanol and 10% sample volume of sodium acetate were added last to the aqueous phase and incubated overnight (16-18 h) at -20 °C. The next day, the sample was centrifuged at 20,000 rcf for one hour. The supernatant was discarded and the pellet was washed twice with 1 ml of 70% ethanol. The pellet was air dried, resuspended in 50 µl H_2O, and DNA concentration and purity were determined using the nanodrop. DNA from organotypic cell cultures for analysis in multiplex qRT-PCR was isolated using the EZ1 DNA Tissue Kit (Qiagen). For this, 190 µl of proteinase K buffer and 10 µl of proteinase K were first added to the tissue and incubated overnight at 65 °C in a shaker. The DNA was then isolated using the BioRobot EZ1 workstation and the corresponding EZ1 DNA Tissue Kit (Qiagen) according to the manufacturer's instructions.

4.2.1.10 Exonuclease V resistance assay

The assay was adapted from Myers et al., 2019, with minor modifications: total cellular DNA (100 ng) was incubated in the presence or absence of 5 U exonuclease V (NEB M0345S) in 1× NEBuffer 4 supplemented with 1 mM ATP for 60 min at 37 °C. Then, the enzyme was inactivated for 10 min at 95 °C. Finally, 10 ng input DNA was measured by qPCR using primers for HPV16 *E2* and *ACTB*.

4.2.2 RNA methods

4.2.2.1 Isolation of total RNA from mammalian cells

To isolate total RNA from cells the RNeasy® mini kit from Qiagen was utilized. As a first step, cells were harvested by adding RLT buffer with beta-mercaptoethanol directly to the wells. Afterwards the cell lysate was passed through QIAshredder® columns (2 min, 21130 rcf, room temperature) to homogenize the sample and remove insoluble cell debris. RNA isolation was then carried out as described in the manual of the kit. The total RNA was eluted in 50 µl of RNase-free water and concentration as well as purity was determined using the NanoDrop 2000 spectrophotometer. Only RNA with a 260/280 ratio of 2.0-2.2 was used for cDNA synthesis. To allow detection of *E6* and *E7* transcripts in transiently transfected cells, mRNA was enriched from total RNA using the RNeasy Pure mRNA bead kit (Qiagen) according to the manufacturer's instruction.

4.2.2.2 Synthesis of complementary DNA (cDNA)

The isolated RNA was subsequently reverse-transcribed to cDNA using the QuantiTect® reverse transcription kit from Qiagen according to the manufacturer's instructions. The prepared cDNA was diluted with RNase-free water to yield a concentration of 5 ng/ µl.

4.2.2.3 Quantitative real-time PCR (qPCR)

Relative quantification of transcription levels was conducted via quantitative real-time PCR using 25 ng of cDNA. cDNA was analyzed in duplicates by qPCR for viral and cellular transcripts using Light-Cycler 480 SYBR green I master mix (Roche Applied Science) and 0.3 µM of the respective primers. All ingredients except the cDNA were prepared as a master mix and stored on ice until usage. The master mix was distributed on a 96 well plate, cDNA was then added. Amplification was performed using the LightCycler 480 and the following program.

Table 23: qPCR cycler program

Step	Temp. (in °C)	Duration	Cycles
Initial denaturation	95	15 min	1
Denaturation	95	15 s	
Annealing/elongation	60	1 min	40
Melt curve	95	15 s	
	60	1 min	
	0.05 °C/s		

The standard SYBR green program of software version 1.5 (Roche Applied Science) was used for cDNA quantification, the second derivate/max analysis was chosen to obtain crossing point values, and melting curves were analyzed to ensure measurement of a single amplicon. The

CP value corresponds to the cycle at which the fluorescence first stands out significantly from the background fluorescence. Afterwards, crossing point values were converted to fold induction compared to the respective control according to Pfaffl, 2001 and *PGK1* as the reference gene transcript, in order to compare different samples and experiments. Copy numbers were determined by plasmid standards run in parallel.

4.2.2.4 Multiplex qPCR

HPV16 copy numbers were quantified in total cellular DNA by multiplex qPCR, which allows the simultaneous determination of HPV16 E2 and the reference gene *ACTB* in one sample. The reaction was prepared in a 96 well plate according to the following scheme:

Table 24: Multiplex qPCR master mix

Component	Amount
DNA (10ng/µl)	2 µl
Fast advanced master mix (10x)	10 µl
Oligonucleotide probe mix (4 µM)	3 µl
H_2O	5 µl

The analysis was performed under the following conditions in the LightCycler 480:

Table 25: Multiplex qPCR cycler program

Temp. (in °C)	Duration	Cycles
95	15 min	1
56	10 s	
72	5 s	45

Color compensation for the VIC, Cy5, and FAM dyes was performed and saved previously (Manawapat-Klopfer, 2013) and could therefore be applied to all multiplex qRT-PCR experiments. To determine the efficiency of oligonucleotide-probe pairs, dilution series of a plasmid containing the HPV16 genome (10^7 copies - 10^1 copy in 1:10 dilution steps) and DNA of human primary keratinocytes (20 ng/µl - 2 pg/µl DNA in 1:2 dilution steps) were prepared. The dilution series were measured using the three pairs of oligonucleotide probes. The determined standard curve was saved and could be applied to all multiplex experiments by carrying a calibrator. Samples were measured in duplicates in each case. Measurement of the reference gene *beta-actin* allowed calculation of the absolute cell number per µl of sample . For this purpose, the amount of genomic DNA (ng) in the sample was divided by the weight of one genome equivalent (6.6 pg/cell). The viral load in the sample was calculated as the number of HPV16 *E2* copies per cell.

4.2.2.5 RNA-Seq and data analysis

Total RNA was isolated from two independently grown organotypic cultures per cell line from HPV16 wt or E8- cell lines from two different donors (Straub et al., 2014). The Institute for Medical Genetics and Applied Genomics (IMGAG) was responsible for NGS data generation and the QBiC at the University of Tübingen for data analysis, long term data storage and management. Raw sequencing data was generated at IMGAG with libraries prepared using the TruSeq Stranded mRNA Library Preparation Kit and samples eventually sequenced on a Hiseq2500 using 1x 65 bp read length (single-end (SE)). Illumina's Casava software was used to de-multiplex the sequenced reads providing individual raw fastq sample files. Raw fastq files was pre-filtered using the chastity filter to remove reads that contain a "Y" flag. FastQC (http://www.bioinformatics.babraham.ac.uk/projects/fastqc/, version v0.11.4) was then used to determine quality of the resulting fastq files. Subsequently adapter trimming/removal process was conducted with Cutadapt (https://pypi.python.org/pypi/cutadapt/), version 1.8.3). This step used FastQC output (see step before) to identify reads that showed a match to some typical overrepresented (Illumina) sequences/adapters. TopHat2 (https://ccb.jhu.edu/software/tophat/index.shtml,version v2.0.12) was used as aligner to map the quality controlled remaining reads to the human genome version hg19, downloaded from UCSC. Read counting to features (e.g. genes or exons) in the genome was performed with HTSeq (http://www-huber.embl.de/users/anders/HTSeq/doc/count.html, version 0.6.0.). Counting was performed using "union' mode on the feature"gene_id" where each gene is considered here as the union of all its exon counts. The stranded option was also set to "–stranded=no" to indicate to count features on both strands. For differential expression analysis the raw read count table outputted from HTSeq was used and fed into the R package DESeq2 (version 1.10.1) to analyze for statistical significant differential expression of genes between the two experimental groups mutant and wt. Genes were considered differentially expressed if the p-adjusted value was $\geqslant$ 0.05. No logFold change cut-off was applied during assessment of DE analysis. Further exploratory analysis graphs were also produced in the R language (R version 3.2.1) mainly using the R package ggplot2 (version 2.1.0). Reports in .html format were produced using the R package rmarkdown (version 0.9.6). Gene set enrichment analysis was performed with g:Profiler (Version e107_eg54_p17_bf42210) with g:SCS multiple testing correction (Raudvere et al., 2019). For this functional enrichment analysis, also known as over-representation analysis (ORA), genes are mapped to known functional information sources and statistically significantly enriched terms are detected. Data from the Ensembl database (Cunningham et al., 2022) is used, in addition to data from Gene Ontology (Dolinski et al., 2000; Consortium, 2021; Mi et al., 2019), pathways from KEGG (Kyoto Encyclopedia of Genes and Genomes; Kanehisa and Goto, 2000; Kanehisa et al., 2023; Sun et al., 2015), Reactome (Fabregat et al., 2018) and WikiPathways (Martens et al., 2021), miRNA targets from miRTarBase (Huang et al., 2022) and regulatory motif matches from TRANSFAC (Matys et al., 2006), tissue specificity from Human Protein Atlas (Uhlén et al., 2015), protein complexes from CORUM (Tsit-

siridis et al., 2023) and human disease phenotypes from Human Phenotype Ontology (Köhler et al., 2021).

4.2.3 Microbiological methods

4.2.3.1 Production of chemical competent bacteria

To generate competent bacteria that can take up plasmid DNA, bacteria were treated with $CaCl_2$, RbCl and $MnCl_2$. Cells were grown in LB medium overnight, this pre-culture was diluted in fresh LB medium and grown to an OD_{600} of 0.45 to 0.55. Bacteria were then incubated on ice and resuspended in buffers containing calcium, rubidium and manganese, followed by snap-freezing in liquid nitrogen and storage at - 80 $^{\circ}\mathrm{C}$ (Ausubel et al., 1990).

4.2.3.2 Transformation of plasmid DNA

Competent bacteria were transformed with the heat shock method (Ausubel et al., 1990). For that, bacteria were thawed on ice and incubated with DNA for 15 min. Next, a 1 min heat-shock at 42 $^{\circ}\mathrm{C}$ was performed. SOC medium was then added and bacteria were grown for 30 min at 37 $^{\circ}\mathrm{C}$ shaking. Next the SOC/bacteria mix was plated on agar plates containing the selection antibiotic and incubated at 37 $^{\circ}\mathrm{C}$ over night (o/n). The next afternoon, clones were picked and inoculated in LB media containing the selection antibiotic. DNA was isolated the next day and sequence was validated by sequencing.

4.2.3.3 Culture of bacteria for DNA amplification and isolation

To amplify DNA, bacteria harboring the plasmid of interest were cultured in LB media with either 100 µg/ml ampicillin or 30 µg/ml kanamycin, depending on the resistance gene of the respective plasmid. Different amounts of LB media were inoculated from frozen bacteria stocks: 3 ml for a mini prep, 50 ml for a midi prep or 200 ml for a maxi prep, dependent on the quantity of DNA needed. The cultures were grown for 16 to 18h at 37 $^{\circ}\mathrm{C}$ and 130-160 rpm. Frozen bacteria stocks were prepared for long-term storage by mixing bacteria with the same amount of freezing medium and transferring them to -80 $^{\circ}\mathrm{C}$.

4.2.3.4 Preparative isolation of plasmid DNA from bacteria

Isolation of plasmid DNA from bacteria was performed using different Qiagen kits depending on the amount of DNA needed. The QIAprep® spin miniprep kit was used to isolate small amounts of plasmid DNA, for larger amounts the QIAgen® plasmid plus midi kit or the QIAgen® plasmid plus maxi kit were used. All kits were used as described in the manufacturer's instructions. Concentration of DNA were measured with the NanoDrop reader, purity was determined by the ratio of absorbance at 260 nm and 280 nm with 1.8 for pure DNA.

4.2.4 Cell culture methods

4.2.4.1 Culture of cells

All cells were grown in Nunc cell culture dishes in a humidified incubator (95% relative humidity) at 37 °C and 5% CO_2. Cells were examined microscopically every other day to determine cell density and morphology. The media was then either exchanged with fresh medium or cells were distributed to new dishes. To passage cells, the media was aspirated and PBS was used to wash away remnants of the medium and dead cells. Trypsin-EDTA was then used to detach cells at 37 °C. Cells were then collected in serum-containing medium to inactivate trypsin and distributed to new dishes. Since keratinocytes are cultivated in serum-free medium, an additional centrifugation step (250 rcf, 5 min) to pellet the cells was performed followed by the resuspension in KSFM and distribution to new dishes. Depending on the cell type, cells were passaged in a ratio of 1:2 up to 1:10.

4.2.4.2 Freezing and thawing of mammalian cells

For long-term storage, cells were kept in liquid nitrogen. Cells were trypsinized, resuspended in serum-containing medium and collected by centrifuging at 250 rcf for 5 min. Afterwards, the pellet was resuspended in 2 ml of freezing medium per 100mm dish and distributed to two cryo tubes. The cryo tubes were placed into a freezing container and immediately transferred to -80 °C. The next day, cells were moved to the liquid nitrogen tank. Freezing media were chosen depending on cell type and consisted of 10% [v/v] DMSO (for J2, NHK and HeLa) or 20% [v/v] glycerol (for HPV genome containing NHK), 10% [v/v] of the preferred serum (CS, FCS) in their standard media. For thawing cells, they were removed from liquid nitrogen, thawed in the 37 °C water bath and immediately transferred to 10 ml of 37 °C warm medium. To remove the remnants of DMSO or glycerol the media was changed the next day.

4.2.4.3 Test for mycoplasma contamination

Cell lines were checked regularly for mycoplasma contamination. The supernatant of cells grown in antibiotic-free medium for at least 48 h was used for a mycoplasma test PCR. After heating the supernatant at 95 °C for 5 min, it was used as a template for the PCR. The following reaction was prepared for the samples in addition to a negative (H_2O) control and a positive control (Table 26). The PCR was run according to the program in table 27. Afterwards, the PCR products were analyzed on a 1% agarose gel. A DNA band at 560 bp indicates the presence of mycoplasma.

Table 26: Mycoplasma PCR reagents and amounts

Reagent	Amount
5x GoTaq Green Reaction Buffer (Promega)	10 µl
dNTPs (10 mM each)	1 µl
Mycoplasma F and R (10 µM), each	2.5 µl
Culture supernatant or H_2O or positive control	1 µl
GoTaq Polymerase (Promega)	0.25 µl
H_2O	32.75 µl

Table 27: Mycoplasma PCR cycler program

Step	Temp. (in $^\circ$C)	Duration	Cycles
Initial denaturation	95	5 min	1
Denaturation	95	20 s	
Annealing	65	20 s	35
Elongation	72	20 s	
Terminal elongation	72	2 min	1

4.2.4.4 Transfection of cells

For transfection of DNA into human cells, cells were seeded on cell culture dishes one day prior to transfection. Transfection was always performed with the complexing agent FuGENE HD (Promega) according to the manufacturer's instructions. In a sterile polystyrene (PS) tube OptiMEM was mixed with the DNA and FuGENE HD was then added in a 5:2 ratio (5 µl FuGENE to 2 µg DNA). The transfection mixture was vortexed and incubated for 15 min at room temperature. Meanwhile, the medium of the cells to be transfected was changed. After incubation, the transfection mixture was added drop wise to the cells. After 24 hours, the medium of the transfected cells was changed again and 48 hours after transfection, the cells were harvested or the corresponding analysis was performed.

4.2.4.5 Harvest of cells

First, feeder cells were removed prior to the harvest by thoroughly washing with PBS or addition of versene (1x PBS with 0.5 mM EDTA), which was removed by washing trice with PBS. To prepare whole cell extracts, the growth medium was removed, the cells were washed with PBS, fresh PBS was added and cells were scraped off the dish with a cell lifter and centrifuged at 4 $^\circ$C to collect them. For subsequent RNA extraction RLT buffer from the RNeasy® mini kit

(Qiagen), supplemented with 1% [v/v] beta-mercaptoethanol, was added directly to the cells, leading to their detachment.

4.2.4.6 Mitomycin C treatment of feeder cells

Before using fibroblasts as feeder cells for keratinocytes carrying viral genomes, they are treated with mitomycin C, which interferes with the formation of the spindle apparatus and inhibits cell division, resulting non-proliferative fibroblasts that are still viable and can support keratinocyte growth but cannot overgrow the keratinocyte population anymore (Blacker et al., 1987). Murine J2 cells, which are kept in DMEM-CS, were treated with 8 µg/ml mitomycin C (stock: 400 µg/ml in PBS) for 1 to 2 h and then thoroughly washed with PBS to remove remnants of the cytostatic agent. For co-cultures the fibroblasts were cultivated in E-medium supplemented with FCS.

4.2.4.7 Isolation of normal human keratinocytes (NHK) from human foreskin

After routine circumcision upon informed consent of patients, tissue samples were collected in PBS. The samples were then rinsed once with PBS and covered with fresh PBS for the preparation procedure under the cell culture hood. After removing the underlying blood vessels and fat tissue with sterile tweezers and scissors, the remaining keratinocyte layer was cut into small pieces, transferred into a 60 mm cell culture dish and covered with 5 ml of dispase. After incubation for 12-16 hours at 4 $^{\circ}\mathrm{C}$, the upper layer of the skin could be detached and cut into small pieces and was then transferred into trypsin-EDTA in a 100 mm cell culture dish. The 10 min incubation at 37 $^{\circ}\mathrm{C}$ was followed by the resuspension of cells in serum-containing medium and passing them through a 100 µm nylon cell strainer. Single cells were then collected by centrifugation at 250 rcf for 5 min and resuspended in KSFM. The isolated keratinocytes were seeded in one or two coated cell culture dishes (Corning Primaria) and grown until near-confluency.

4.2.4.8 Generation of HPV16 positive keratinocyte cell lines

For the establishment of stable HPV16 positive NHK cells, a plasmid containing the HPV16 genome was first cleaved with BamHI to release the viral genome from the bacterial vector. The viral DNA was then purified with an agarose gel, and the DNA was subjected to overnight religation at 16 $^{\circ}\mathrm{C}$ using T4 DNA ligase (10 µg/ml, Fermentas). To concentrate the DNA, the next day 2.5 times sample volume of ethanol and 10% sample volume of sodium acetate were added to samples and incubated overnight (16-18 h) at -20 $^{\circ}\mathrm{C}$. The next day, the samples were centrifuged at 20,000 g for one hour, the supernatant was discarded, and the pellet was washed twice with 1 ml of 70% ethanol. The pellet was air dried and then resuspended in H_2O. NHK cells to be transfected were seeded in KSFM culture medium on 60 mm cell culture dishes and transfected the next day using FuGENE HD (Promega) with 4 µg of religated genome and 2 µg of the selection plasmid pSV2neo, which encodes resistance to G418. Twenty-four hours after

transfection, cells were transferred to 100 mm cell culture dishes containing mitomycin C treated neomycin-resistant 3T3-J2-NHP and E medium. Another 24 hours later, cells were selected with the neomycin analog G418 (100 µg/ml). Selection was performed for approximately one week. Cell culture medium was removed and replaced with fresh medium with added G418 every other day. Uninfected NHK were included as a selection control. After selection was complete, cells were cultured with mitomycin C treated J2.

4.2.4.9 Isolation of normal mouse tail keratinocytes (NMTK)

Tails from mice were stored in ethanol until use and then transferred to a petri dish with PBS, and about 2 mm of the tail tip was discarded. To peel the skin off the bone, a scalpel was used to cut along the tail. The skin was then cut into 1 to 2 cm pieces, and placed with the epidermis side up in a 60 mm petri dish with 10 U dispase (Gibco) overnight in a 4 $^{\circ}\mathrm{C}$ refrigerator. The next day, the epidermis was removed with forceps and incubated in trypsin in a 37 $^{\circ}\mathrm{C}$ incubator. Single cells were scratched out and resuspended in 5 ml DMEM/ 10% FCS, the suspension was passed through to a 100 µm cell strainer. After centrifugation for 5 min at 250 rcf, cells were resuspended in keratinocyte serum-free medium without $CaCl_2$ (catalog no. 37010022; Thermo Scientific) supplemented with 50 mM $CaCl_2$ and seeded in 6-well plates or 60 mm dishes coated with bovine collagen I.

4.2.4.10 Organotypic cultures

To induce differentiation, HPV16-positive keratinocytes were seeded onto collagen plugs (rat tail collagen type I) in which NIH 3T3 J2 cells were embedded in cell culture inserts. After the keratinocytes reached confluence, the medium was completely removed from the inside of the inserts. Inserts were then placed in 100 mm culture dishes, and complete E medium without epidermal growth factor (EGF) was added to the culture dishes and changed every other day. Organotypic cultures were harvested 16 days after exposure to the air-liquid interface. To harvest the organotypic cell cultures, they were excised from the cell culture inserts together with the underlying collagen matrix and the polycarbonate membrane was removed. The epithelium was then peeled away from the collagen matrix. The tissue was lastly cut with a scalpel into smaller pieces for DNA or RNA isolation.

4.2.5 Analysis of eukaryotic cells

4.2.5.1 Western blot analysis

For western blot (WB) analysis, proteins are firstly separated electrophoretically according to their molecular weight under denaturing conditions in a polyacrylamide (PAA) gel and then transferred from the gel onto a membrane. Next, the proteins can be detected by applying antisera or antibodies directed against the proteins of interest.

All WB samples were either directly resuspended in Roti®-Load (Carl Roth, 4x) or lysed with lysis buffer and then supplemented with Roti®-Load to yield an at least 1x concentrated Roti®-Load suspension. The samples were stored at -20 °C and were heated at 95 °C for 5 min before usage. To shear the viscous DNA, samples were sonified using the SonoPuls Sonifier UW 2200 (Bandelin) for 15s with 40% power before loading them on a PAA gel.

Protein extracts were separated in a one-dimensional polyacrylamide gel electrophoresis (SDS-PAGE). The stacking gel contained 4% PAA, the separation gel 8-15% PAA, depending on the size of the proteins to be analyzed. The PageRuler prestained protein ladder (Thermo Fisher) was included as a size standard in each electrophoresis. The PAGE was conducted in 1x SDS-PAGE running buffer at 160-200V for 45-90 min.

The separated proteins were then transferred to a nitrocellulose membrane with a pore size of 0.22 µm (Whatman plc) using the wet blot technique. All items used for the blotting sandwich were soaked in freshly prepared CAPS transfer buffer and assembled, starting from the cathode as following: - sponge - two blotting papers - gel - membrane - two blotting papers - sponge. The transfer was carried out at 90V for 90 min using a cooling coil and a magnetic stirrer. The membrane was then incubated with blocking buffer (milk powder or BSA in PBS depending on antibody) and gently moved for 30-60min to reduce unspecific binding. Afterwards, the blocking buffer was washed away and the membrane was incubated overnight with the primary antibodies at 4 °C shaking. The next day, 3x5 min washing steps with PBS-T were performed, followed by 1 h of incubation with the secondary, fluorescence-labeled antibodies (LI-COR, 1:15000) in the dark. After 3 more 5 min washing steps, protein bands were detected using the Odyssey® Fc imaging system (LI-COR Biosciences).

4.2.5.2 Coomassie staining of SDS gels

In addition to immunological detection, separated proteins were also detected directly by staining SDS gels with coomassie. For this purpose, the SDS gel was incubated in a coomassie staining solution (0.05% [w/v] coomassie brilliant blue R-250, 10% [v/v] acetic acid, 25% [v/v] isopropanol) for 20 to 30 min at RT. Subsequently, the SDS gel was destained for at least one hour with a destaining solution (10% [v/v] acetic acid). The stained SDS gels were then scanned for documentation.

4.2.5.3 Co-immunoprecipitation (Co-IP)

C33A or HeLa (2.5 x 10^6 cells) were seeded in 100 mm cell culture dishes. The next day they were transfected, 48h later they were harvested and then lysed in IP-buffer (50 mM HEPES [pH 7.5], 150 mM NaCl, 10% [v/v] glycerol, 5 mM EDTA, 1 mM DTT, protease and phosphatase inhibitors or 50 mM HEPES [pH 7.9], 150 mM NaCl, 0.3% [v/v] igepal 630, 1 mM DTT, protease and phosphatase inhibitors). IP was carried out using magnetic anti-HA-beads or protein G-beads (Miltenyi Biotech). Beads were washed with IP-buffer using µMACS columns and µMACS Separator (Miltenyi Biotech). Bound proteins were eluted in elution buffer (50 mM Tris-HCl [pH 6.8], 50 mM DTT, 1% SDS, 1 mM EDTA, 0.005% bromphenol blue, 10% glycerol) heated to 95 $^{\circ}\mathrm{C}$ and analyzed by immunoblotting.

4.2.5.4 Immunofluorescence (IF)

For IF analyses cells were seeded on coverslips in 6 well plates and transfected with expression plasmids for the protein of interest the next day or left untransfected for endogenous proteins. Cells were fixed 48h later by addition of 4% paraformaldehyde and incubated for 15 min at room temperature. Afterwards, cells were washed three times with PBS and blocked with blocking buffer (1 x PBS, 5% [v/v] normal goat/donkey serum, 0.3% [v/v] triton-X 100) for 1h at RT. After that the primary antibody was diluted in antibody dilution buffer (1x PBS, 1% [w/v] BSA fraction V, 0.3% [v/v] triton-X 100) and incubated at 4 $^{\circ}\mathrm{C}$ overnight. The next day, coverslips were washed three times in PBS and then incubated with the secondary fluorescence labelled antibody for 1h at room-temperature. After three PBS washing steps, the coverslips were incubated in DAPI solution (0.01 µg/mL in 1 x PBS) for 20 s, followed by three more washing steps with PBS and one washing step with H_2O. Afterwards, coverslips were placed on one droplet of mounting medium on a microscope slide and fixed using nail varnish. The prepared slides were analyzed with the fluorescence microscope Axio Observer.Z1 (Zeiss). Colocalization was quantified with the Colco2 plugin from ImageJ.

4.2.5.5 Reporter gene assays

C33A or NMTK were seeded into 24-well dishes one day before transfection. Cells were transfected with reporter plasmids alone or together with pSG HPV16 E1, pSG HPV16 E2, pSG MmuPV1 E8^E2, or MmuPV1E8^E2 mt expression constructs or the empty vector pSG5 using the Fugene HD reagent (Promega) and Opti-MEM (Life Technologies). Furthermore, 10 ng of renilla plasmid was cotransfected as an internal control. Renilla and firefly luciferase assays were carried out 48 h after transfection. No delay before measurement and a counting time of 5 s was used.

4.2.5.6 Flow cytometry analysis (FCA)

After trypsinization, the cells were centrifuged for 5 min at 600 rcf and the supernatant was discarded. All following centrifugation steps were performed with 600 rcf for 5 min unless otherwise stated. The pellet was then resuspended in FCA buffer and centrifuged, the supernatant was discarded. The cells were fixed with 4% PFA for 10 min at 37℃ shaking and centrifuged for 10 min at 600 rcf. The pellet was resuspended in FCA buffer (1x PBS and 1% FCS) and centrifuged. To permeabilize the cells, the pellet was resuspended in 100 µl of permeabilization buffer (FCA buffer + 0.1% triton-X-100), after incubation at RT for 5 min, the cells were washed twice with FCA buffer. After centrifuging, the pellet was resuspended in 150 µl blocking buffer (FCA buffer + 10% FCS) and incubated at RT for 30min. Cells were then centrifuged again and the primary antibody was added in FCA buffer and incubated for 1h at 4 $^{\circ}\mathrm{C}$ (rabbit-anti-E4, 1:200, 100 µl total volume). After that, the cells were washed twice in FCA buffer, stained with the secondary antibody (anti-rabbit-AF405, 1:1000) for 1h at 4 $^{\circ}\mathrm{C}$ and washed again before PI staining. The PI solution (working concentration 50 µg/ml) was supplemented with 0.33 mg/ml RNAse A and incubated for 30min at 37 $^{\circ}\mathrm{C}$. Cells were then analyzed with MACS Quant Analyzer VYB Flow Cytometer (Miltenyi Biotec).

4.2.6 Expression and purification of HPV16 E2 for antibody production

4.2.6.1 Test expression in E. coli

A fragment encompassing the codon optimized HPV16 E2 fragment as a His_6-MBP-TEV-HPV16 E2C co fusion protein (E2 hinge aa202-286, DBD/Dimerization aa286-365) was cloned in pETm41. The plasmid was transformed in *Escherichia coli* strain BL21(DE3), which was cultured at 37 $^{\circ}\mathrm{C}$ and 130 rpm o/n in 20 ml TB medium (24 g/L yeast extract, 12 g/L peptone, 0.4% [v/v] glycerol, 5 g/L NaCl, 17 mM KH_2PO_4, 72 mM K_2HPO_4, 2 mM $MgSO_4$, 0.05% [w/v] glucose) supplemented with 30 µg/ml kanamycin. The next day, 20 mL TB medium were inoculated with the preculture and incubated at 37 $^{\circ}\mathrm{C}$ and 130 rpm until optical density at 600 nm (OD_{600}) = 0.5 was reached and 1 mM isopropyl beta-d-1 thiogalactopyranoside (IPTG) was added to induce expression of recombinant protein and incubated for 4 h at 37 $^{\circ}\mathrm{C}$. Samples were taken to monitor cell growth according to the OD_{600} and protein expression via SDS-PAGE. After 4 h the culture was harvested (6,000 rcf, 4 $^{\circ}\mathrm{C}$, 20 min). To analyze the solubility of the expressed proteins, the cell pellet was resuspended in 2 ml cell lysis puffer (50 mM Tris-HCl [pH 8 at 8 $^{\circ}\mathrm{C}$], 200 mM NaCl, 5% [v/v] glycerol, 1 mM EDTA) and lysed via ultra-sonification (3 cycles with 30 s ultrasound each, Ms 72, 25% power, SonoPuls UW 2200). To separate the soluble (supernatant) and insoluble (pellet) fraction, the cell lysate was centrifuged at 12,000 rcf, 30 min at 4 $^{\circ}\mathrm{C}$ and analyzed.

4.2.6.2 Expression and purification of HPV16 E2

For purification of recombinant protein, the His_6-MBP-TEV-HPV16 E2C co plasmid was transformed in *E. coli* BL21(DE3) and plated on a LB agar plate with 30 µg/ml kanamycin, a single clone was picked to start an overnight pre-culture, which was then used to inoculate the 4 liter production culture. This culture was grown at 37 °C to an OD_{600} of ~ 0.5 and recombinant-protein production was induced by addition of IPTG. The cells were harvested after 4h (6,000 rcf, 4 °C, 30 min) and the cell pellet was resuspended in 40 ml lysis buffer (40 mM Tris-HCl [pH 8 @ 8 °C], 50 mM NaCl, 3 mM $MgCl_2$, 5% [v/v] glycerol, 1 mM Tris(2-carboxyethyl)phosphine hydrochloride (TCEP)). After resuspending the cell pellet 5 µl benzonase (Merck, 500,000 U, activity $\geqslant$ 250 U/ µl), 3.5 mg/ml lysozyme, and a complete EDTA-free protease inhibitor cocktail pill (Roche, Germany) were added and incubated for 30 min at 4 °C. Cells were lysed by French press (Thermo Spectronic French Pressure Cell Press Model FA-078 With Pressure Cell) in 3 cycles at a pressure of 600-1,000psi. After re-adjusting the pH to 8.0, the suspension was incubated for 1 h at 4 °C and subsequently centrifuged at 30,000 g for 1 h at 4 °C to remove cell debris. The clarified supernatant was filtered with an 0.45 µm syringe filter (Whatman 25 mm Roby Syringe Filters, GE Healthcare, USA) and the recombinant protein was enriched by affinity chromatography with 2 x 5 ml MBP Trap columns in row (Cytiva Life Sciences™ MBP-Trap™HP), and washed with running buffer (40 mM Tris-HCl [pH 8 @ 8 °C], 50 mM NaCl 5% [v/v] glycerol, 3 mM $MgCl_2$, 1 mM TCEP). Bound protein was eluted with elution buffer containing 20 mM maltose, as well as 20 mM Tris-HCl [pH 8 @ 8 °C], 600 mM NaCl, 5% [v/v] glycerol, 1 mM TCEP. The eluted protein was incubated o/n with 600 mM NaCl at 4 °C, followed by size exclusion chromatography (SEC) with a S200 column (HiLoad® 16/600 Superdex® 200 prep grade, GE Healthcare Life Sciences, UK), pre-equilibrated with running buffer (20 mM HEPES [pH 7.5], 600 mM NaCl, 5% [v/v] glycerol, 1 mM TCEP). Protein concentrations were determined spectroscopically (Specord 200, Analytik Jena, Germany).

4.2.6.3 Cleavage of the fusion protein

His_6-MBP-TEV-HPV16 E2C was incubated with tobacco etch virus (TEV) protease in a 1:20 mass ratio (protease:protein) at 4 °C o/n and centrifuged the next day (30,000 rcf, 4 °C, 30 min), the reaction was analyzed by SDS-PAGE. The supernatant was used as input for SEC with a S75 column (HiLoad® 16/600 Superdex® 75 prep grade, GE Healthcare Life Sciences, UK) and a running buffer containing 20 mM HEPES [pH 7.5], 600 mM NaCl, 5% [v/v] glycerol, 1 mM TCEP. The eluate was subsequently concentrated with Pierce™ protein concentrator PES (10K MWCO), followed by a 1ml MBPTrap HP (1ml MBPTrap™HP, Cytiva Life Sciences™) run with the same HEPES running buffer as previously used.

4.2.6.4 Polyclonal antibody production in rabbits

The purified protein was sent to Davids Biotechnology (Regensburg) for polyclonal antibody production in New Zealand white rabbits. Rabbits were immunized five times according to the following schedule (Table 28).

Table 28: Immunization schedule for antibody production

Day	Step
1	First Immunization
14	Second Immunization
28	Third Immunization
42	Fourth Immunization
56	Fifth Immunization
63	Final bleed for Antiserum harvest

The antiserum was then affinity purified by Davids Biotechnology and used for WB, IF and IP assays.

4.2.7 Animal experiments

All animal studies were carried out by Margaret Wong and Richard B.S. Roden (Department of Pathology, The Johns Hopkins University) in accordance with the recommendations in the Guide for the Care and Use of Laboratory Animals of the National Institutes of Health and with the prior approval of the Animal Care and Use Committee of Johns Hopkins University.

4.2.8 Statistical analysis and generation of figures

After processing the results of different experiments as described in the respective section, the calculated values of the single biological replicates were used to do statistical analysis and create graphical representations of the data. This was done using the GraphPad Prism software (GraphPad Software Inc., San Diego, US; software version 9.1.2).
The GraphPad statistics guide (H. J.Motulsky, GraphPad Statistics Guide) was used to decide what statistical test to use.

5 Results

5.1 Deregulation of host gene expression by HPV16 E8^E2 is due to enhanced productive replication

It has previously been shown that HPV16 genomes lacking E8^E2 replicate to higher levels in stable cell lines and express higher levels of early and late transcripts than wt genomes under both undifferentiated and differentiated conditions (Lace et al., 2008; Straub et al., 2014). In differentiated cells HPV16 E8- genomes additionally express increased levels of the late viral E4 and L1 proteins (Straub et al., 2014). The advantage of the expression of E8^E2 for HPV16 remains unclear on the other hand. To further explore this, the cellular transcriptome of HPV16 wt and E8- cell lines from two different donors grown in organotypic cultures were compared. The data discussed in this chapter are published in Kuehner et al., 2023.

5.1.1 RNA sequencing of organotypic cultures

The expression of only 43 cellular genes were significantly deregulated (P adj<0.05) in the RNA-seq analysis. Of those 27 were upregulated and 16 downregulated in HPV16 E8- cell lines (Figure 7 A). Over-representation analysis (ORA) or gene set enrichment analysis, maps genes to known functional information sources and detects statistically significantly enriched terms (Raudvere et al., 2019). Gene set enrichment analyses with g:Profiler identified only the hypertrophy and the photodynamic therapy-induced unfolded protein response pathways as significantly enriched, most likely due to the small number of differentially expressed genes (Figure 7 B). Neither keratinocyte differentiation genes, cell cycle nor DNA replication genes were deregulated, which confirms previous observations that HPV16 E8- cell lines lack changes in differentiation patterns or induction of cell cycle and DNA replication markers despite increased early and late viral transcription (Straub et al., 2014).

A

gene_ID	log2 FC	padj	gene_ID	log2 FC	padj
ACSL4	0.76	3.49E-02	*AQP5*	-1.14	4.63E-02
ANKRD1	2.00	1.83E-06	*BAIAP2-AS1*	-0.73	1.68E-02
ASNS	1.33	1.89E-02	*BIN2*	-1.13	4.63E-02
ATF3	1.25	3.61E-04	*CAPS*	-1.28	2.04E-02
AUNIP	0.92	3.68E-03	*CPTP*	-1.05	2.85E-02
CD274	1.14	1.62E-04	*CRNN*	-0.80	1.46E-02
CXCL3	1.23	3.23E-02	*DMBT1*	-1.42	7.43E-03
CYR61	1.50	8.65E-04	*EEF1A2*	-1.09	1.70E-03
DSCAM	1.55	1.72E-03	*METRN*	-1.22	3.26E-02
FLNC	1.97	1.59E-06	*PPP1R1B*	-1.25	2.18E-02
HOXD8	0.91	4.63E-02	*RHOD*	-0.76	2.48E-03
INHBE	1.59	9.65E-04	*RIN3*	-0.74	4.15E-02
KBTBD8	1.30	8.65E-04	*RNF225*	-1.23	4.15E-02
KCTD12	0.93	1.72E-03	*SYDE1*	-1.18	1.46E-02
KRTAP2-3	2.36	1.29E-09	*TNFSF9*	-0.95	4.76E-02
LOC100134391	1.29	2.25E-02	*TTYH3*	-1.03	4.15E-02
M1AP	1.25	2.23E-02			
PLCXD2	1.19	2.84E-02			
PLCXD2-AS1	1.56	1.62E-03			
RND1	1.32	3.61E-04			
ROCK1P1	2.13	1.19E-07			
SH2D5	1.11	2.04E-02			
SNHG20	1.13	4.15E-02			
SPX	1.51	1.79E-03			
SULT1E1	0.95	3.34E-04			
TTTY15	0.68	3.91E-02			
ULBP1	2.11	1.29E-09			

B

source	term_name	term_id	adjusted p value	intersections
WP	Hypertrophy model	WP:WP516	0.001	*ANKRD1. CYR61.ATF3*
WP	Photodynamic therapy-induced unfolded protein response	WP:WP3613	0.003	*ASNS.ATF3. SULT1E1*

Figure 7: Differential host cell gene expression of HPV16 wt and E8- cell lines grown in organotypic cultures. (**A**) RNA-seq analysis identified 27 upregulated (left table, red) and 16 downregulated (right table, blue) genes with an adjusted P-value (padj) <0.05; log2FC= log2 fold change by comparison of HPV16 E8- with wt cell lines. (**B**) Gene set enrichment analysis was performed with g:Profiler (Raudvere et al., 2019) with g:SCS multiple testing correction method applying a significance threshold of 0.05. Figure from Kuehner et al., 2023.

5.1.2 Analysis of copy number and integration frequency of wt and E8- cell lines

NHK from different donors were used to generate cell lines by transfection with recircularized HPV16 wt or E8- genomes and selection to validate these findings. Viral copy numbers were increased in E8- cell lines compared to the wt (Figure 8 A), which supports previous results (Straub et al., 2014). The extrachromosomal HPV16 genome fraction, resistant to exonuclease V digestion (Myers et al., 2019), was similar in wt (38%) and E8- cell lines (34%) indicating that E8^E2 does not influence integration events (Figure 8 B).

Quantification of spliced viral transcripts revealed significant increase of *E1^E4* and *E4^L1* in undifferentiated HPV16 E8- cell lines compared to the wt. Both transcripts were further increased in organotypic cultures (Figure 8 C+D) consistent with previously published data (Straub et al., 2014). Increased amounts of both transcripts in organotypic cultures indicates the successful induction of the productive cycle (Kuehner et al., 2023).

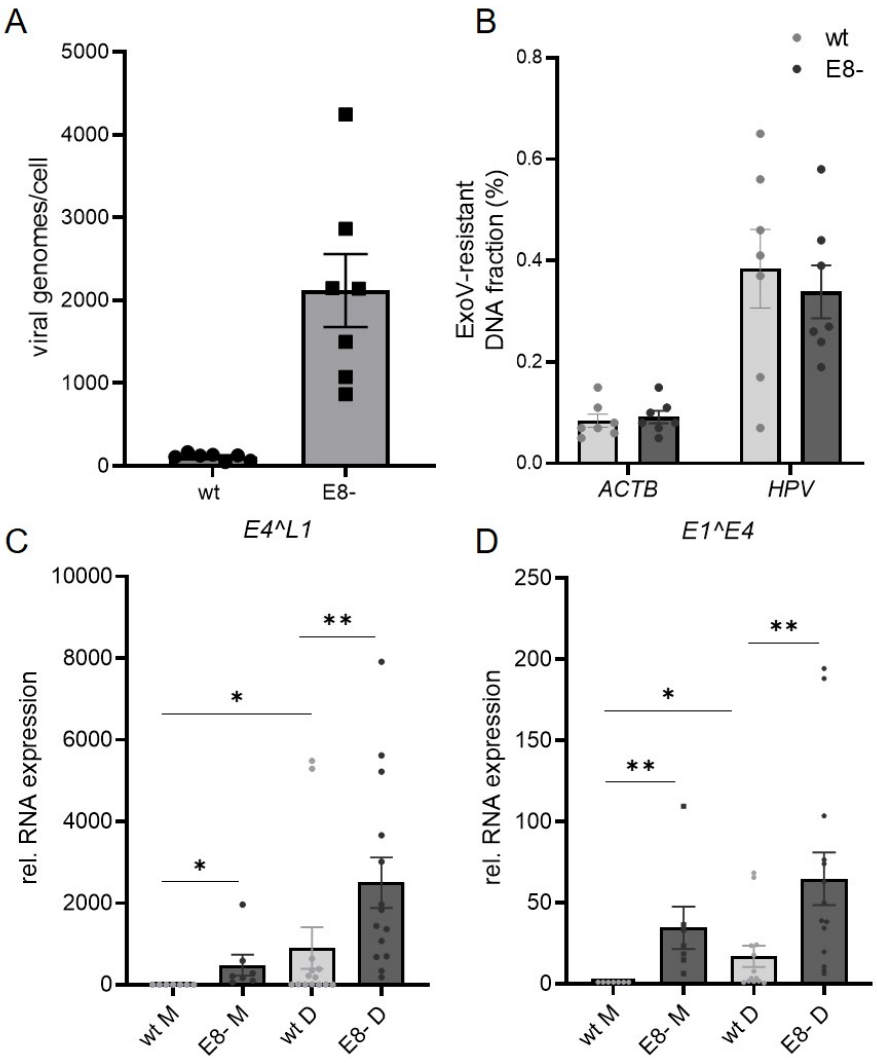

Figure 8: Increased copy number and *E1^E4* as well as *E4^L1* expression in E8- cell lines, but similar integration frequency. (**A**) Total cellular DNA was isolated from HPV16 wt and E8- cell lines and viral copy numbers were determined by qPCR using amplicons in HPV16 *E2* and the cellular *ACTB* genes and copy number standards. (**B**) Total cellular DNA was treated with or without exonuclease V (ExoV) and then the copy numbers were determined by qPCR as described in (A). (**C**+**D**) The spliced viral *E1^E4* and *E4^L1* transcripts were quantified with qPCR in cells grown in monolayer (M) or organotypic (D) cultures using *PGK1* as a cellular reference gene. Data are presented relative to wt cells grown in monolayer cells. Averages are derived from at least seven independent experiments, and the error bars represent the Standard Error of the Mean (SEM). Statistical significance was determined by wilcoxon signed rank test (*, $P \leq 0.05$; **, $P \leq 0.01$).
Figure from Kuehner et al., 2023.

5.1.3 Deregulation of host gene expression after differentiation

Four cellular genes were used to validate the transcriptome data:
The Activating Transcription Factor 3 (*ATF3*) as it is part of both identified enriched pathways. Cysteine-rich Angiogenic Inducer 61 (*CYR61*, also known as *CCN1*) since it belongs to the hypertrophy pathway. Lastly, the immune regulators *CD274* (also known as Programmed Cell Death 1 Ligand 1 (*PDL1*)) and UL16 Binding Protein 1 (*ULBP1*) were chosen for further analysis (Sharpe and Pauken, 2018; Schmiedel and Mandelboim, 2018).
The expression of all four genes was significantly different in qPCR analysis in HPV16 wt compared to E8- cells grown in organotypic cultures confirming the RNA-seq results (Figure 9). Interestingly, no significant differences could be observed between monolayer wt and E8- cells. Furthermore, expression in wt cells grown in monolayer was significantly upregulated for *ATF3* or downregulated for *CYR61* compared to organotypic cultures.

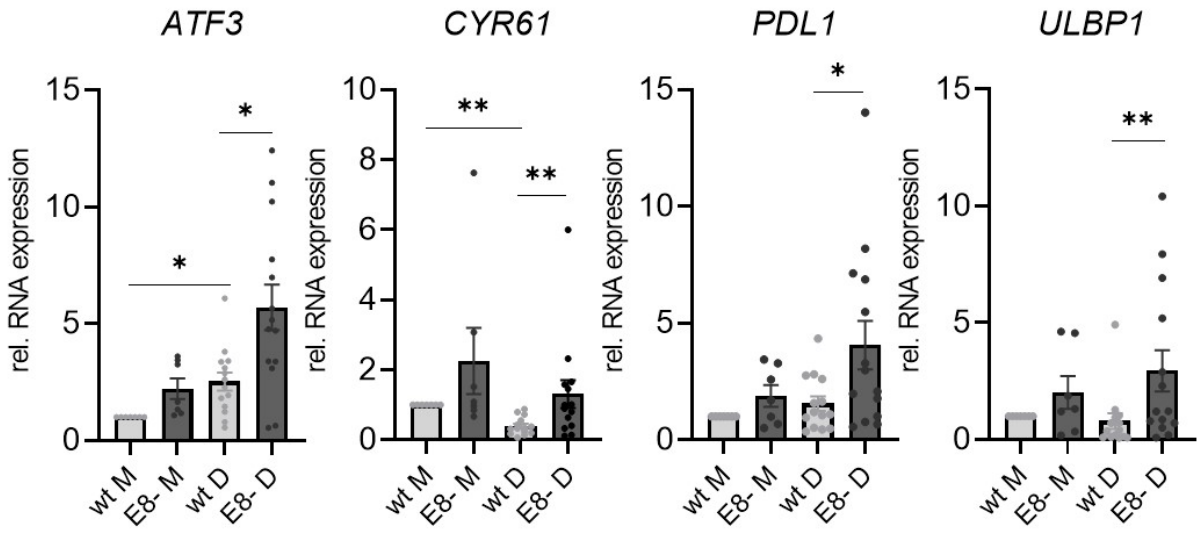

Figure 9: Deregulation of host gene expression after differentiation. RNA was isolated from monolayer (M) and 3D organotypic cultures (D) of HPV16 wt and E8- cell lines, transcribed to cDNA and used for qPCR with *ATF3*, *CYR61*, *PDL1* and *ULBP1*, and *PGK1* reference gene primers. Averages are derived from at least seven independent experiments, and the error bars represent the SEM. Statistical significance was determined by Kruskal Wallis uncorrected Dunns (*, $P \leq 0.05$; **, $P \leq 0.01$).
Figure from Kuehner et al., 2023.

Differential expression of ATF3 at the protein level could be confirmed by immunoblotting (Figure 10) revealing an increased ATF3 expression in a HPV16 E8- cell line grown in organotypic cultures compared to the monolayer and the associated wt cell line.

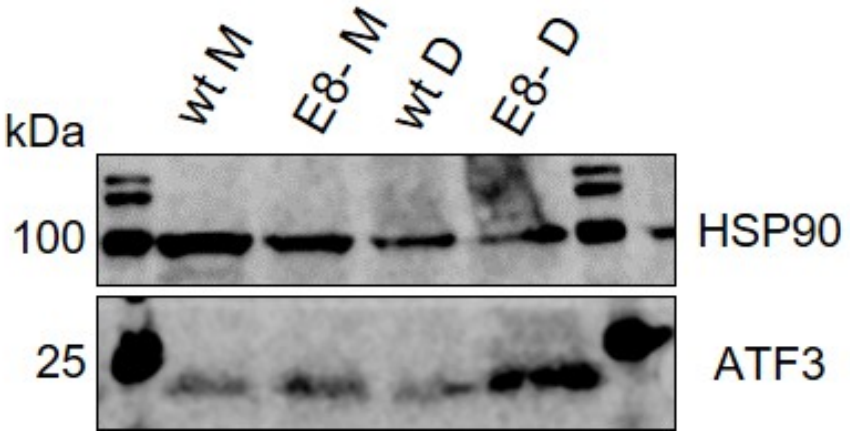

Figure 10: ATF3 expression changes on the protein level after differentiation. Monolayer (M) and 3D organotypic cultures (D) of HPV16 wt and E8- cell lines were harvested and lysed with 4xSDS lysis buffer. The expression of ATF3 (bottom) and HSP90 (top) was analyzed with specific antibodies by WB.

5.1.4 Increased expression of viral late transcripts but not early transcripts contribute to the deregulation of cellular genes

The induction of the viral late promoter that drives expression of E4- and L1-encoding mRNAs is a key event upon differentiation in the HPV replication cycle. Correlation analyses were performed to investigate if the expression of early or late viral mRNAs influences the expression of *ATF3, CYR61, PDL1* and *ULBP1* (Figure 11). These revealed that an increased expression of both *E1^E4* and *E4^L1* transcripts was significantly positively correlated with *ATF3*, *PDL1*, and *ULBP1*, but not *CYR61* expression. The expression of the early *E6*I* transcript however did not correlate with any of the deregulated genes. These data suggested that the increased expression of viral late transcripts but not early transcripts contributes to the deregulation of the majority of analyzed cellular genes.

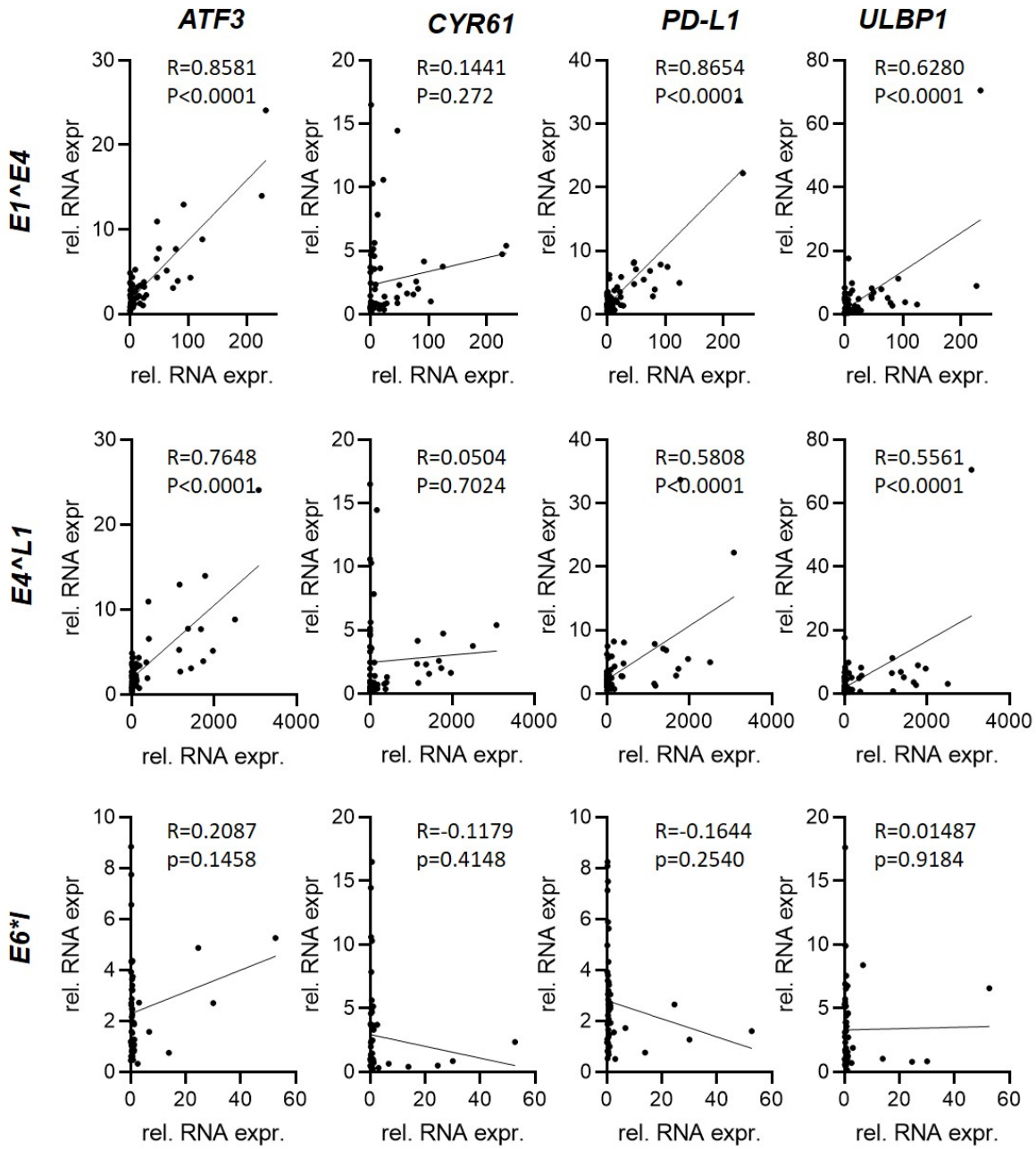

Figure 11: Correlation analysis of viral and cellular transcripts. The correlation between viral transcripts *E1^E4*, *E4^L1* or *E6*I* and the cellular genes *ATF3, CYR61, PDL1*, or *ULBP1* was analyzed by simple linear regression (GraphPad Prism 9) of more than 50 samples. Figure from Kuehner et al., 2023.

5.1.5 E4 and E5 influence copy number but not integration frequency in HPV16 E8-/E4- and E8-/E5- cell lines

HPV16 *E4* and *E5* modulate genome amplification and late gene transcription (Egawa and Doorbar, 2017; Fehrmann et al., 2003; Genther et al., 2003; Nakahara et al., 2005; Wilson et al., 2005). Therefore, the previously described HPV16 *E4* mutation st15 (Nakahara et al., 2005) or a stop codon at residue 3 of *E5* was introduced into the HPV16 E8- genome to prevent E4 or E5 expression, respectively. HPV16 E8-/E4- or HPV16 E8-/E5- genomes were then used to generate stable cell lines. In undifferentiated cells copy numbers of HPV16 E8-/E4- and E8-/E5- genomes were similar to E8- genomes (Figure 12 A). This indicates that the over replication phenotype of E8- genomes is independent from E4 and E5 in undifferentiated cells. In contrast, copy numbers of cells differentiated in organotypic cultures were lower for E8-/E4- and E8-/E5- genomes compared to E8- genomes (Figure 12 A). The levels of integration determined by resistance to exonuclease V were similar for all tested cell lines (Figure 12 B).

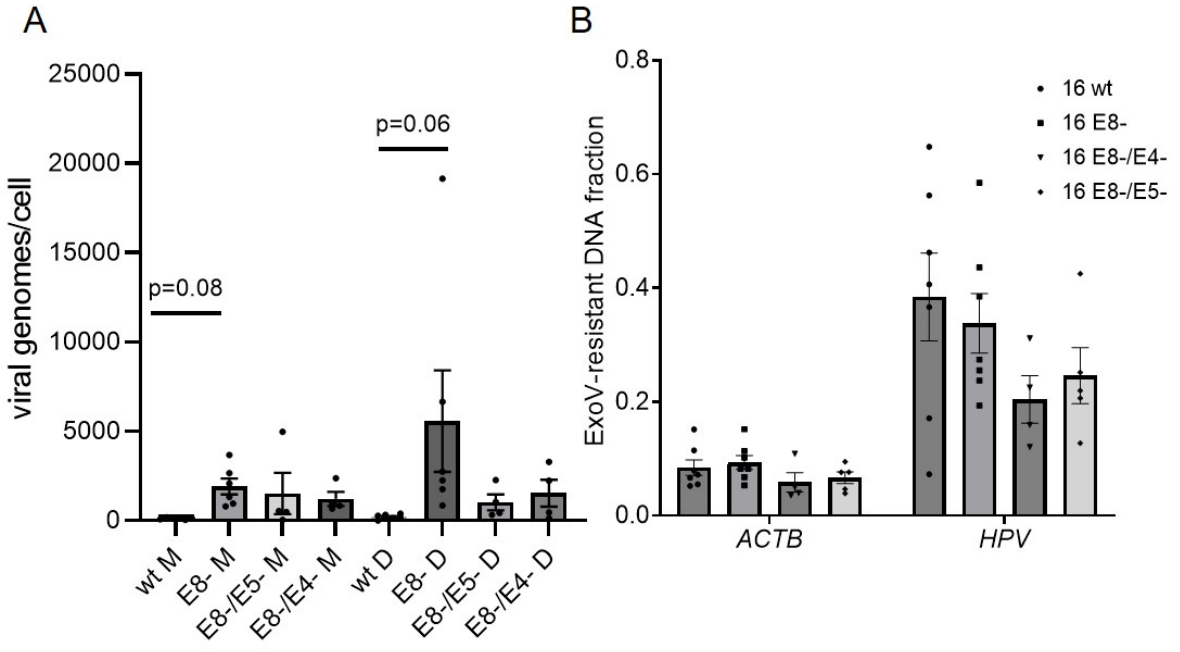

Figure 12: Characterization of HPV16 wt, E8-, E8-/E4- and E8-/E5- cell lines. (**A**) Total cellular DNA was isolated from HPV16 wt, E8-, E8-/E5- and E8-/E4- monolayer (M) and organotypic (D) cultures and viral copy numbers were determined by multiplex qPCR using amplicons in HPV16 *E2* and the cellular *ACTB* genes and copy number standards. (**B**) Total cellular DNA was treated with or without ExoV and then the copy numbers were determined by qPCR. Averages are derived from at least seven independent experiments, and the error bars represent the SEM. Statistical significance was determined by ordinary one-way ANOVA. Figure from Kuehner et al., 2023.

5.1.6 Reduced expression of late transcripts in HPV16 E8-/E4- and E8-/E5- cell lines compared to E8- cell lines

Analysis of the late *E1^E4* and *E4^L1* viral transcripts revealed a reduced expression of both transcripts in E8-/E4- and E8-/E5- cell lines compared to E8- cell lines maintained in both monolayer or organotypic cultures (Figure 13). This indicated that not only copy number but also late viral transcription is reduced consistent with the published phenotypes of E4- and E5-genomes.

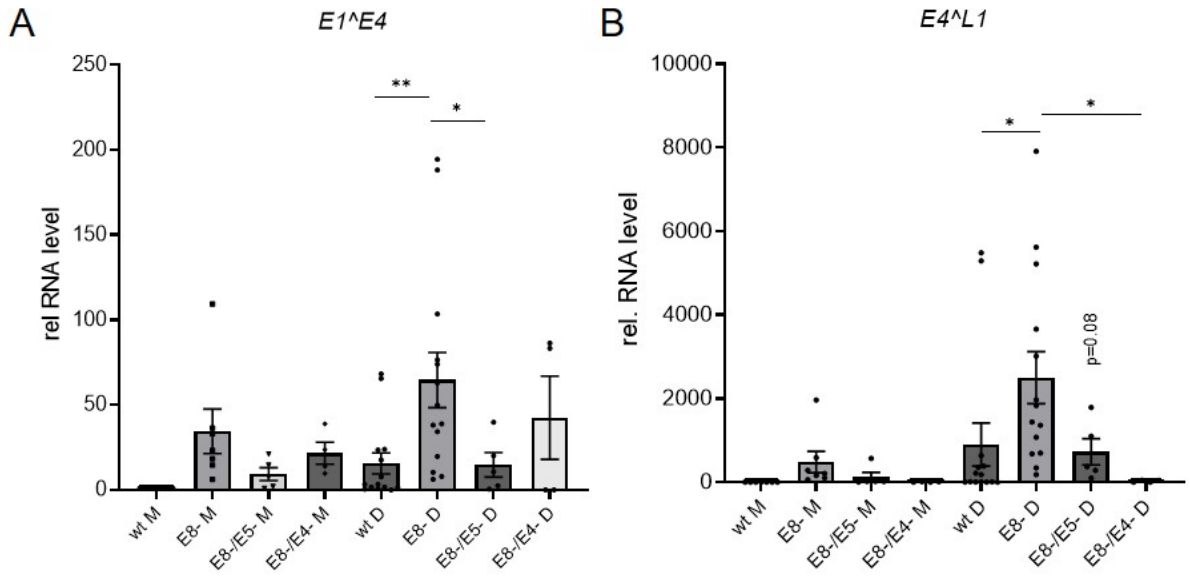

Figure 13: Viral transcript analysis in E8-/E4- and E8-/E5- cell lines compared to E8- cell lines. RNA was isolated from monolayer (M) and 3D organotypic cultures (D) of HPV16 wt, E8-, E8-E5- and E8-E4- cell lines, transcribed to cDNA and used for qPCR with **(A)** *E1^E4* and **(B)** *E4^L1* primers to quantify their expression and using *PGK1* as a cellular reference gene. Averages are derived from at least four independent experiments, and the error bars represent the SEM. Statistical significance was determined by ordinary one way ANOVA (*, $P \leq 0.05$; **, $P \leq 0.01$).
Figure from Kuehner et al., 2023.

5.1.7 Reduced expression of cellular genes in HPV16 E8-/E4- and E8-/E5- cell lines compared to E8- cell lines

The expression of *ATF3, CYR61, PDL1* and *ULBP1* in 3D organotypic cultures was reduced in E8-/E4- and E8-/E5- cell lines compared to E8- cell lines, this was only significant for ATF3 (Figure 14). The amounts of the analyzed cellular transcripts in E8-/E5- and E8-/E4- cell lines in monolayer cultures were similar to E8- cells.

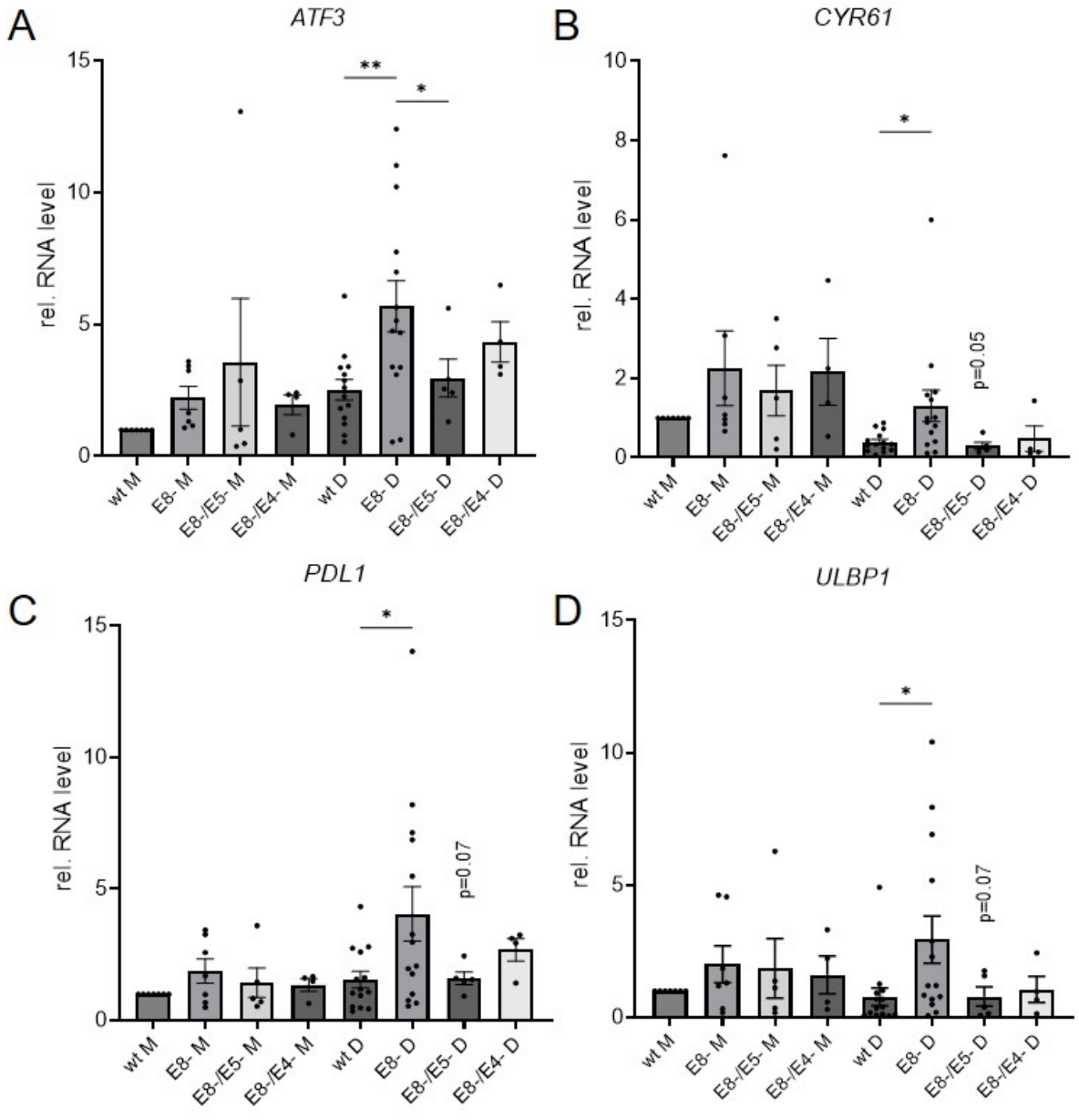

Figure 14: Cellular transcript analysis in E8-/E4- and E8-/E5- cell lines compared to E8- cell lines. RNA was isolated from monolayer (M) and 3D organotypic cultures (D) of HPV16 wt, E8-, E8-E5- and E8-E4- cell lines, transcribed to cDNA and used for qPCR with **(A)** *ATF3*, **(B)** *CYR61*, **(C)** *PDL1* and **(D)** *ULBP1* primers to quantify their expression and using *PGK1* as a cellular reference gene. Averages are derived from at least four independent experiments, and the error bars represent the SEM. Statistical significance was determined by ordinary one way ANOVA ($*, P \leq 0.05$; $**, P \leq 0.01$).
Figure from Kuehner et al., 2023.

Taken together these data support the idea that the deregulation of cellular genes by E8-genomes is a consequence of genome amplification and late gene transcription in differentiated cells.

5.2 Characterization of HPV16 E2 and E8^E2

E2 is involved in the viral DNA replication, genome maintenance, and transcription and is expressed at early and intermediate stages of the viral life cycle. E8^E2 mediates transcriptional repression of the viral promoter. The amounts of E2 and E8^E2 protein during the PV replication cycle have not been investigated so far. In a 2010 paper by Xue and colleagues, cervical intraepithelial neoplasia lesions (CIN) stained with a HPV16 E2 antibody, mainly resulted in a signal in the upper parts of the lesions (Xue et al., 2010). The antibody used recognized the C-terminal part of HPV16 E2 and thus both HPV16 E8^E2 as well as E2. To better understand E2 and E8^E2 expression in HPV positive cell lines, I purified the HPV16 E2 protein for antibody generation. Additionally, a monoclonal HPV16 E2 antibody from Andreas Wieland was used to validate the following results further. This HPV16 E2 antibody was generated from HPV16 E2-specific activated B-cells, which were single cell sorted, and their IgG heavy and light chain genes were then cloned. Recombinant monoclonal Abs were expressed as mouse IgG2c and purified using protein A agarose (Wieland et al., 2020).

5.2.1 Expression and Purification of HPV16 E2 for antibody production

A codon optimized HPV16 E2 fragment (E2 hinge aa202-286, DBD/Dimerization aa286-365) was expressed as a His_6-MBP-TEV-HPV16 E2C fusion protein in *E. coli* BL21(DE3) and then purified before sending it off for antibody production. The recombinant protein was enriched by affinity chromatography with 2x 5 ml MBP Trap columns in row (Cytiva Life Sciences™ MBPTrap™HP). Bound protein, which is about 68 kDa in size, was then eluted with buffer containing 20 mM maltose. Analysis by SDS-PAGE showed that a band at the expected size of about 68 kDa could be detected for the four fractions from the elution peak (Figure 15).

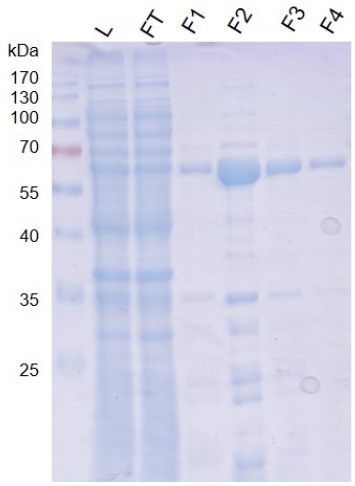

Figure 15: Affinity purification of His_6-MBP-TEV-HPV16 E2C with MBP trap column. Coomassie stained SDS gel of the purification progress after affinity chromatography with a MBP trap column. Fractions 1-4 (F1-4) with the target fusion protein were pooled and used for further purification steps. L= load, FT= flow through.

The eluted protein was then incubated o/n with 600mM NaCl to remove contamination by DNA and/or RNA, followed by SEC with a S200 column (HiLoad® 16/600 Superdex® 200 prep grade, GE Healthcare Life Sciences, UK) to remove protein impurities (Figure 16).

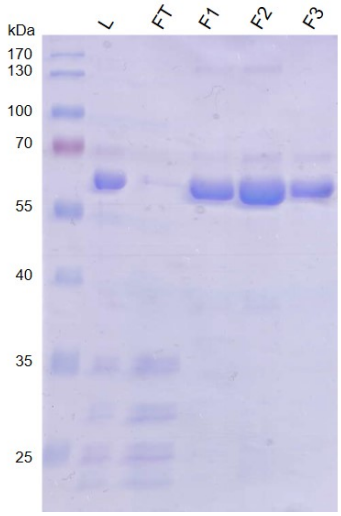

Figure 16: Result of the SEC with a S200 column. SDS-PAGE analysis (after Coomassie staining) of the purification progress after SEC with a S200 column. Fractions 1-3 (F1-3) with the target protein were pooled and used for further purification steps. L= load, FT= flow through.

To remove the MBP tag, the His_6-MBP-TEV-HPV16 E2C protein was incubated with tobacco etch virus (TEV) protease in a 1:20 mass ratio (protease:protein) at 4°C for one to four hours or o/n and centrifuged (30,000 g, 4°C, 30 min), the reaction was analyzed by SDS-PAGE (Figure 17). The simultaneous decrease of the fusion protein (68 kDa) and the increase of free MBP tag (40 kDa) and of cleaved HPV16 E2 protein (18 kDa) over time is clearly visible on the gel.

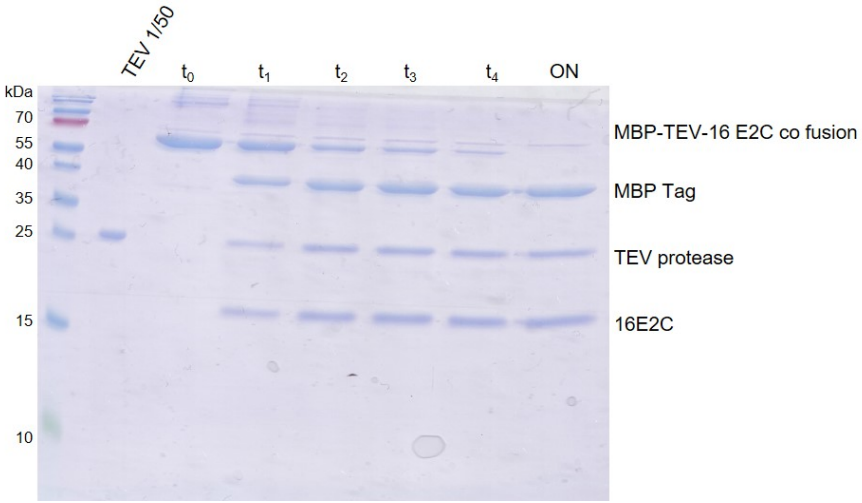

Figure 17: Result of the TEV cleavage of His_6-MBP-TEV-HPV16 E2C. His_6-MBP-TEV-HPV16 E2C (68 kDa) was cleaved with TEV protease for different time points (t_0= before cleavage, $t_{1\text{-}4}$= cleavage for 1-4h or ON= over night) and analyzed by SDS page and coomassie staining. Specific bands for the fusion protein, the MBP tag (40 kDa), the TEV protease (27 kDa) and 16 E2C (18 kDa) are clearly visible on the gel.

Since the o/n cleavage of His_6-MBP-TEV-HPV16 E2C showed the best result, I decided to use it as input for SEC with a S75 column (HiLoad® 16/600 Superdex® 75 prep grade, GE Healthcare Life Sciences, UK) and a HEPES running buffer. The eluate was subsequently concentrated with a Pierce™ Protein Concentrator PES (10K MWCO), followed by a 1 ml MBPTrap HP (1 ml MBPTrap™HP, Cytiva Life Sciences™). The purified protein was then sent to Davids Biotechnology for antibody generation in rabbits (Section 4.2.6.4).

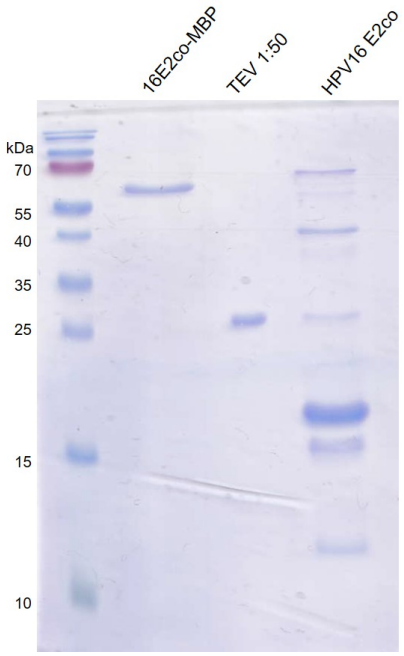

Figure 18: Final purified and concentrated HPV16 E2C protein. SDS-PAGE analysis (after Coomassie staining) of the HPV16 E2 protein after SEC with a S75 column and MBP trap. The protein was concentrated and then sent for antibody production.

5.2.2 HPV16 E2 antibodies detect transfected E2 and E8^E2 in IF and WB

To compare and validate the mono- and polyclonal HPV16 E2 antibodies, C33A cells were transfected with expression vectors encoding HPV16 E2, E8^E2 or E8^E2 KWK mt and analyzed 2 dpt by western blot. Both the polyclonal HPV16 E2 antibody as well as the monoclonal B9 antibody was able to detect HPV16 E2, E8^E2 and E8^E2 KWK mt proteins (Figure 19).

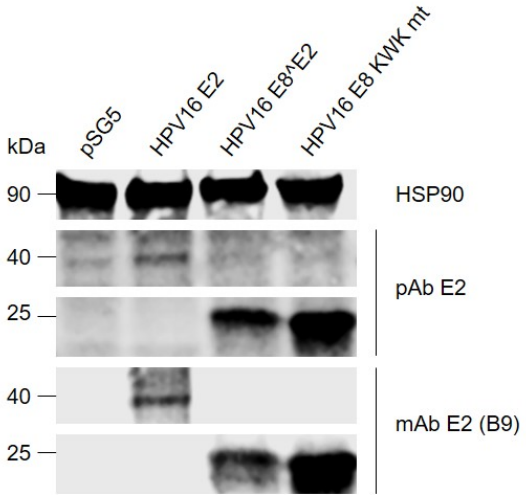

Figure 19: WB of C33A transfected with HPV16 E2, E8^E2 or E8^E2 KWK mt. C33A cells were transfected with the indicated expression plasmids and harvested 48 hpt (hours post transfection), lysed and analyzed with WB. Both polyclonal and monoclonal HPV16 E2 antibodies detected the HPV16 E2/E8^E2 /E8^E2 KWK mt proteins, n=4.

Furthermore, the HPV16 E2 antibodies were validated with an IP assay. C33A cells were transfected with expression vectors encoding HPV16 E2 and E8^E2 and analyzed 2 dpt (days post transfection). The monoclonal HPV16 E2 B9 antibody was used to coat the protein G beads, the polyclonal antibody was used for detection. The enrichment of HPV16 E2 and E8^E2 is clearly visible on the right side of the blot with some minor signal in the samples without monoclonal antibody (Figure 20).

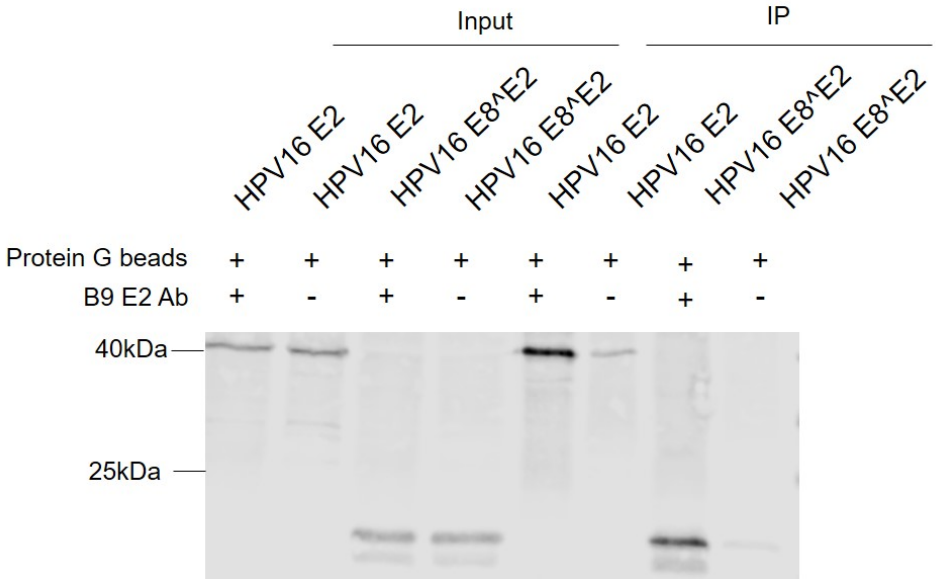

Figure 20: IP assay of C33A transfected with HPV16 E2 or E8^E2 expression plasmids. C33A cells were transfected with the indicated expression plasmids, harvested 48 hpt and lysed. IP was performed with protein G beads and the monoclonal HPV16 E2 antibody B9 and analyzed by WB, n=3.

The signal for the monoclonal B9 and the polyclonal HPV16 E2 antibody colocalized in an IF assay where C33A cells were transfected with expression vectors encoding HPV16 E2 and E8^E2 (Figure 21).

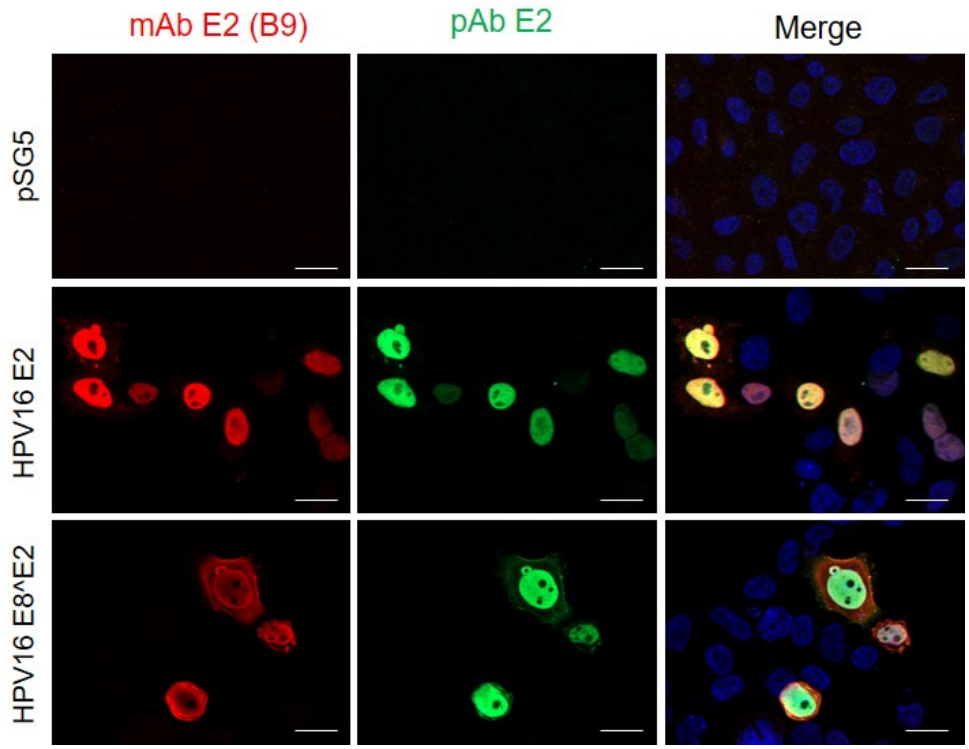

Figure 21: IF of C33A transfected with HPV16 E2 or E8^E2 expression plasmids. C33A cells were transfected with the indicated expression plasmids and stained with the indicated Antibodies 48 hpt. Both polyclonal (pAb) and monoclonal (mAb) HPV16 E2 antibodies detected the HPV16 E2 proteins with little background. Magnification 630x, scale bar is 20 µm, n=3.

5.2.3 HPV16 E2 antibodies recognize endogenous E2 and E8^E2 in IF in HPV16 wt and E8- cell lines

Since both antibodies detected transfected HPV16 E2 and E8^E2 by IF, NHK cell lines immortalized with either HPV16 E6 and E7, HPV16 wt or E8- genomes were stained with them. In the HPV16 E6/E7 negative control, where E2 and E8^E2 are absent, neither the monoclonal B9 nor the polyclonal E2 antibody detected anything. Interestingly, E2 RNA levels in HPV16 E8- cell lines have been described to be increased by 4-fold compared to wt cell lines (Straub et al., 2014). E2 foci of different sizes were visible in the nuclei of wt and E8- cell lines (Figure 22), but they could be found only in a fraction of cells and not all of them. There were generally more and bigger foci in E8- than in wt cell lines. E8^E2 has been shown to localize to E1-E2 induced replication foci (Dreer et al., 2016; Dreer et al., 2017; Khurana et al., 2021).

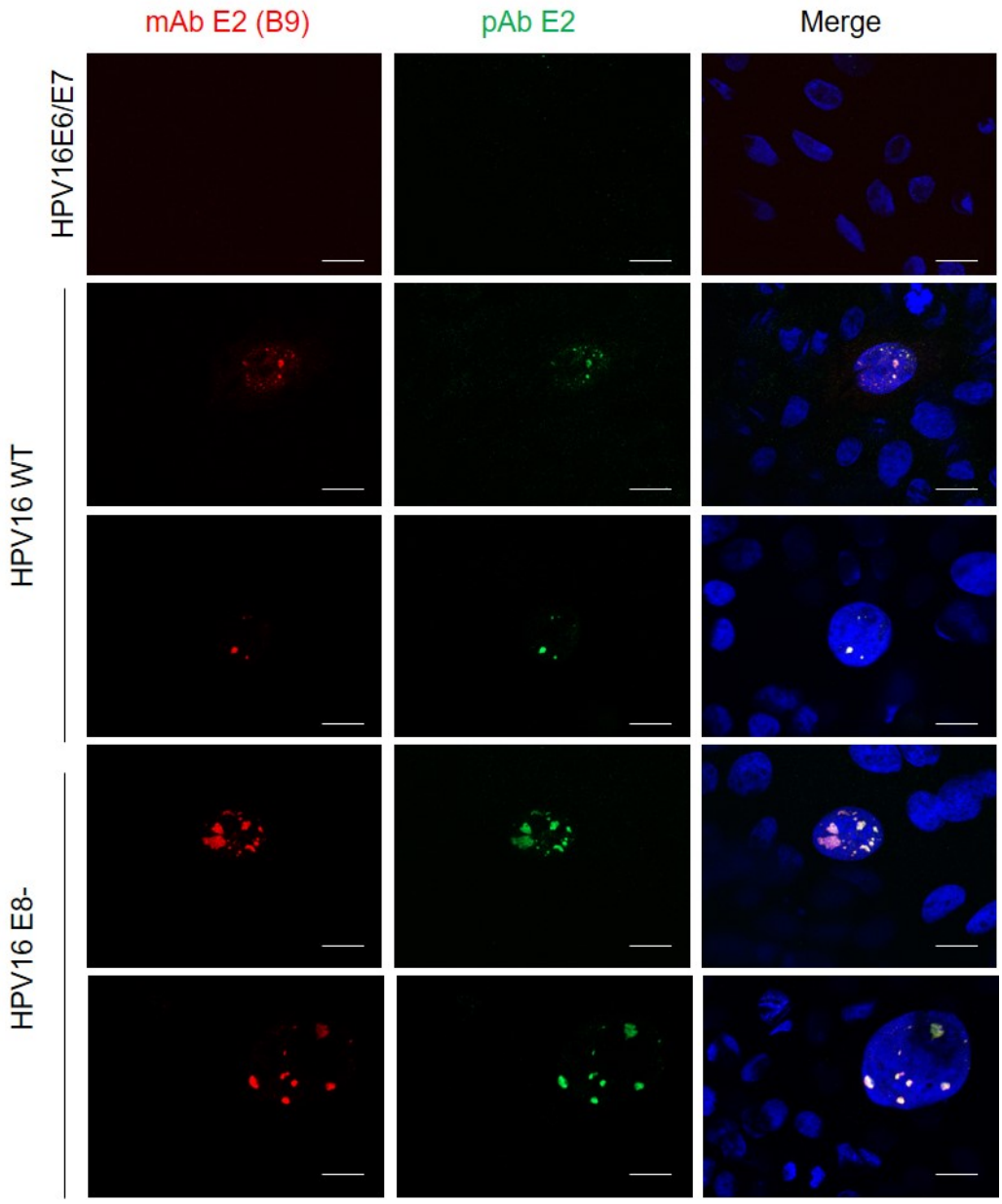

Figure 22: IF of HPV16 E6/E7, HPV16 wt or E8- cell lines with mono- and polyclonal HPV16 E2 antibodies. NHK cell lines expressing either HPV16 wt or E8- genomes or HPV16 E6/E7 cell lines were stained with monoclonal or polyclonal HPV16 E2 antibodies to detect endogenous E2/E8^E2 and imaged. Magnification 630x, scale bar is 20 µm, n=3.

5.2.4 Detection of endogenous E8^E2 by IP in HPV16 KWK mt cell lines

The IF assay of different HPV positive cell lines (Figure 22) confirmed the expression of HPV16 E2 and possibly E8^E2, but also revealed the relatively low expression levels of the proteins. Therefore, I decided to enrich HPV16 E2/E8^E2 by IP before analysis by WB. I was able to detect E8^E2 in a E8 KWK mt cell line after IP, but not in HPV16 wt nor E8- cell lines (Figure 23). Nevertheless, none of the samples showed a specific band at around 40kDa for E2 protein, indicating very low levels of E2 expression.

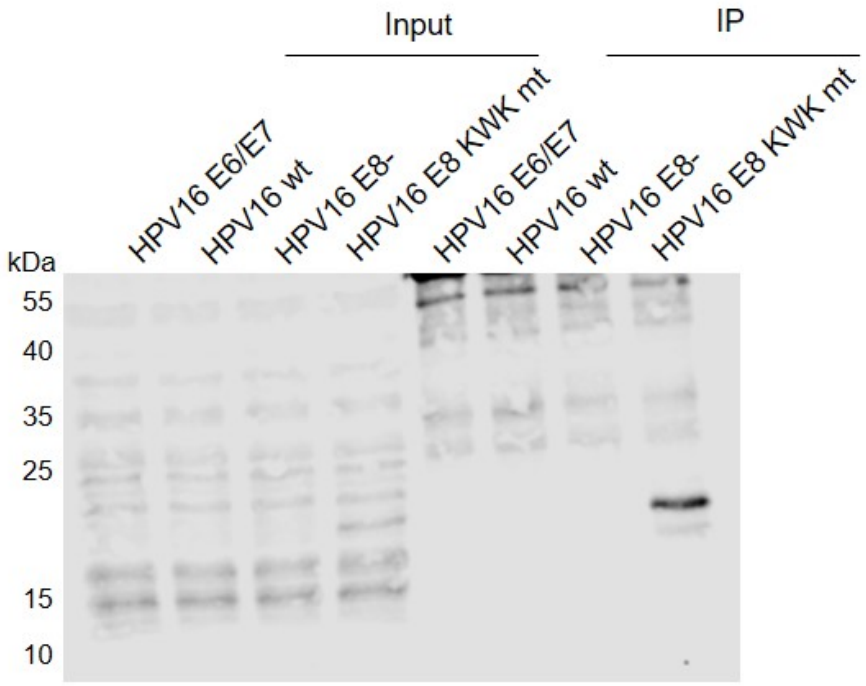

Figure 23: IP assay of endogenous HPV16 E2/E8^E2 in different HPV16 cell lines. IP assay of endogenous HPV16 E2/ E8^E2 in HPV16 E6/E7, wt, E8- and KWK mt cell lines. IP was performed with Protein G beads and the monoclonal HPV16 E2 antibody B9 and analyzed with WB, n=2.

5.2.5 E2 foci and RPA32 partially colocalize in HPV16 E8- cell lines

Next, HPV16 E6/E7 and E8- cell lines were stained with the monoclonal HPV16 E2 antibody and an antibody that recognizes the replication protein A 32 (RPA32). It is known that the heterotrimeric RPA complex, composed of the 70, 32, and 14 kDa subunits, binds single-stranded DNA, and is involved in cell cycle, DNA damage checkpoints, and DNA repair (Kastan and Bartek, 2004; Sancar et al., 2004; Wold and Kelly, 1988; Zhou and Elledge, 2000). It was shown that RPA32 localized to HPV DNA foci, suggesting that these were sites of viral DNA synthesis (Gillespie et al., 2012). Some, but not all of the E2 foci colocalized with RPA32 in HPV16 E8- cell lines (Figure 24), indicating active replication.

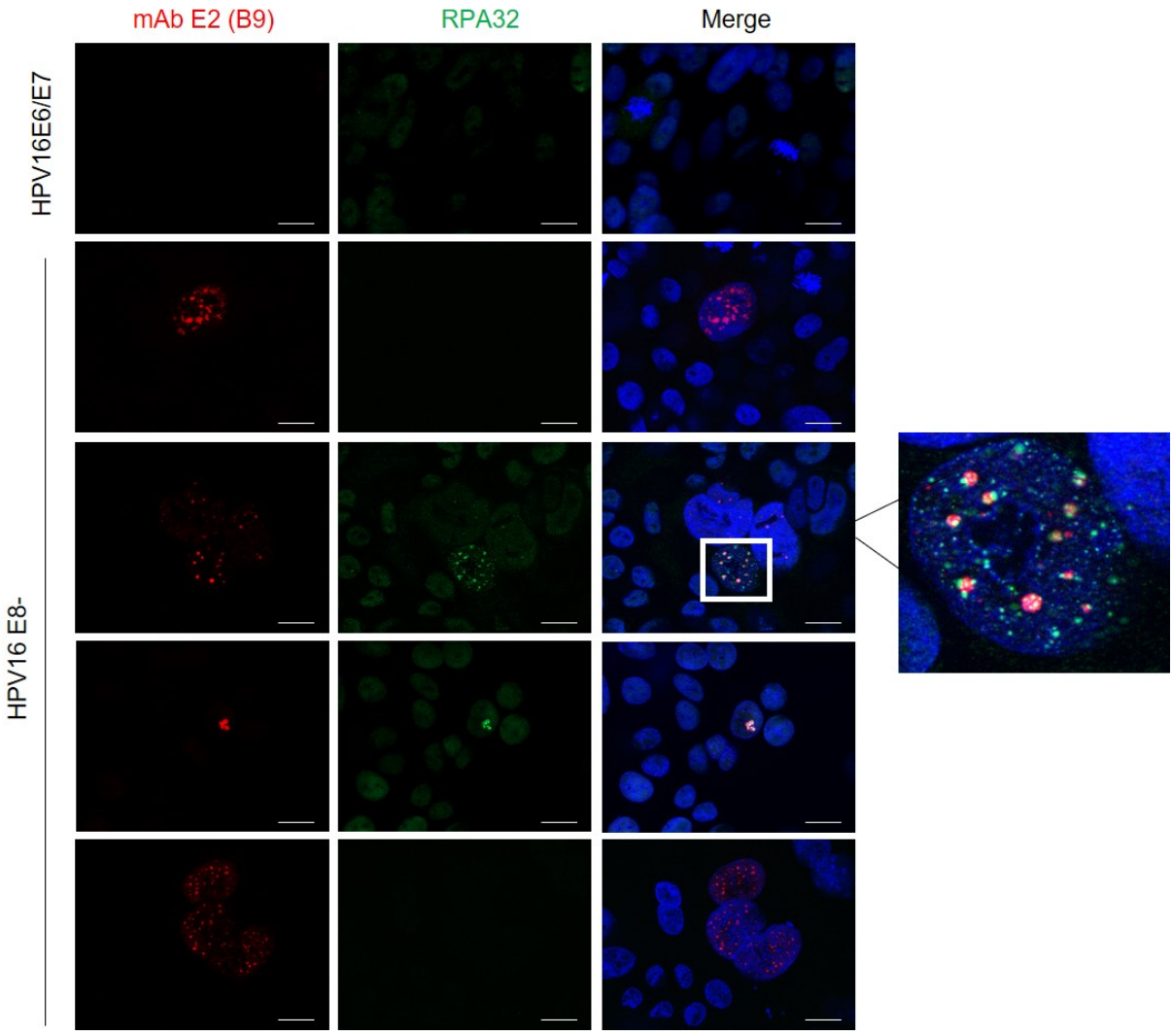

Figure 24: IF of HPV16 E6/E7 or E8- cell lines with HPV16 E2 and RPA32 antibodies. NHK cell lines expressing either HPV16 E8- genomes or HPV16 E6/E7 were stained with the monoclonal HPV16 E2 Antibody B9 as well as a RPA32 antibody. Magnification 630x, scale bar is 20 µm, n=3.

5.2.6 Late E4 protein and keratin 10 (K10) expression in HPV16 E8- cell lines

Lastly, HPV16 E6/E7 or E8- cell lines were co-stained with antibodies for HPV16 E2 and HPV16 E4 or K10. Productive replication of HPV is characterized by genome amplification and expression of the E4 protein and takes place within suprabasal, differentiated keratinocytes (Grassmann et al., 1996; Hummel et al., 1992; Pray and Laimins, 1995; Sterling et al., 1993). K10 is a suprabasal keratinocyte differentiation marker (Coulombe et al., 1991; Fuchs and Green, 1980). Some HPV16 E2 positive cells expressed the late viral E4 protein (Figure 25 A). Furthermore, E4 positive cells expressed the suprabasal keratinocyte differentiation marker keratin 10 (Figure 25 B). This suggests that E2 accumulation might precede E4 protein expression and E4 protein expression may require cellular differentiation as evidenced by K10 expression.

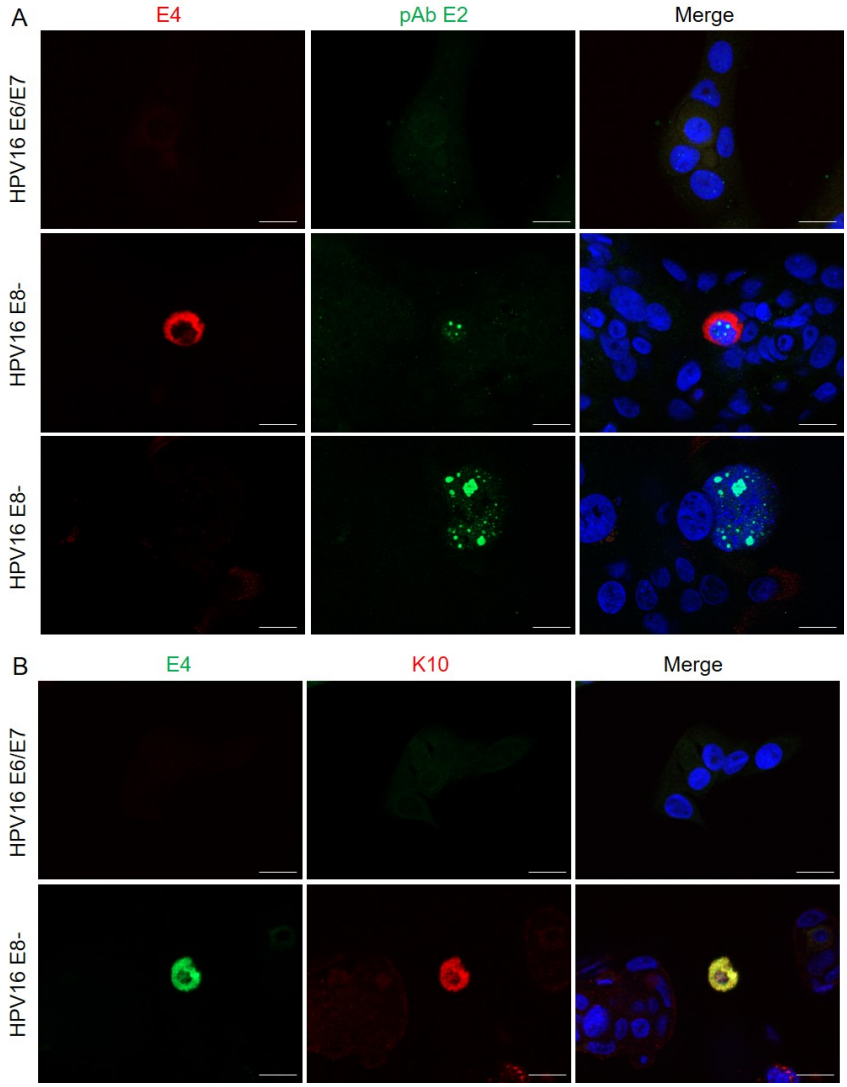

Figure 25: IF of HPV16 E6/E7 or E8- cell lines with HPV16 E2, E4 and K10 antibodies. NHK cell lines expressing either HPV16 E8- genomes or HPV16 E6/E7 were stained with either **(A)** the monoclonal HPV16 E2 antibody B9 (green) and a E4 antibody (red) or **(B)** the HPV16 E4 antibody (green) as well as a K10 antibody (red). Magnification 630x, scale bar is 20 µm, n=3.

5.3 Inactivation of the MmuPV1 E8^E2 protein induces late E4 protein expression but prevents wart formation

It has recently been shown that MmuPV1 E8- genomes did not induce warts in T cell-deficient Foxn1$^{nu/nu}$ mice suggesting that E8^E2 is necessary for tumor formation *in vivo* (Stubenrauch et al., 2021). The data in this chapter are part of the accepted manuscript Kuehner et al., (*Mus musculus* papillomavirus 1 E8^E2 represses expression of late protein E4 in basal-like keratinocytes via NCoR/SMRT-HDAC3 co-repressor complexes to enable wart formation *in vivo*, mBio, accepted 22.05.2023).

5.3.1 Mutation of the MmuPV1 E8 splice donor but not a stop codon in E8 increases viral transcription

To provide further evidence that the lack of wart formation *in vivo* is due to the lack of E8^E2 and not cis-elements overlapping with the E8 start codon, additional mutations in E8 predicted to prevent E8^E2 expression by introducing a stop codon in E8 (G9X; E8 Stop mt) or disrupting the splice donor signal AG|GT (AA|GT; E8 SD mt) were generated (Figure 26 A).
NMTK were transfected with wt, E8-, E8 Stop mt, or E8 SD mt genomes and the amount of *E1^E4* transcripts was measured by qPCR 6 dpt (Figure 26 B). E8 SD mt increased *E1^E4* transcripts to significantly higher levels than the wt, the levels were even higher than for E8- genomes. Surprisingly, gene expression from E8 Stop mt genomes was only slightly, but not significantly, increased compared to wt.
The *E1* coding sequence in E8 Stop mt genomes is affected and E1 G126 is exchanged to V, in contrast to E8- and E8 SD mt genomes, where the *E1* ORF is not changed (Figure 26 A).
However, reporter assays using the pGL mURR/E1-luc plasmid, which harbors several MmuPV1 promoters and the viral origin of replication (Figure 27), revealed similar activation levels for wt mE1 and mE1 G126V in the absence and presence of mE2 (Figure 26 C). This suggests that the lack of a transcriptional phenotype of E8 Stop mt is not due to changes of mE1. When evaluating the mutated sequence of E8 Stop mt, it became evident that the change from G to T created a potential novel splice donor sequence (GGTGA, Figure 26 D). RT-PCR was therefore performed using RNA isolated from wt or E8 Stop mt transfected murine keratinocytes and primers in the E8 and E4 region. DNA sequencing of gel-purified amplicons revealed that in E8 Stop mt transfected cells nt 1116 was linked to nt 3139 (wt: nt 1125 to nt 3139) confirming that the introduction of the stop codon accidentally created a novel splice donor sequence. The novel splice donor removes the artificial stop codon in E8 and produces an in-frame fusion of E8^E2 from which residues 9-11 are deleted (mE8^E2 d9-11).

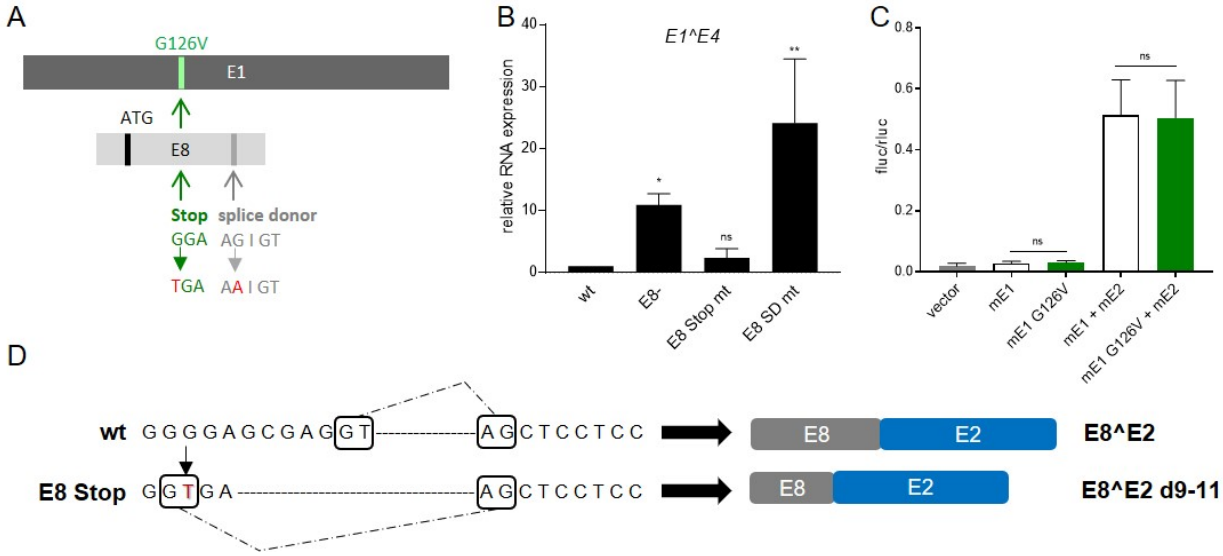

Figure 26: mE8 Stop mutation creates a new splice donor site resulting in a truncated E8^E2 d9-11. (**A**) Schematic representation of the *E8* ORF (light grey) with the overlapping *E1* reading frame (dark grey) and the impact of the E8 Stop mutation on E1 (G126V in light green) and the lack of E1 involvement for E8 splice donor mutation. (**B**) NMTK were transfected with ligated wt or mutant MmuPV1 genomes. RNA was harvested 6 dpt and qPCR was performed with *E1^E4* and *Pgk1* as a reference. Averages from at least three independent experiments, error bars= SEM, one way ANOVA test (ns, not significant; *, P, 0.05; **, P, 0.01). (**C**) There is no significant difference between mE1 G126V and mE1 wt on replication. C33A cells were transfected with 100 ng of pGL mURR/E1-luc reporter plasmid, 10 ng Renilla-luc, 1,000 ng wt or d9-11 pSG5 mE1; 100 ng pSG5 mE2, plus empty vector (pSG5), to obtain equal amounts of plasmid DNA. Luciferase activities were determined 48 hpt. Data are presented as ratios between firefly luciferase (Fluc) and renilla luciferase (Rluc) activities. Averages are derived from three independent experiments, the error bars represent the SEM. Statistical significance was determined by unpaired t-test (ns, not significant). (**D**) The G to T mutation in the mE8 stop mutant creates a new splice donor site resulting in a truncated E8^E2 d9-11. Figure from Kuehner et al., accepted for publication in mBio.

Murine E8^E2 d9-11 is expressed at similar levels as wt mE8^E2 in C33A cells after transfection of the respective HA-tagged expression vectors indicated by immunoblot (Figure 27 A). To test whether the deletion of residues 9-11 has an impact on it's repression activity, the pGL mURR/E1-luc reporter plasmid was co-transfected with mE1 and mE2, and different amounts of mE8^E2 or mE8^E2 d9-11 expression vectors. This revealed that E8^E2 d9-11 behaves as a repressor comparable to wt E8^E2 (Figure 27 B+D). Similar results were obtained with an pC18-Sp1-luc-reporter containing E2BSs (Figure 27 C+E). The lack of increased gene expression from E8 Stop mt genomes is most likely due to the expression of E8^E2 d9-11 which compensates for wt E8^E2.

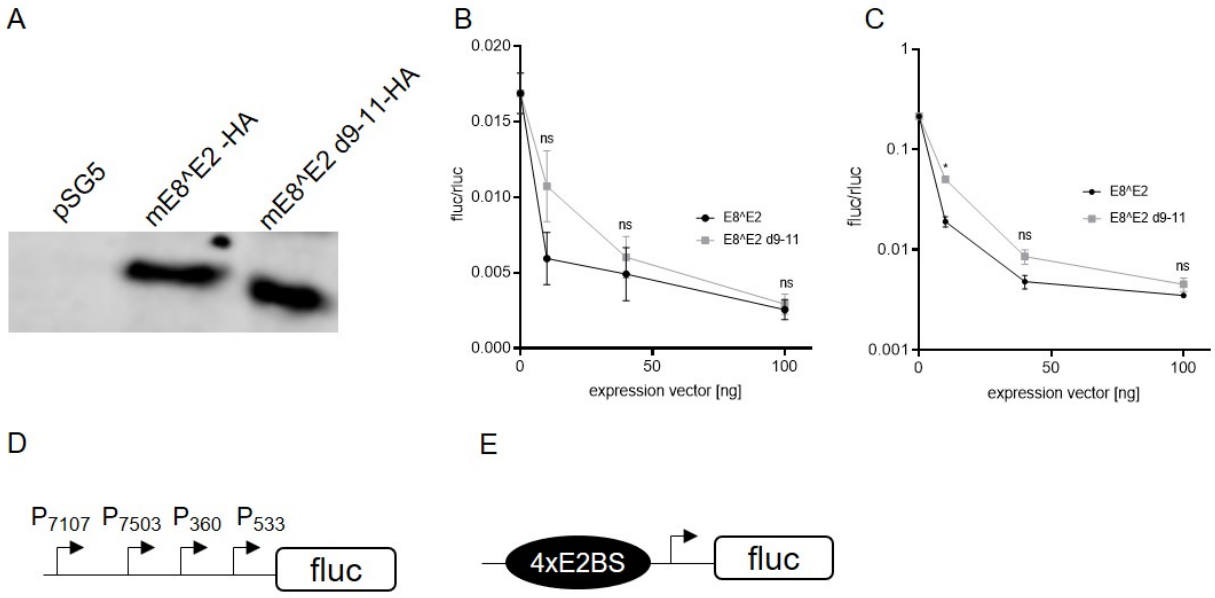

Figure 27: Expression of mE8^E2 d9-11 compensates for wt mE8^E2. (**A**) WB of C33A cells transfected with either pSG5, mE8^E2-HA wt or d9-11 indicates similar levels of expression when stained with anti-HA antibody, n=2. (**B**) C33A cells were transfected with 100 ng of pC18-Sp1-luc reporter plasmid, 10ng renilla-luc, and the indicated amounts of pSG5 mE8^E2 -HA wt or d9-11, plus empty vector (pSG5), to obtain equal amounts of plasmid DNA. Luciferase activities were determined 48 hpt. Data are presented as ratios between Fluc and Rluc activities. Averages are derived from three independent experiments, and the error bars represent the SEM. Statistical significance was determined for mE8^E2 (black) and mE8^E2 d9-11 (grey) by ordinary one way ANOVA (ns, not significant). (**C**) C33A cells were transfected with 100 ng of pGL mURR/E1-luc reporter plasmid, 10 ng renilla-luc, 1,000 ng pSG5 mE1, 100 ng pSG5 mE2, and the indicated amounts of pSG5 mE8^E2 -HA wt or d9-11, plus empty vector (pSG5), to obtain equal amounts of plasmid DNA. Luciferase activities were determined 48 hpt. Data are presented as ratios between Fluc and Rluc activities. Averages are derived from at least three independent experiments, and the error bars represent the SEM. Statistical significance was determined by ordinary one way ANOVA (ns, not significant; *, $P < 0.05$). (**D**) Schematic structure of the pGL mURR/E1-luc plasmid. Localization of the upstream regulatory region (URR), the E6 and E7 genes, and transcription start sites of the P7107, P7503, P360, and P533 promoters are indicated. (**E**) Schematic structure of the pC18-SP1-luc plasmid with four E2 binding sites is shown. Figure from Kuehner et al., accepted for publication in mBio.

5.3.2 mE8^E2 interacts with NCoR/SMRT complex components

It has been previously shown that HPV1, 8, 16, and 31 E8^E2 proteins interact with NCoR/SMRT co-repressor complexes. These complexes consist of NCoR1 and/or SMRT, HDAC3, TBL1 and/or TBLR1, and GPS2 and the conserved K5/W6/K7 residues in HPV16 and 31 E8 or K2/L3/K4 residues in HPV1 and 8 E8 are required for the interaction (Dreer et al., 2017). MmuPV1 harbors conserved K2/L3/K4 residues, elucidated in the sequence alignment of HPV1, 5, 8, 38, 49, and MmuPV1 E8, making it possible that MmuPV1 also functionally interacts with NCoR/SMRT complexes (Figure 28 A). The conserved K2/L3/K4 residues were also exchanged to RPR in mE8^E2 (E8^E2 RPR mt). To test this possible interaction and the importance of the conserved KLK motif, HA-tagged mE8^E2 was co-expressed with GPS2, HDAC3 or TBLR1 fused to sYFP in C33A cells and analyzed by co-IP analysis. Immunoblot

and IF analysis revealed that E8^E2 RPR mt is stably expressed and localizes to the nucleus comparable to the wt protein (Figure 28 B). Co-IP analyses revealed that mE8^E2 interacts with HDAC3, GPS2 and TBLR1, whereas interaction with E8^E2 RPR mt, despite being expressed at similar levels in the nucleus, was greatly impaired (Figure 28 C). Attempts to express full length NCoR1 as a sYFP fusion protein to analyze the interaction with mE8^E2 failed for unknown reasons. However, since HDAC3 and GPS2 interact with mE8^E2, which are known to directly bind to NCoR/SMRT but not directly to each other (Watson et al., 2012), it can be assumed that NCoR/SMRT complexes interact with mE8^E2. In line with this, the endogenous NCoR/SMRT complex components HDAC3 and TBL1 can be immunoprecipitated with HPV16 E8^E2, mE8^E2 but not with the E8^E2 RPR mt in HeLa cells transfected with expression vectors for HPV16 E8^E2 as a positive control, mE8^E2, or E8^E2 RPR mt (Figure 28 D).

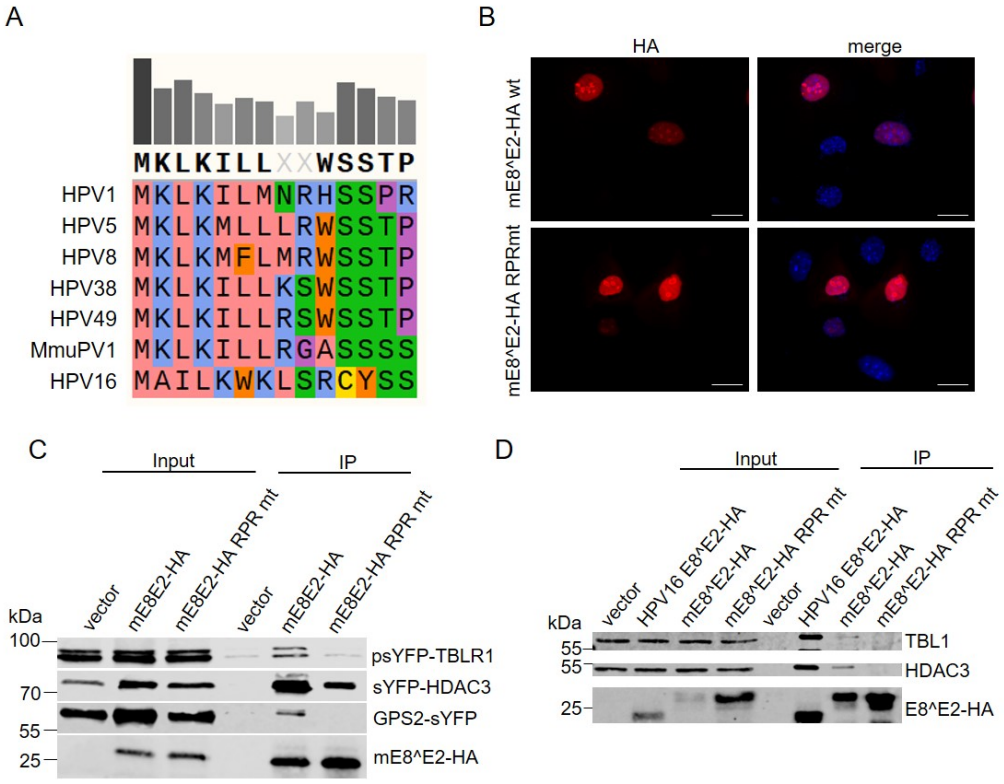

Figure 28: mE8^E2 interacts with the NCoR/SMRT complex. (**A**) E8 consensus sequence of different papillomaviruses, highly conserved KLK motif. E8 sequences were retrieved from the PAVE database (pave.niaid.nih.gov, Van Doorslaer et al., 2017) and analyzed with Snapgene. (**B**) NMTK were transfected with mE8^E2 -HA wt or RPR mutant pSG5 expression plasmids and fixed and stained with HA antibodies 48 hpt. Magnification 630x, scale bar is 20 µm, three independent experiments. (**C**) Co-IP analysis reveals an interaction of wt MmuPV1 E8^E2 with transfected sYFP tagged GPS2, TBLR1, and HDAC3, which is decreased/abolished with RPR mt E8^E2. Cell lysates from C33A cells were directly analyzed (input) or precipitated with anti-HA antibody (IP) and subjected to immunoblot analysis, n=3. (**D**) Co-IP analysis reveals an interaction of HPV16 E8^E2 and mE8^E2 with HDAC3 and TBL1. Cell lysates from HeLa cells were directly analyzed (input) or precipitated with anti-HA antibody (IP) and subjected to immunoblot analysis, n=4. Figure from Kuehner et al., accepted for publication in mBio.

5.3.3 Lack of repression by mE8^E2 correlates with binding to NCoR/SMRT complexes

Next, reporter assays were conducted to evaluate if the interaction of mE8^E2 with NCoR/SMRT components is important for repression activity. In contrast to the repression effect of wt mE8^E2 on pC18-Sp1-luc activity in both human C33A cells and murine keratinocytes, E8^E2 RPR mt has no inhibitory activity (Figure 29 A+B). Furthermore, the pGL mURR/E1 construct is repressed by low amounts of mE8^E2 expression vector whereas E8^E2 RPR mt even slightly activates the reporter at low input in C33A cells (Figure 29 C). The addition of mE1 and mE2 to pGL mURR/E1-luc to induce replication, the differences between mE8^E2 and E8^E2 RPR mt are even more pronounced. Whereas E8^E2 represses the reporter almost completely at 10 ng input, E8^E2 RPR mt only slightly inhibits at 100 ng input (Figure 29 D). These data indicate that the conserved KLK residues are not only important for the interaction with NCoR/SMRT complex components, but also for repression activity in both human and murine cells.

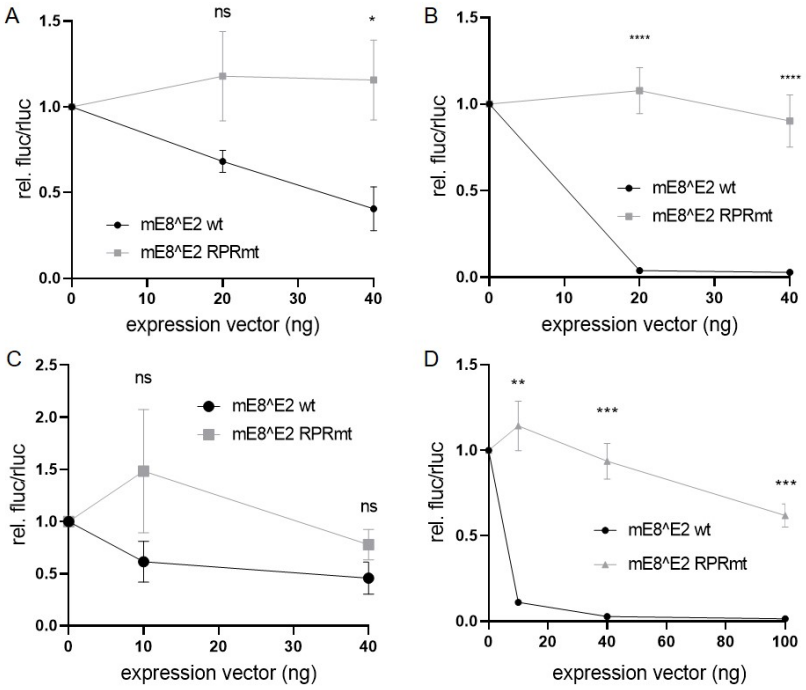

Figure 29: Lack of repression by mE8^E2 correlates with binding to NCoR/SMRT complexes. (**A**) C33A cells or (**B**) NMTK were transfected with 100 ng of pC18-Sp1-luc reporter plasmid, 10ng renilla-luc, and the indicated amounts of pSG5 mE8^E2 -HA wt or E8^E2 RPR mt, plus empty vector (pSG5), to obtain equal amounts of plasmid DNA. Luciferase activities were determined 48 hpt. (**C**+**D**) mE8^E2 inhibits MmuPV1 promoter activity in the presence of mE1 and mE2. C33A cells were transfected with 100 ng of pGL mURR/E1-luc reporter plasmid, 10 ng renilla-luc, and the indicated amounts of pSG5 mE8^E2 -HA wt or RPR, empty vector (pSG5), to obtain equal amounts of plasmid DNA and in (**D**) additionally 1,000 ng pSG5 mE1 and 100 ng pSG5 mE2. Luciferase activities were determined 48 hpt. Data are presented as ratios between Fluc and Rluc activities relative to those of pSG5-transfected cells. Averages are derived from three independent experiments, and the error bars represent the SEM. Statistical significance was determined by unpaired t-test (ns, not significant; *, $P \leq 0.05$; **, $P \leq 0.01$; ***, $P \leq 0.001$).
Figure from Kuehner et al., accepted for publication in mBio.

To further corroborate the importance of NCoR/SMRT complexes for mE8^E2 repression activity, RNA interference experiments were carried out. Previous studies have indicated that combinations of siRNAs against different complex components are necessary to relieve repression activity of E8^E2, which is most likely due to the dimeric nature of these complexes and the functional redundancy of NCoR and SMRT on the one side and TBL1 and TBLR1 on the other side (Dreer et al., 2016). Therefore I tested combinations of siNCoR and siSMRT or of siHDAC3 and siTBLR1, in addition to siGPS2, which was previously not tested. All siRNAs reduced gene expression of the respective target genes in human or mouse cells (Figure 30 A,D; Figure 31 A). The effect of siNCoR/siSMRT and siHDAC3/siTBLR1 on the reporters themselves were not significant (Figure 30 B+C) in C33A cells. Repression of the pC18-Sp1-luc by mE8^E2 was significantly relieved by both siNCoR/siSMRT and siHDAC3/siTBLR1, whereas the effect on E8^E2 RPR mt is far less pronounced (Figure 30 B). Repression of the pGL-mURR/E1-luc reporter in the presence of mE1 and mE2 by mE8^E2 was also significantly relieved by both siRNA combinations, whereas no effect on E8^E2 RPR mt is seen (Figure 30 C). In contrast, the knockdown of GPS2 had no effect on the repression by mE8^E2 of pC18-Sp1-luc or pGL-mURR/E1-luc in the presence of E1 and E2 (Figure 30 E+F) in C33A.

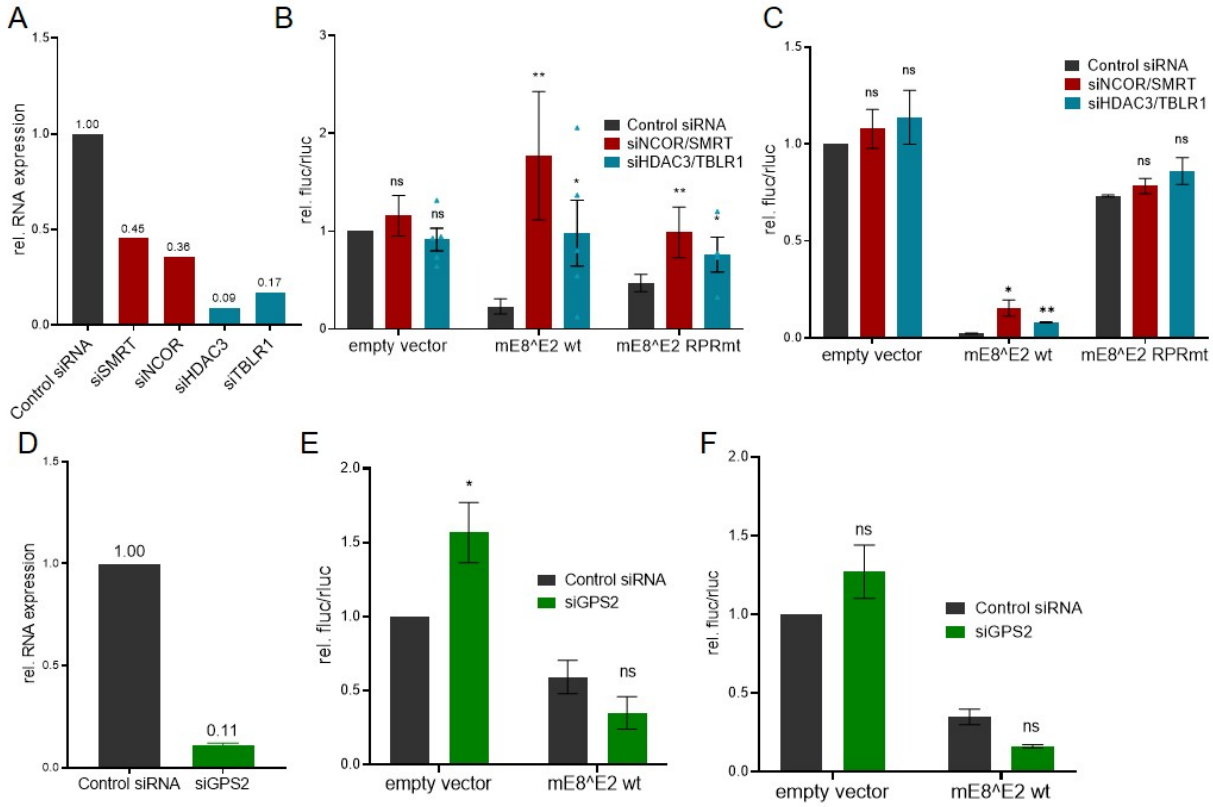

Figure 30: NCoR/SMRT complex mediates repression of transcription and replication by mE8^E2 in C33A. (**A**) Knockdown Efficiency of siRNAs for SMRT, NCoR1, HDAC3 and TBLR1 in C33A cells compared to control siRNA. (**B**+**C**) siRNA against NCoR/SMRT and HDAC3/TBLR1 relieves the repression of transcription (**B**) and replication (**C**). C33A cells were transfected with siRNA combinations and 24 h later with the pC18-Sp1-luc reporter (**B**) or mURR/E1-luc (**C**) as well as the expression vectors for mE8^E2 wt or mE8^E2 RPR mt. Luciferase activities were determined 48 hpt. Averages from at least three independent experiments, error bars= SEM. . (**D**) Knockdown Efficiency of siRNAs for GPS2 in C33A cells compared to control siRNA. (**E**+**F**) siRNA against GPS2 does not relieve the repression of transcription (**E**) and replication (**F**). C33A cells were transfected with GPS2 siRNA and 24 h later with the pC18-Sp1-luc reporter (**E**) or mURR/E1-luc (**F**) as well as the expression vectors for mE8^E2 wt. Luciferase activities were determined 48 hpt. Averages from at least three independent experiments, error bars= SEM, ratio-paired t-test (ns, not significant; *, $P \leq 0.05$; **, $P \leq 0.01$).
Figure from Kuehner et al., accepted for publication in mBio.

A similar effect of siNcor1/siSmrt on the repression of pC18-Sp1-luc by mE8^E2 could also be observed in mouse keratinocytes (Figure 31 B). Taken together these reporter experiments strongly indicate that NCoR/SMRT complexes contribute to the repression activity of mE8^E2.

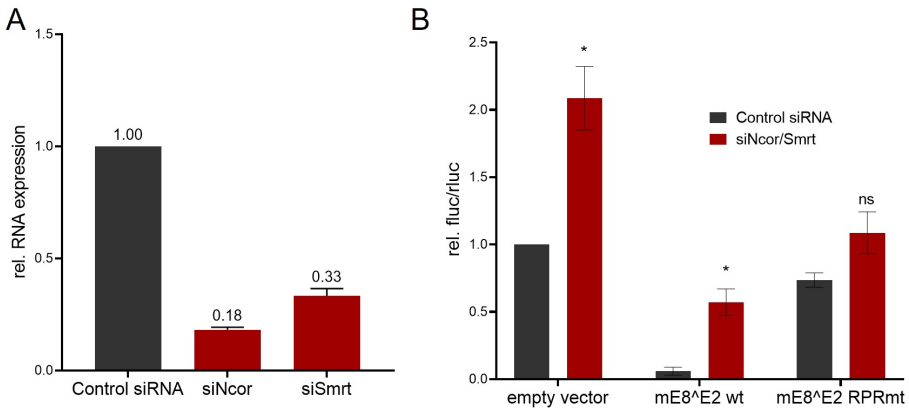

Figure 31: NCoR/SMRT complex mediates repression of transcription by mE8^E2 in NMTK. (**A**) Knockdown Efficiency of siRNAs for Smrt and Ncor1 in NMTK compared to control siRNA. (**B**) siRNA against Ncor1/Smrt relieves the repression of transcription in mouse keratinocytes. NMTK were transfected with siRNAs for Ncor1 and Smrt and 24 h later with the pC18-Sp1-luc reporter as well as the expression vectors for mE8^E2 wt or mE8^E2 RPR mt. Luciferase activities were determined 48 hpt. Averages from four independent experiments, error bars= SEM, ratio-paired t-test (ns, not significant; *, $P \leq 0.05$).
Figure from Kuehner et al., accepted for publication in mBio.

5.3.4 Higher expression of spliced viral transcripts in E8- and E8^E2 RPRmt MmuPV1 than wt in NMTK

I next evaluated the contribution of NCoR/SMRT complexes to gene expression from MmuPV1 wt, E8- or E8^E2 RPR mt genomes in NMTK. In the presence of control siRNA, E8^E2 RPR mt genomes displayed higher levels of *E1^E4* (13-fold), *E8^E2* (16-fold), and *URR^E4* (54-fold) transcripts than wt genomes (Figure 32). The simultaneous knock-down of Ncor1 and Smrt by siRNA significantly increased *E1^E4* (2.9-fold), *E8^E2* (2.5-fold), and *URR^E4* (7.1-fold) transcripts from wt genomes (Figure 32 B-D), but reduced transcription from E8- and E8^E2 RPR mt genomes. These data are consistent with the idea that mE8^E2 interacts with NCoR/SMRT complexes to limit viral gene expression in NMTK.

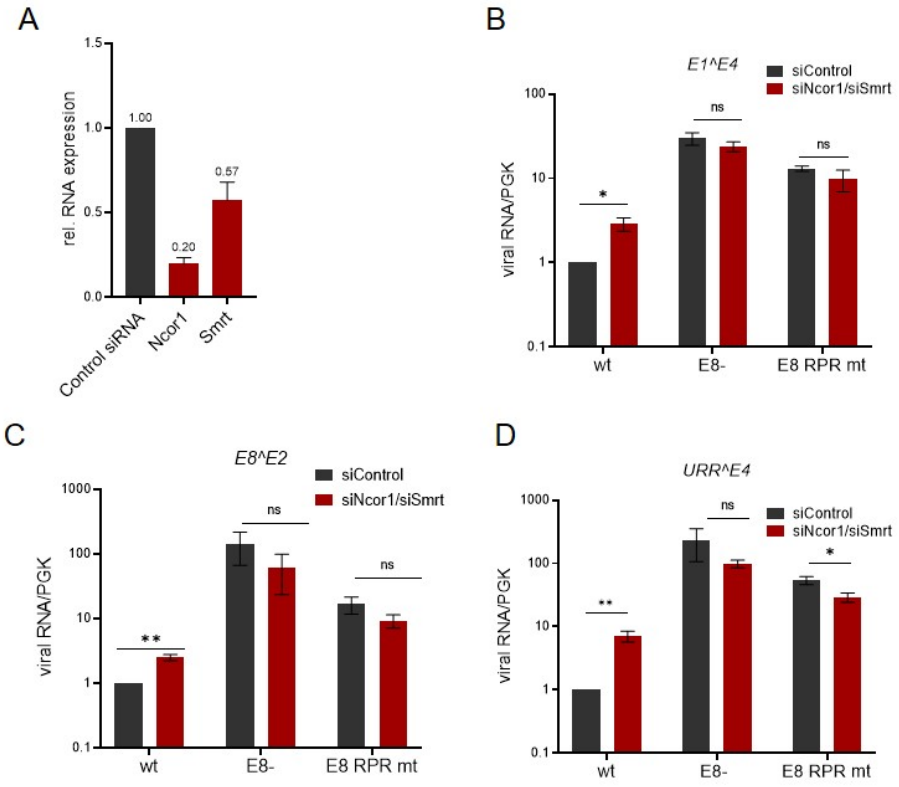

Figure 32: Increased expression of spliced viral transcripts from MmuPV1 E8- and E8 RPR mt genomes in NMTK. (**A**) Knockdown Efficiency of siRNAs for *Ncor1* and *Smrt* in NMTK compared to control siRNA determined by qPCR using PGK1 as a reference. (**B**-**D**) NMTK were transfected with ligated wt or mutant MmuPV1 genomes and transfected with control siRNA or siNcor/siSmrt the next day. RNA was harvested 5 dpt and qPCR was performed with *E1^E4*, *E8^E2* or *URR^E4* primers and *Pgk1* as a reference. Averages from four independent experiments, error bars= SEM, unpaired t-test, Log10 scale (ns, not significant; *, $P \leq 0.05$; **, $P \leq 0.01$).
Figure from Kuehner et al., accepted for publication in mBio.

5.3.5 Disruption of E8^E2 activity prevents tumor formation by MmuPV1 genomes in athymic nude Foxn1$^{nu/nu}$ mice

Next, it was determined if MmuPV1 E8 Stop mt, E8 SD mt, or E8^E2 RPR mt genomes induce warts Foxn1$^{nu/nu}$ mice using the wt genome as a control. Foxn1$^{nu/nu}$ mice are nude, athymic and T cell-deficient (Pantelouris, 1968), their phenotype is caused by null mutation of the transcription factor Forkhead Box N1 (Foxn1), which is an important regulator for thymus development as well as homeostasis (Vaidya et al., 2016). MmuPV1 genomes were introduced in two independent experiments in the tail skin of ten Foxn1$^{nu/nu}$ mice per genome and analyzed after 4 and 5 months, respectively. All *in vivo* animal studies were carried out by Margaret Wong and Richard B.S. Roden (Department of Pathology, The Johns Hopkins University). This revealed that the wt induced warts in 9/10 mice and the E8 Stop mt in 7/10 mice (Figure 33). In contrast, the E8 SD mt and E8^E2 RPR mt genomes failed to induce warts (0/10 and 0/9 mice respectively).

Study 1					
mouse #	Challenge DNA	tail warts	MmuPV1 DNA detected	MmuPV1 RNA Cq	*Capzb* RNA Cq
1	WT	Yes	Yes	X	20.13
2	WT	Yes	Yes	16.27	20.93
3	WT	X	Yes	14.33	20.27
4	WT	Yes	Yes	12.58	19.80
5	WT	Yes	Yes	14.46	20.04
6	E8 Stop mt	Yes	Yes	13.79	20.54
7	E8 Stop mt	X	Yes	19.20	20.77
8	E8 Stop mt	Yes, died[a]	Yes	n/a[a]	n/a[a]
9	E8 Stop mt	Yes, died[b]	Yes	n/a[b]	n/a[b]
10	E8 Stop mt	Yes	Yes	12.81	20.30
11	E8 SD mt	X	X	X	20.24
12	E8 SD mt	Yes, died[c]	n/a[c]	n/a[c]	n/a[c]
13	E8 SD mt	X	X	X	19.80
14	E8 SD mt	X	X	34.52	19.37
15	E8 SD mt	X	X	X	19.34
16	E8 RPR mt	X	X	X	19.62
17	E8 RPR mt	X	X	X	19.93
18	E8 RPR mt	X	X	X	19.51
19	E8 RPR mt	X	X	X	19.66
20	E8 RPR mt	X	X	X	19.80

Study 2					
mouse #	Challenge DNA	tail warts	MmuPV1 DNA detected	MmuPV1 RNA Cq	*Capzb* RNA Cq
1	WT	Yes	Yes	26.44	19.24
2	WT	Yes	Yes	14.51	19.09
3	WT	Yes	Yes	15.81	19.14
4	WT	Yes	Yes	15.08	18.88
5	WT	Yes	Yes	14.54	18.94
6	E8 Stop mt	Yes	Yes	12.82	18.39
7	E8 Stop mt	Yes	Yes	38.93	20.02
8	E8 Stop mt	Yes	Yes	35.39	19.00
9	E8 Stop mt	X	Yes	22.89	19.83
10	E8 Stop mt	X	Yes	24.38	20.00
11	E8 SD mt	X	X	X	19.30
12	E8 SD mt	X	X	X	18.63
13	E8 SD mt	X	X	X	18.53
14	E8 SD mt	X	X	X	18.79
15	E8 SD mt	X	X	X	18.97
16	E8 RPR mt	X	X	X	18.77
17	E8 RPR mt	X	X	X	18.47
18	E8 RPR mt	X	Yes	X	18.74
19	E8 RPR mt	X	X	X	18.56
20	E8 RPR mt	X	X	X	18.56

Figure 33: Disruption of E8^E2 binding to co-repressor by defined mutants prevents tumor formation by MmuPV1 genomic DNA in athymic nude Foxn1$^{nu/nu}$ mice. Wt and mutant MmuPV1 genomic DNA was introduced in the tail skin of five Foxn1$^{nu/nu}$ mice per genome in two different studies. All mice were euthanized and examined for tail warts (at 5 or 4 months after DNA challenge in studies 1 and 2 respectively), excepting animals that died at [a] 3.5 months, [b] 4 months and [c] 0.25 months post DNA challenge for unrelated reasons. Tail tissues were excised and analyzed for the presence of MmuPV1 DNA and transcripts. *In vivo* experiments were done by Margaret Wong and Richard B.S. Roden. Figure from Kuehner et al., accepted for publication in mBio.

Challenge sites were analyzed by qPCR for the presence of MmuPV1 mRNA and PCR for viral DNA. The presence of viral RNA at visible lesions could be confirmed, indicating that they were indeed viral warts. Except for one E8 SD mt challenged mouse where MmuPV1 mRNA was found, no mRNA was detected at sites without lesions. Viral sequences could be amplified by PCR from wt and E8 Stop mt DNA challenge sites but not the E8 SD mt or E8^E2 RPR mt challenges, with one exception (1/10 E8^E2 RPR mt). Sequencing of the PCR products confirmed the expected wt and E8 Stop mt genomes and ruled out contamination with wt virus. Interestingly, one mouse challenged with wt DNA produced tail warts positive for viral DNA but no mRNA was detected, possibly due to an integration event.
In summary, these data confirm and extend previous findings that MmuPV1 E8- genomes display increased gene expression in tissue culture but do not form warts or are maintained in the skin of athymic nude Foxn1$^{nu/nu}$ mice. These data strongly suggest that the complete inactivation of E8^E2 or expression of a repression-defective E8^E2 protein is incompatible with tumor growth *in vivo* even in the absence of T-cells.

5.3.6 E8^E2 regulates E4 expression from MmuPV1 genomes in cultured murine keratinocytes

The differentiation-dependent genome amplification of PV resembles the increased genome replication and expression of *E1^E4* and *L1* transcripts of E8^E2 mt genomes in undifferentiated NMTK. The loss of MmuPV1 E8^E2 might therefore induce the switch to productive replication and result in the expression of E4 in murine keratinocytes maintained in monolayer culture. To test this, I constructed an expression vector for HA-tagged MmuPV1 E4 and analyzed E4 protein expression 2 dpt in murine tail keratinocytes by IF (Figure 34 A). This revealed a complete absence of signals in empty vector-transfected cells for either anti-HA or anti-E4. The overlap of signals for anti-HA and anti-mE4 antibody in HA-E4 transfected NMTK (average Pearson correlation coefficient of 0.801 (range: 0.6451 - 0.950)) confirming the specificity of the E4 antiserum (Egawa et al., 2021). As expected, mE4 is mainly expressed as a cytoplasmic protein consistent with data for other PV E4 proteins.
Furthermore, E4-positive cells could be seen for murine keratinocytes transfected with wt, E8-, E8 Stop mt, E8 SD mt, or E8^E2 RPR mt genomes 2 dpt (Figure 34 B). However, the number of E4-positive cells appeared greatly increased in E8-, E8 SD mt and E8^E2 RPR mt compared to wt or E8 Stop mt transfected cells.

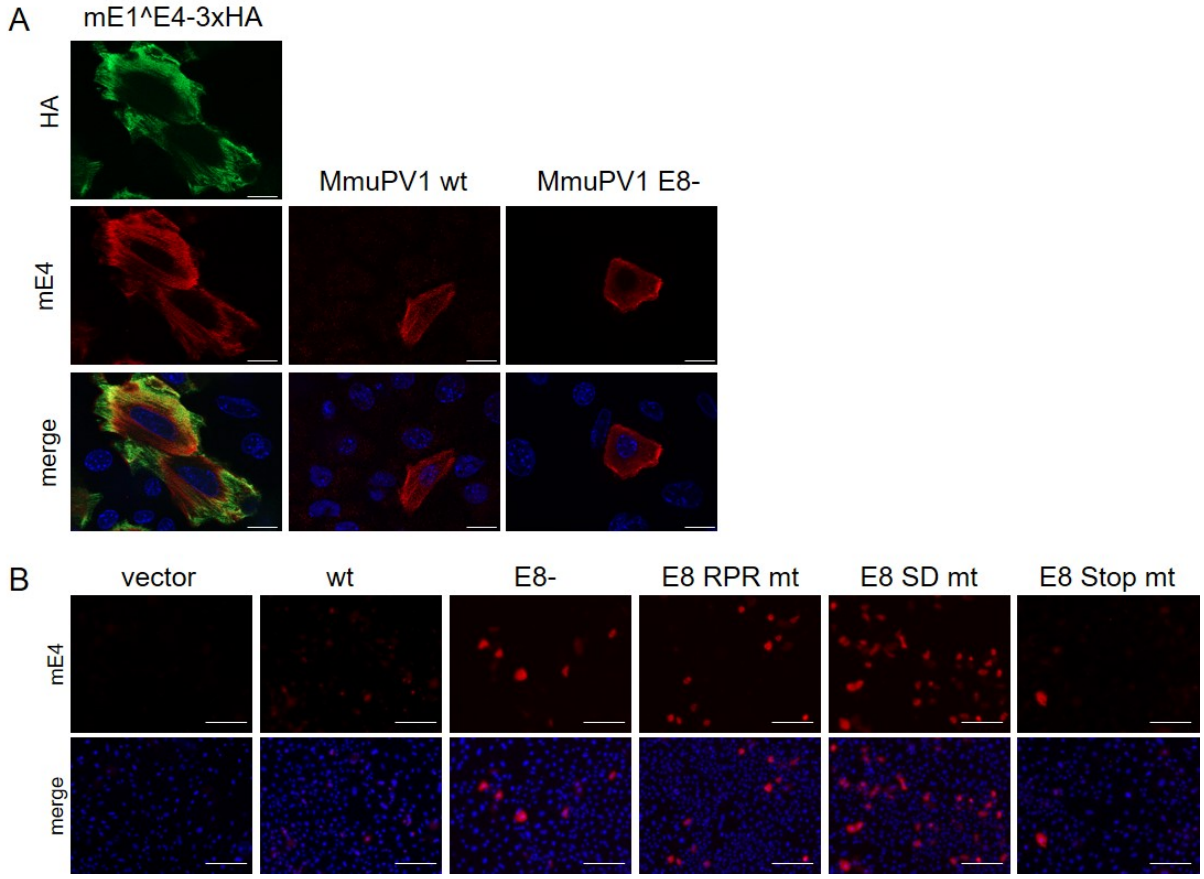

Figure 34: E8^E2 regulates E4 expression from MmuPV1 genomes in NMTK. (**A**) NMTK were transfected with mE1^E4-3xHA, MmuPV1 wt or E8- and stained 2 dpt with HA and mE4 antibodies (Egawa et al., 2021), magnification 630x, scale bar is 20 µm, n=3. (**B**) NMTK were transfected with MmuPV1 wt, E8-, E8^E2 RPR mt, E8 SD mt or E8 Stop mt genomes and fixed and stained 2 dpt with mE4 antibody, magnification 100x, scale bar is 200 µm, n=3. Figure from Kuehner et al., accepted for publication in mBio.

To quantify this more accurately, flow cytometry experiments were carried out (Figure 35). Consistent with the IF experiments, wt (0.33%) and E8 Stop mt (0.83%) transfected cells displayed much lower numbers of E4-positive cells than E8- (2.31%), E8 SD mt (3.36%) or E8^E2 RPR mt (1.99%) transfected cells. This indicates that the loss of functional E8^E2 induces expression of the late E4 protein.

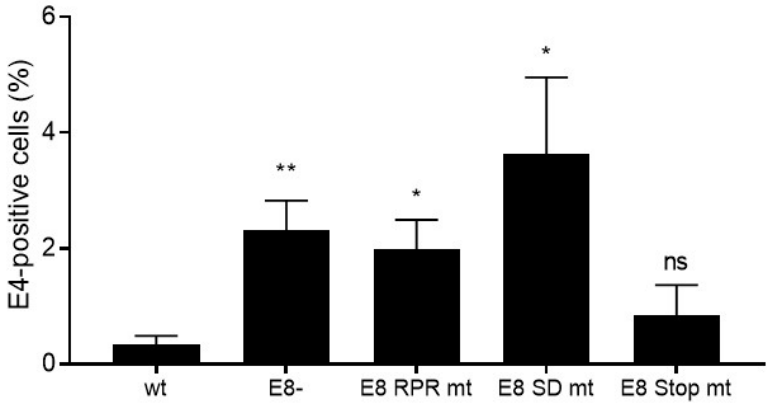

Figure 35: MmuPV1 E8^E2 mt genomes increase the percentage of E4-expressing cells. Flow cytometry analysis of NMTK 2 dpt transfected with MmuPV1 wt or different mt genomes using an anti-mE4 antibody. Data were analyzed with FlowLogic and the averages are derived from five independent experiments, error bars indicate the SEM. Statistical significance was determined by one way ANOVA and Fisher's LSD (ns, not significant; *, $P \leq 0.05$; **, $P \leq 0.01$).
Figure from Kuehner et al., accepted for publication in mBio.

HPV E4 expression has been linked to an arrest in the G2-phase of the cell cycle (Doorbar, 2013), I therefore quantified DNA content in E4-positive and -negative cells by flow cytometry. Propidium Iodide staining, which passes through permeabilized membranes and intercalates into cellular DNA, was used to analyze the cell cycle state, since the intensity of the PI signal is directly proportional to DNA content. In the G0/G1 phase cells are active and growing, in S phase, they are actively replicating DNA. In G2/M phase, cells are preparing for mitosis and contain twice the normal amount of DNA (Fried et al., 1976). Figure 36 A depicts the histograms, Figures 36 B, C and D show the Watson improved analysis to quantify the cell cycle states.

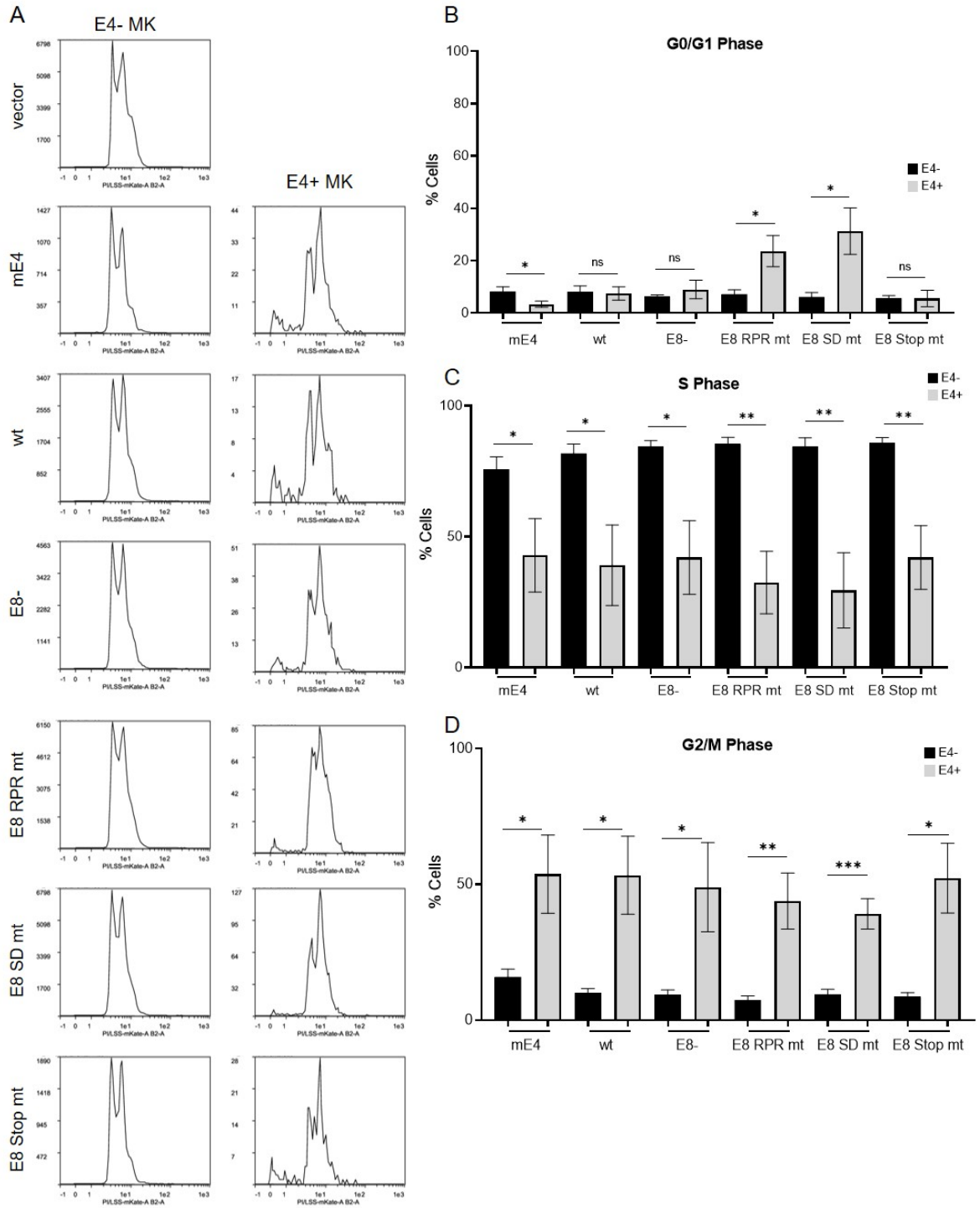

Figure 36: E4 protein expression changes the cell cycle profile in NMTK. Flow cytometry analysis of NMTK transfected with pSG5 (vector), pSG 3xHA-mE4 (mE4) or MmuPV1 wt or different mt genomes using anti-mE4 antibody and propidium iodide to stain DNA. (**A**) DNA content analysis in E4-negative and positive cells 2 dpt. Quantification of E4-negative and positive cell fractions in the G0/G1 (**B**), S (**C**), or G2/M (**D**) phase using FlowLogic and the Watson Improved analysis. Data are derived from 3 independent experiments and error bars indicate the SEM. Statistical significance was determined by unpaired t-test. (ns, not significant; *, $P \leq 0.05$; **, $P \leq 0.01$; ***, $P \leq 0.001$).
Figure from Kuehner et al., accepted for publication in mBio.

To understand if the loss E8^E2 overcomes the need for cellular differentiation, I stained NMTK after transfection of wt, E8-, E8^E2 RPR mt, and E8 SD mt genomes with markers for keratinocyte differentiation. Keratin 14 is a marker for basal-like keratinocytes, and keratin 10 is a marker for suprabasal keratinocytes (Hsu and Fuchs, 2022). Consistent with the culture of NMTK in serum free medium with a low concentration of Ca^{2+} to preserve their basal-like phenotype, almost all cells were positive for keratin 14 and only very few cells expressed keratin 10 (Figures 37). All E4-positive cells in wt and E8^E2 mt transfections were positive for keratin 14 (Figure 37 A), only a minority was positive for keratin 10 (14.5% (wt), 6.1% (E8-), 12.5% (E8 RPR mt), and 12.5% (E8 SD mt)) (Figure 37 B). This suggests that E4 expression in cultured mouse keratinocytes occurs mainly in cells with a basal-like phenotype.

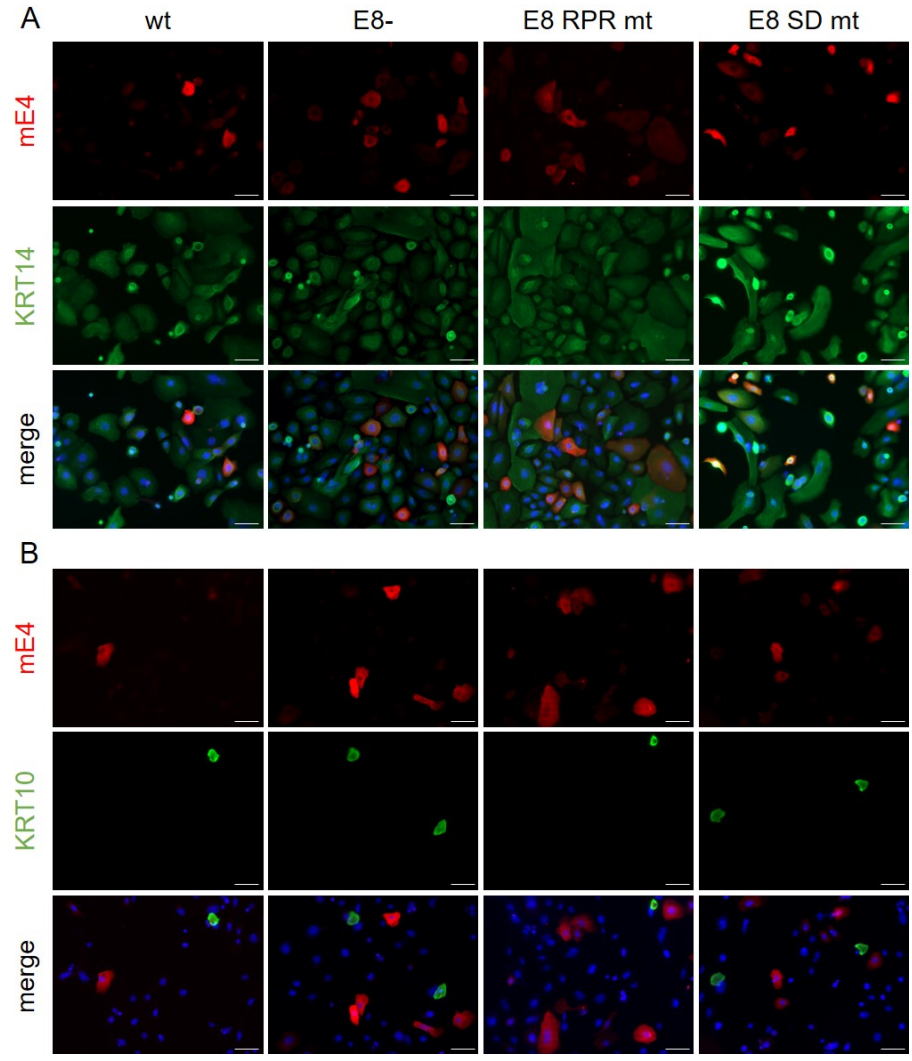

Figure 37: IF staining for mE4 and the keratinocyte differentiation markers keratin 14 and 10. NMTK were transfected with MmuPV1 wt, E8-, E8^E2 RPR mt, E8 SD mt genomes, fixed 2 dpt, and stained with anti-mE4 (red) and either **(A)** -keratin 14 (KRT14, green) or **(B)** -keratin 10 (KRT10, green) antibodies and DAPI to visualize DNA (blue). Magnification 200x, scale bar is 50 µm, n=2. Figure from Kuehner et al., accepted for publication in mBio.

To further evaluate if the loss of E8^E2 induces the late phase in cultured NMTK, I analyzed transcripts for the early *E6* and *E7* genes derived from the early P7503 and P360 promoters and the *E1^E4* and *URR^E4* transcripts that are mainly transcribed from the late P7107 and P533 promoters (Xue et al., 2017). To avoid the detection of genomes in the case of *E6* and *E7* as no splicing occurs in these genes, mRNA was isolated via polyA+ selection and then subjected to qPCR (Figure 38). *E6* levels were 2.5-fold increased at 3 dpt, and 6-fold at 6 dpt in E8- compared to wt-transfected cells. Similar increases were observed for *E7* levels. However, *E1^E4* levels were increased 16.4-fold (3 dpt) and 17.6-fold (6 dpt) and *URR^E4* levels were activated 29.6-fold (3 dpt) and 33.8-fold (6 dpt). This strongly indicates that the loss of mE8^E2 activates viral late transcription to a much greater extent than viral early transcription consistent with a switch to the productive phase.

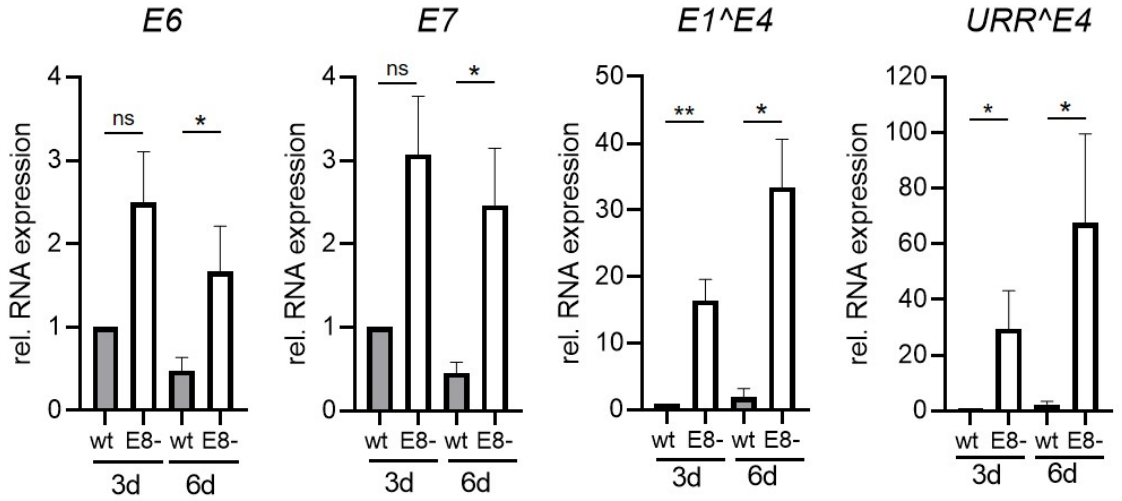

Figure 38: MmuPV1 E8- genomes preferentially increase viral late transcripts. NMTK were transfected with the indicated MmuPV1 genomes and RNA was harvested 3 dpt or 6 dpt. Poly-A+ RNA was analyzed by qPCR to detect *E6*, *E7*, *E1^E4* or *URR^E4* transcripts and *Pgk1* as a reference. Averages are derived from three independent experiments and are presented relative to the wt on day three. Error bars indicate the SEM. Statistical significance was determined by a ratio-paired t-test (ns, not significant; *, $P \leq 0.05$; **, $P \leq 0.01$).
Figure from Kuehner et al., accepted for publication in mBio.

6 Discussion

6.1 Deregulation of host gene expression by HPV16 E8^E2 is due to enhanced productive replication

The inactivation of E8^E2 in HPV16 genomes leads to increased viral gene expression and genome replication in undifferentiated cells and late viral protein expression in organotypic cultures (Lace et al., 2008; Straub et al., 2014). To gain insight into E8^E2's role, the host cell transcriptome of HPV16 wt and E8- cell lines grown in organotypic cultures was analyzed. This revealed only a small number of deregulated cellular genes. I then further investigated the *ATF3*, *CYR61*, *PDL1* and *ULBP1* host genes and was able to validate their upregulation in E8- cell lines only in organotypic cultures but not in undifferentiated cells maintained in monolayer culture (Figure 9).

6.1.1 Increased expression of viral late transcripts but not early transcripts contribute to the deregulation of cellular genes

There was a strong correlation of *ATF3*, *PDL1* and *ULBP1* transcript levels with viral late *E1^E4* and *E4^L1*, but not early *E6*I* transcripts (Figure 11). This might indicate that the differential gene expression is a consequence of increased genome amplification and late promoter induction, which is consistent with a greater number of E4-expressing cells in E8- compared to wt organotypic cultures (Straub et al., 2014).

6.1.2 E4 and E5 contribute to the productive replication cycle of HPV16

Both E4 and E5 have been reported to contribute to the productive replication cycle of HPV16 and the closely related HPV31 (Egawa and Doorbar, 2017; Fehrmann et al., 2003; Genther et al., 2003; Nakahara et al., 2005; Wilson et al., 2005). To modulate genome amplification, the E8- mutation was combined with an E4- or E5- mutation. No influence of E4- or E5- on viral copy numbers in undifferentiated E8- monolayer cultures could be observed, whereas in organotypic cultures viral copy numbers only increase in E8-, but not in E8-/E4- or E8-/E5- cell lines (Figure 12 A). Furthermore, spliced *E1^E4* and *E4^L1* transcripts, mainly derived from the viral late promoter P670, were also reduced in the double knockout cell lines (Figure 13). Likewise, expression of deregulated host cell genes was reduced upon the additional inactivation of E4 or E5 (Figure 14). These data confirm that E4 and E5 contribute to the productive replication cycle of HPV16 and strongly indicate that the differentiation-dependent deregulation of host cell gene expression in HPV16 E8- cell lines is a consequence of the increased number of cells entering the productive cycle. This suggests for the first time that productive replication impacts the host transcriptome.

6.1.3 Integration of HPV genomes and the productive replication cycle

Cell lines with exclusively integrated HPV genomes do not enter the productive replication cycle (Frattini et al., 1996). The identification of changes due to productive replication is further complicated by the use of mixed cell populations, which is likely responsible for the large degree of variability in viral and host cell gene expression observed. A significant fraction of wt and E8- positive cells harbor integrated genomes (Figure 8 B), determined with the exonuclease V resistance assay that enables distinguishing between extrachromosomal and integrated viral genomes in a quantitative manner (Myers et al., 2019). Bulk analyses of uninfected and infected cells (Bienkowska-Haba et al., 2020; Chatterjee et al., 2019) may have missed those changes since only a fraction of HPV16 cells in organotypic cultures enter the productive cycle (Nakahara et al., 2005; Straub et al., 2014). This could be circumvented by single cell RNA sequencing (scRNA-seq). Nevertheless, in summary our data strongly suggest that the productive replication cycle of HPV16 induces host cell gene changes that have not been reported before.

6.1.4 Role of *ATF3*, *CYR61*, *PDL1* and *ULBP1* in the productive replication cycle

It is currently unclear if *ATF3*, *CYR61*, *PDL1* or *ULBP1* play a direct role in the productive replication cycle. ATF3 has been reported to interact with HPV16 E6. Overexpression of ATF3 in the cervical cancer cell line SiHa results in the activation of p53, cell cycle arrest and apoptosis (Wang et al., 2010). Furthermore, ATF3 was recently described to mediate apoptotic functions through a p53-independent pathway in HeLa cells (Kooti et al., 2022). The overexpression of *ATF3* in HPV16-positive CaSki cells was shown to lead to a significant cell cycle arrest in the G1 phase, as well as a significant reduction of nuclear factor kappa B (NF-kB) level (Akbarpour Arsanjani et al., 2022). Unfortunately, the stable knock-down of ATF3 in HPV16 E8- cell lines using different shRNA expression constructs was not achievable during this thesis (data not shown), making it impossible to address its influence on viral replication in organotypic cultures. Global expression profiling of HaCaT cells, transfected with HPV genomes to identify interactions between HPV and the host cell at early stages of infection, identified *CYR61* upregulation by high-risk HPV16 and -45 (Kaczkowski et al., 2012). Furthermore, *CYR61* has been described as an *ATF3* target gene in hepatocellular cancer cell lines (Chen et al., 2018). However, *CYR61* expression, in contrast to *ATF3*, does not correlate with viral late expression (Figure 11), suggesting that this regulation does not occur in HPV16-positive keratinocyte cell lines. Furthermore, while the deregulation of *CYR61* is independent from late viral transcript expression, it still is modulated by E4 and E5 (Figure 14), indicating that several pathways regulate differential host gene expression in E8- cell lines. *PDL1* and *ULBP1* are known to be involved in directing T-cell and natural killer cell responses towards tumor and virus-infected cells (Schmiedel and Mandelboim, 2018; Sharpe and Pauken, 2018). Thus, they do most likely do not play a direct role in the productive replication cycle, but may modulate immune responses

towards HPV16. While high expression of *ULBP1* is an indicator of good prognosis in cervical cancer (Cho et al., 2014), numerous studies for PD-1 and PDL1 inhibitors as monotherapy or as part of combination therapy for cervical cancer were conducted in recent years (Colombo et al., 2021; Friedman et al., 2020; Lan et al., 2020; Naumann et al., 2019; O'Malley et al., 2021; Rischin et al., 2020; Tewari et al., 2021). Interestingly, MmuPV1 E8- genomes do not induce warts in T-cell deficient mice, making it unlikely that an upregulation of *PDL1* contributes to the failure to induce warts (Stubenrauch et al., 2021).

6.2 Characterization of HPV16 E2 and E8^E2

E2 is involved in the viral DNA replication, genome maintenance, and transcription and is expressed at early and intermediate stages of the viral life cycle. E8^E2 mediates transcriptional repression of the viral promoter (Kuehner and Stubenrauch, 2022). To better understand E2 and E8^E2 expression in HPV positive cell lines, I purified the HPV16 E2 protein for antibody generation. Due to the lack of protocols in the literature for the purification of HPV16 E2 hinge and DBD and the vague description in Xue et al., 2010, protocols for purification of HPV16 E2 DBD (Hegde and Androphy, 1998; Sanders and Maitland, 1994; Mok et al., 1996), HPV31 E2 DBD (Bussiere et al., 1998) and full length cottontail rabbit papillomavirus E2 (Schneider et al., 2020) were consulted. The codon optimized HPV16 E2 fragment was expressed as a His-MBP-TEV-HPV16 E2C fusion protein (E2 hinge aa202-286, DBD/Dimerization aa286-365) in *E. coli* BL21(DE3), purified and cleaved (Purification strategy described in 4.2.6) before sending it off for antibody production to Davids Biotechnology. Additionally, the monoclonal HPV16 E2 antibody B9, kindly provided by Andreas Wieland (Wieland et al., 2020), was used to validate the following results further.

6.2.1 Validation of HPV16 E2 antibody specificity

Both the polyclonal E2 antibody as well as the monoclonal B9 antibody were able to detect transfected HPV16 E2, HPV16 E8^E2 and HPV16 E8^E2 KWK mt proteins in C33A cells in western blot (Figure 19). The signal for both antibodies colocalized in an immunofluorescence assay where C33A cells were transfected with expression vectors encoding HPV16 E2 and E8^E2 (Figure 21). Furthermore, the HPV16 E2 antibodies were validated with an IP assay (Figure 20). All together, these data clearly demonstrated the specificity of the 16E2 antibodies and made further experiments in the characterization of E2 and E8^E2 possible.

6.2.2 Localization of HPV16 E2 in replication foci

Since both antibodies recognized transfected HPV16 E8^E2 and E2, NHK cell lines immortalized by either HPV16 E6/E7, HPV16 wt or E8- genomes were stained next. The nuclei of HPV16 wt and E8- cell lines showed clear E2 foci of different sizes (Figure 22), which were generally bigger and more abundant in HPV16 E8- than in wt cell lines. Papillomaviruses are

dependent on the host replication machinery for replication of their genome, it is known that the PV E1 proteins bind RPA and recruit it to sites of DNA replication (Han et al., 1999; Loo and Melendy, 2004). Furthermore, HPV DNA foci indicate compartments that contain actively replicating genomes (Gillespie et al., 2012). CIN 612 cell, stably maintaining HPV31 genomes (De Geest et al., 1993), were stained by IF for RPA32 followed by fluorescence in situ hybridization (FISH) to visualize HPV DNA, the localization of RPA32 to HPV DNA foci suggested that these were sites of viral DNA synthesis (Gillespie et al., 2012). Some, but not all of the E2 foci colocalized with the replication protein RPA32 (Fairman and Stillman, 1988; Liu and Weaver, 1993; Wobbe et al., 1987) in E8- cell lines (Figure 24), indicating that they were replication foci. It was described before that undifferentiated HPV16 cell lines show an increase in early and late transcripts in the absence of E8^E2 (Straub et al., 2014), this derepression might contribute to the higher number of E2 foci in HPV16 E8- cell lines. The inhibition of E1/E2 dependent-origin replication by E8^E2 does not only result from binding site competition between E2 and E8^E2 since the E8 part has repression activity on its own (Ammermann et al., 2008; Zobel et al., 2003). PV E2 proteins can associate with the cellular Brd4 (Bromodomain-containing protein 4) protein and DNA damage response markers. These foci do not contain viral DNA and are hypothesized to be immature nuclear foci (Baxter et al., 2005; Iftner et al., 2017; Jang et al., 2014; McPhillips et al., 2005; Sakakibara et al., 2013; You et al., 2004), which might explain the RPA negative HPV16 E2 foci.
Since the levels of integration were similar for the HPV16 wt and E8- cell lines I tested (Figure 12), it is unlikely that the integration frequency is the reason for lower foci numbers in HPV16 wt cell lines. Productive replication of HPV is characterized by genome amplification and expression of the E4 protein (Grassmann et al., 1996; Hummel et al., 1992; Pray and Laimins, 1995; Sterling et al., 1993) and takes place within suprabasal, differentiated keratinocytes, positive for the suprabasal keratinocyte differentiation marker keratin 10 (Coulombe et al., 1991; Fuchs and Green, 1980). The loss of HPV16 E8^E2 possibly leads to spontaneous differentiation and productive replication. Consistent with that, many HPV16 E2 positive cells expresses the late viral E4 protein (Figure 25 A). Furthermore, E4 positive cells express the suprabasal keratinocyte differentiation marker K10 (Figure 25 B).

6.2.3 HPV16 *E2* transcripts versus HPV16 E2 protein

The HPV16 genome can be either maintained extrachromosomally as episomes or can be integrated in the host genome, both forms can even coexist in the same cell (Arias-Pulido et al., 2006; Huang et al., 2008; Li et al., 2008; Matovina et al., 2009; Tsakogiannis et al., 2014). Integration of the virus can result in the disruption of the E1 and/or E2 ORFs, transcriptional activation of the viral oncogenes E6 and E7, loss of function of tumor suppressor genes, inter- and intrachromosomal rearrangements, as well as changes in global promoter methylation and transcription that can lead to carcinogenesis (Akagi et al., 2014; Kadaja et al., 2009; Rusan et al., 2015; Tsakogiannis et al., 2015; Wentzensen et al., 2004; Xu et al., 2013). There is no

expression of E2 in the vast majority of HPV-associated cervical cancers (Nulton et al., 2017; Skeate et al., 2016). Cervical intraepithelial neoplasia (CIN) I/II stained with a polyclonal rabbit antiserum that recognized the C-terminal domain of HPV16 E2, resulted in a signal in the intermediate or upper layers but never in the basal layers of the lesions. In CIN III this expression was either maintained in upper layers or completely lost. Due to the nature of the antibody, the distinction of 16E2 and E8^E2 is unfortunately impossible (Xue et al., 2010). Maitland and colleagues also saw E2 expression in the intermediate and upper layers of CIN especially in koilocytes, which are squamous epithelial cells with perinuclear cavitation, nuclear enlargement, coarse chromatin, and irregular nuclear membranes (Krause et al., 2022; Maitland et al., 1998). Both full-length and repressor forms of E2 protein were detectable in BPV1 infected wart tissue at low levels along the basal cell layer and at high levels in a some cells in the spinous layer (Burnett et al., 1990; Penrose and McBride, 2000). HPV6 E2 could be detected in nuclei in the middle and upper layers of genital warts and laryngeal papillomas (Sekine et al., 1989).
My immunofluorescence assay of different HPV positive cell lines (Figure 22) confirmed the expression of HPV16 E2, but also revealed a relatively low expression level. The HPV16 E2 foci could be only found in a fraction of cells and not all of them. Furthermore, I was able to detect HPV16 E8^E2 protein in a HPV16 E8 KWK mt cell line by immunoblot (Figure 23), but not E2. The inevitable use of mixed cell population with integrated and episomal PV genomes might explain this.
Expression of HPV16 E2 protein in normal, spontaneously immortalized keratinocytes stably transfected with HPV16 genomes (NIKS16) (Allen-Hoffmann et al., 2000; Isaacson Wechsler et al., 2012), differentiated by culturing to high density in 1.2 mM Ca^{2+} media, could only be observed after 13 days and not mid-differentiation (8 days), indicating the importance of differentiation for E2 expression (Klymenko et al., 2017).
Even though it was described that E2 RNA levels in HPV16 E8- and E8 KWK mt cell lines were significantly increased compared to wt cell lines (4 and 3.8-fold) (Straub et al., 2014), immunoprecipitation with an E2 antibody (Figure 23) did not detect E2 protein. Interestingly, the cervical squamous cell carcinoma cell line CaSki (Pattillo et al., 1977), harboring truncated but also full-length HPV16 integrates with an intact E2 region (Baker et al., 1987; Mincheva et al., 1987), have been shown to transcribe all HPV16 early genes including *E2* (Schmitt and Pawlita, 2011), but lack E2 protein expression (Xue et al., 2012). Intriguingly, a similar phenotype was also described for clinical samples of various grades of HPV16-associated cervical neoplasias: the E2 ORF was not always disrupted and transcripts reduced by integration of the viral DNA in the cellular genome, on the other hand expression of the E2 protein was always drastically reduced. This suggests that downregulation of the E2 protein expression has to be mediated by additional pathways linked to either transcriptional or translational control (Xue et al., 2012).

6.3 Inactivation of the MmuPV1 E8^E2 protein induces late E4 protein expression but prevents wart formation

Papillomaviruses replicate and propagate in keratinocytes. A key property of all PV investigated is, that productive genome replication, capsid protein expression and synthesis of infectious progeny only occur in the suprabasal layers of the epithelium which consist of keratinocytes that have entered their terminal differentiation program. In line with keratinocyte differentiation being required for productive replication, the propagation of HPV *in vitro* only occurs in organotypic keratinocyte cultures which strongly resemble differentiated epithelium *in vivo*. Despite intensive research, the key differentiation events required for HPV propagation are only partially understood. A hallmark for the start of productive replication in suprabasal keratinocytes is the activation of the viral late promoter in *E7* and genome amplification which results in the abundant expression of the viral E4 protein (Grassmann et al., 1996; Hummel et al., 1992; Pray and Laimins, 1995; Sterling et al., 1993).

6.3.1 Mutation of the MmuPV1 E8 splice donor but not a stop codon in E8 increases viral transcription

Previous studies have shown that the knock-out of E8^E2 expression in different HPV types results in increased genome replication and viral gene expression in undifferentiated cells (Lace et al., 2008; Straub et al., 2014). The mutation of the putative start codon for E8^E2 in the MmuPV1 genome (E8-) resulted in increased viral transcription in undifferentiated NMTK. Surprisingly, despite being more transcriptionally active, MmuPV1 E8- genomes were unable to induce warts or being maintained in tail or vaginal epithelium of T-cell deficient mice (Stubenrauch et al., 2021). To validate that this phenotype is caused by a lack of E8^E2 expression, additional mutations disrupting E8^E2 expression were generated. Mutation of the conserved E8 splice donor site (E8 SD mt) greatly increased viral gene expression in undifferentiated NMTK consistent with the spliced E8^E2 transcript being responsible for the translation of an inhibitory protein. Surprisingly, the introduction of a translation termination codon at codon 9 of E8 did not increase viral gene expression (Figure 26 B). Transcript analyses revealed that this mutation accidentally created a novel splice donor at nt 1116 leading to a transcript in which the stop codon and also E8 residues 9-11 are removed (Figure 26 D). The analysis of mE8^E2 d9-11 expression constructs revealed that this protein acts a transcriptional repressor comparable to wt mE8^E2 (Figure 27 B+C). Thus mE8^E2 d9-11 may compensate for mE8^E2 expression and prevent the induction of viral gene expression. Consistent with E8 residues 9-11 not being important for repression activity, G9 and A10 are not conserved and conserved S11 is followed by three consecutive serines which may compensate for the loss of S11 (Figure 28 A). Mutation of residues 8 to 12 in HPV31 E8^E2 also had no impact on transcriptional repression supporting the idea that this part of E8 is not important for the repression activity (Stubenrauch et al., 2001).

6.3.2 Lack of repression by mE8^E2 correlates with binding to NCoR/SMRT complexes

High risk HPV16 and 31 and beta-HPV8 E8^E2 proteins interact via conserved residues in E8 (K5/W6/K7 in HPV16 and 31; K2/L3/K4 in HPV8) with NCoR/SMRT complexes to inhibit transcription and replication (Dreer et al., 2016). In line with this, mutation of K2/L3/K4 residues of mE8^E2 attenuates the repression of transcription and replication reporters in human and mouse cells by mE8^E2 and also increases transcription from MmuPV1 genomes in keratinocytes. Furthermore, mE8^E2 interacts with GPS2, HDAC3, TBLR1 and TBL1 which are different components of NCoR/SMRT complexes in co-immunoprecipitation assays in a KLK-dependent manner (Figure 28). SiRNA knockdown experiments confirm that NCoR and SMRT or HDAC3 and TBLR1 relieve repression in an E8^E2 dependent manner (Figure 30 B+C). Interestingly, the single knock-down of GPS2 had no impact on E8^E2 repression activity indicating that repression is largely independent from GPS2 and also that GPS2 cannot be the unknown direct interactor in NCoR/SMRT complexes of E8^E2 proteins (Figure 30 E+F). These data confirm that E8^E2 proteins from animal and human PV use NCoR/SMRT complexes to limit viral gene expression and replication.

6.3.3 Disruption of E8^E2 activity prevents tumor formation by MmuPV1 genomes in athymic nude Foxn1$^{nu/nu}$ mice

Consistent with the phenotype of the MmuPV1 E8- genome, E8 SD mt and E8 RPR mt genomes displayed increased viral gene expression in cultured NMTK but failed to induce tail warts in athymic Foxn1$^{nu/nu}$ mice (Figure 33). This strongly suggests that the loss of E8^E2 activity by a complete knock-out (E8-, E8 SD mt) or by an interference with its repression activity (E8 RPR mt) is responsible for increased gene expression from viral genomes and the failure to induce warts *in vivo*. The increase in *E1^E4* as well as *E4^L1* transcripts pointed to the possibility that a loss of E8^E2 activity facilitates the switch to the productive phase in cells being maintained in an undifferentiated state (serum free medium, low Ca^{2+}). Consistent with this idea, E8^E2 mt genomes displayed a greatly increased number of cells expressing the late viral E4 protein (Figure 35). This suggests that the loss of E8^E2 induces productive replication.

6.3.4 E8^E2 regulates E4 expression from MmuPV1 genomes in NMTK

Remarkably, MmuPV1 E8^E2 mt genomes displayed an increased number of cells expressing the late viral E4 protein in monolayer culture. Expression of HPV E4 proteins has been shown to induce a G2 arrest in monolayer cultures independent from other viral gene products (Davy et al., 2002; Knight et al., 2004; Nakahara et al., 2002). The expression of mE4 from wt or mt MmuPV1 genomes in NMTK induces a shift in the cell cycle consistent with a G2 arrest. Remarkably, almost all E4-positive cells stained positive for keratin 14, a marker for basal keratinocytes, but were only very rarely positive for keratin 10, a marker for suprabasal keratinocytes (Figure 37). The analysis of L1 expression of these cells would certainly be very

interesting. This strongly indicates that the loss of mE8^E2 greatly increases the probability to induce productive replication independent from keratinocyte differentiation. This is further supported by the finding, that the late *E1^E4* and *URR^E4* transcripts are induced to a much greater extent than the early *E6* and *E7* transcripts from E8- genomes. The induction of E4 protein expression from HPV31 E8^E2 mt genomes in undifferentiated keratinocytes may also explain the inability to stably maintain these genomes as autonomously replicating elements. However, replicating HPV16 E8^E2 mt genomes can be maintained in keratinocytes and the number of E4-positive cells is increased only in the suprabasal layers in organotypic cultures (Straub et al., 2014). This suggests that HPV16, in contrast to MmuPV1, may require in addition to the loss of E8^E2, a second differentiation-dependent signal to initiate productive replication. Consitent with this, HPV16 E4 positive cells were sometimes K10 positive (Figure 37).
Similarly, HPV49 E8- genomes can be stably maintained at high extrachromosomal copy numbers in undifferentiated keratinocytes suggesting that HPV49 may also require a differentiation signal to efficiently express E4 or that the HPV49 E4 protein has different activities than the mE4 protein. However, since *E6* and *E7* levels are also induced upon a loss of E8^E2 (Figure 38; Lace et al., 2008; Rehm et al., 2022b; Rehm et al., 2022a; Straub et al., 2014; Stubenrauch et al., 2000) it is also possible, that not only E4, but also the activities of E6 and E7 determine the fate of E8^E2 mt genomes. Cell cycle analyses indicated that mE4-expressing keratinocytes are preferentially in the G2/M compared to the S and G1/G0 phase. This is consistent with findings that HPV E4 proteins induce a G2-arrest in undifferentiated cells (Davy et al., 2002; Knight et al., 2004; Nakahara et al., 2002). HR-HPV genome amplification and E4 protein expression in differentiated keratinocytes preferentially takes place in the G2 phase, these cells then exit the cell cycle and do not undergo cell division before being shed from the epithelium (Banerjee et al., 2011; Wang et al., 2009). Based on the tissue culture data, it can be proposed that the infection of basal layer keratinocytes with MmuPV1 E8^E2 mt genomes greatly enhances the probability of an immediate switch to the productive replication phase leading to genome amplification which induces high-levels of E4 protein. The resulting shift to the G2 phase prevents the cells from dividing. This would prevent an efficient expansion of infected cells in the basal layer and in turn the development of warts. Furthermore, the DNA content analysis provided evidence that a small fraction of E4-positive cells undergoes cell death which is consistent with the induction of apoptosis by HPV16 E4 in HeLa cells (Raj et al., 2004). This would further diminish the number of infected cells over time and could account for the complete absence of viral RNA and DNA at E8- infected sites (Stubenrauch et al., 2021).

6.3.5 E8^E2 as a possible therapeutic target

HPV E8^E2 was hypothesized to be part of a copy number control mechanism required to maintain viral genomes in dividing cells at a low, but relatively constant copy number (Straub et al., 2015). The highly conserved E8^E2 might represent an attractive anti-viral target even in settings without functional T-cells (Stubenrauch et al., 2021). HPV16 E8^E2 mt genomes

express high levels of E4 only in suprabasal, differentiated cells indicating that HPV16 uses additional mechanisms to prevent productive replication in undifferentiated cells (Straub et al., 2014). My data suggest that the primary function of MmuPV1 E8^E2 is to prevent the initiation of productive replication in basal-like cells in order to allow for lateral expansion of infected cells and thus maximizing virus production. The manipulation of E8^E2 activity in lesions might have the unintended consequence of enhancing productive replication and virion production. However, it is also possible that an inappropriate induction of the viral late phase in more basal cells, which are not destined for this, might interfere with cell survival or lesion growth and thus have a therapeutic effect. While the tissue culture data for HPV16 argue against a clinical benefit of an interference with E8^E2, it is still possible that the outcome might be different *in vivo*. However, one should also consider that an interference with E8^E2 activity might induce malignant tumors from HPV49-infected cells (Rehm et al., 2022b). Nevertheless, different patient groups have been identified which display generalized wart or papilloma growth and recent data suggest that this is often due to an inherited immunodeficiency (Béziat et al., 2021). Since E8^E2 is highly conserved and required for wart growth in T-cell deficient mice, such patients might benefit from an inhibition of E8^E2. The high conservation of E8^E2 and the observation that the inactivation of E8^E2 facilitates the switch to the productive phase makes it likely that the inhibition by E8^E2 needs to be at least partially overcome to allow the differentiation-dependent switch in wt infected cells. Data obtained for HPV16 and 31 do not indicate that E8^E2 expression is transcriptionally down-regulated upon differentiation (Stubenrauch et al., 2000; Straub et al., 2015). However, it has been proposed that the activation of the late promoter leads to increased E2 protein levels which might out-compete E8^E2 protein levels (Klumpp and Laimins, 1999; Zheng et al., 2020). Therefore, it might be worthwhile to identify means to interfere with E8^E2´s activity in order to evaluate if E8^E2 is a suitable target for the treatment of HPV infections. In summary, MmuPV1 E8^E2 may inhibit E4 protein expression to prevent a cell cycle arrest in order to enable the expansion of infected cells in the basal layer which is required for wart formation *in vivo*. Future studies are required to understand how E2 and E8^E2 regulate productive genome amplification and late gene expression in differentiating cells, which might be useful to combat persistent infections and decrease HPV-related cancer cases.

7 Abbreviations

µl	microliter
µg	microgram
µm	micrometer
$^{\circ}C$	Degrees Celsius
aa	Amino acid
AP1	Activator protein 1
ATM kinase	Ataxia telangiectasia mutated kinase
ATP	Adenosine triphosphate
BRD4	Bromodomain-containing protein 4
BSA	Bovine serum albumin
C	Cysteine
CAPS	Cyclohexaminopropanesulfonic acid
cDNA	Complementary DNA
Chk2	Checkpoint kinase 2
CIN	Cervical intraepithelial neoplasia
CK2	Casein kinase 2
CP	Crossing point
CRPV	Cottontail rabbit papillomavirus
CS	Calf serum
cSCC	Cutaneous squamous cell cancer
CYR61	Cysteine-rich angiogenic inducer 61, also known as CCN1
DAPI	4,6-diamidine-2-phenylindole
DBD	DNA binding and dimerization domain
ddH_2O	Double deionized water
DDR	DNA damage response
DEPC	Diethylpyrocarbonate
DMEM	Dulbecco's Modified Eagle Minimum Essential Medium
DMSO	Dimethyl sulfoxide
DNA	Deoxyribonucleic acid
dNTP	Deoxyribonucleoside triphosphate
dpt	days post transfection
DTT	Dithiothreitol
E	Early genes or early gene products of HPV or or glutamic acid
E. coli	*Escherichia coli*
E1BS	E1 binding sites
E2BS	E2 binding sites
EDTA	Ethylenediaminetetraacetate

EGF	Epidermal growth factor
EGFR	Epidermal growth factor receptor
EtOH	Ethanol
EV	Epidermodysplasia verruciformis
F	Forward for primers in a PCR
FCS	Fetal calf serum
FISH	Fluorescence in situ hybridization
Fluc	Firefly luciferase
FOXN1	Forkhead Box N1
h	Hours
HA	Hemagglutinin
HC-FKS	Defined fetal calf serum
HDAC3	Histone deacetylase 3
HIF1α	Hypoxia-inducible factor 1 α
HNSCC	Head and neck squamous cell carcinoma
hpt	hours post transfection
HR	High Risk
IgG	Immunoglobulin G
IMAG	Institute for Medical Genetics and Applied Genomics
IP	Immunoprecipitation
ISG	Interferon stimulated gene
ISGF3	Interferon stimulated gene factor 3
JNK	c-Jun N-terminal kinase
kb	Kilobase(s)
KDM6A	L ysine-specific demethylase 6A
KSFM	Keratinocyte serum-free medium
L	Late reading frame of papillomavirus or leucine
LB	Complex medium for bacterial culture (lysogeny broth)
log2FC	Log2 fold change
LR	Low risk
Luc	Luciferase gene
M	Molar
mAb	Monoclonal antibody
MAML1	Mastermind-like protein 1
MAPK	Mitogen-activated protein kinase
MBP	Maltose binding protein
min	Minutes
MmuPV1	Mus musculus papilloma virus 1

mRNA	Messenger RNA
NCoR1	Nuclear Receptor Corepressor 1
NCoR2/SMRT	Nuclear Receptor Corepressor 2, also known as SMRT
NF-κB	Nuclear factor kappa B
NHK	Normal human keratinocytes
NIKS	Normal, spontaneously immortalized keratinocytes
NLS	Nuclear localization signal
NMTK	Normal mouse tail keratinocytes
NRs	Nuclear hormone receptors
nt	Nucleotide
NTD	N-terminal domain
N-terminal	amino-terminal
o/n	Over night
OD	Optical density
ORA	Over-representation analysis
ORF	Open reading frame
ORI	Origin of replication
padj	Adjusted P-value
PAGE	Polyacrylamide gel electrophoresis
pA_E	early polyadenylation site
pA_L	late polyadenylation site
PBS	Phosphate buffered saline solution
PCR	Polymerase chain reaction
PDL1	Programmed Cell Death 1 Ligand 1, also known as CD274
P_E	early promotor
PGK1	Phosphoglycerate kinase 1
pH	Negative decadic logarithm of H^+ ion concentration
PKA	Protein kinase A
P_L	late promoter
pmol	Picomol
pRb	Retinoblastoma protein
pt	post transfection
PTM	Post-translational modification
(H)PV	(Human) papillomavirus
qRT-PCR	Quantitative real-time PCR
R	Reverse for primer in a PCR
rcf, g	Relative centrifugal force
Rluc	Renilla luciferase

RNA	Ribonucleic acid
RNase	Ribonuclease
rpm	Revolutions per minute
RT	Room temperature
s	Seconds
SA	Splice acceptor
SCJ	Squamo-columnar junction of cervix
scRNA-seq	Single-cell RNA-sequencing
SD	Splice donor
SDS	Sodium dodecyl sulfate
SEM	Standard error of the mean
SIL	Squamous intraepithelial lesion
SMRT	Silencing mediator for retinoid or thyroid-hormone receptor
SOC	Super Optimal broth with Catabolite repression (medium)
SP1	Specificity protein 1
SSC	Sodium citrate (saline-sodium citrate)
STAT3	Signal transducer and activator of transcription 3
STIKO	German Standing Committee on Vaccination
SV40	Simian Virus 40
TBL1	Transducin beta like 1
TBLR1	Transducin beta like-related protein 1
TCEP	Tris(2-carboxyethyl)phosphine hydrochloride
TEMED	Tetramethylethylenediamine
TERT	Telomerase reverse transcriptase
Tris	Trishydroxymethylaminomethane
U	Unit
ULBP1	UL16 Binding Protein 1
URR	Upstream regulatory region
UV(B)	Ultra violet (B) irradiation
V	Volt
v/v	Volume percent
VEGF	Vascular endothelial growth factor
VLP	Virus-like particle
w/v	Mass concentration
WT	Wild type
X	Any amino acid

8 List of Figures

9 List of Tables

10 Bibliography

Keiko Akagi, Jingfeng Li, Tatevik R Broutian, Hesed Padilla-Nash, Weihong Xiao, Bo Jiang, James W Rocco, Theodoros N Teknos, Bhavna Kumar, Danny Wangsa, et al. Genome-wide analysis of hpv integration in human cancers reveals recurrent, focal genomic instability. *Genome research*, 24(2):185–199, 2014.

Amirhossein Akbarpour Arsanjani, Haniyeh Abuei, Abbas Behzad-Behbahani, Zahra Bagheri, Rita Arabsolghar, and Ali Farhadi. Activating transcription factor 3 inhibits nf-κb p65 signaling pathway and mediates apoptosis and cell cycle arrest in cervical cancer cells. *Infectious Agents and Cancer*, 17(1):1–10, 2022.

B Lynn Allen-Hoffmann, Sandra J Schlosser, Cathy AR Ivarie, Lorraine F Meisner, Sean L O'Connor, and Carol A Sattler. Normal growth and differentiation in a spontaneously immortalized near-diploid human keratinocyte cell line, niks. *Journal of Investigative Dermatology*, 114(3):444–455, 2000.

Vincent G Allfrey, R Faulkner, and AE Mirsky. Acetylation and methylation of histones and their possible role in the regulation of rna synthesis. *Proceedings of the National Academy of Sciences*, 51(5):786–794, 1964.

Ingo Ammermann, Markus Bruckner, Frank Matthes, Thomas Iftner, and Frank Stubenrauch. Inhibition of transcription and dna replication by the papillomavirus e8 e2c protein is mediated by interaction with corepressor molecules. *Journal of virology*, 82(11):5127–5136, 2008.

Hugo Arias-Pulido, Cheri L Peyton, Nancy E Joste, Hernan Vargas, and Cosette M Wheeler. Human papillomavirus type 16 integration in cervical carcinoma in situ and in invasive cervical cancer. *Journal of clinical microbiology*, 44(5):1755–1762, 2006.

Nelly Auersperg. Long-term cultivation of hypodiploid human tumor cells. *Journal of the National Cancer Institute*, 32(1):135–163, 1964.

Frederick M. Ausubel, R Brent, RE Kingston, DD Moore, JG Seidman, JA Smith, and K Struhl. Current protocols in molecular biology." greene pub. assoc. and wilcy—interscience, new york. 1990.

Carl C Baker, William C Phelps, Valerie Lindgren, Michael J Braun, Matthew A Gonda, and Peter M Howley. Structural and transcriptional analysis of human papillomavirus type 16 sequences in cervical carcinoma cell lines. *Journal of virology*, 61(4):962–971, 1987.

N Sanjib Banerjee, Hsu-Kun Wang, Thomas R Broker, and Louise T Chow. Human papillomavirus (hpv) e7 induces prolonged g2 following s phase reentry in differentiated human keratinocytes. *Journal of Biological Chemistry*, 286(17):15473–15482, 2011.

Om Basukala and Lawrence Banks. The not-so-good, the bad and the ugly: Hpv e5, e6 and e7 oncoproteins in the orchestration of carcinogenesis. *Viruses*, 13(10):1892, 2021.

Michael K Baxter, Maria G McPhillips, Keiko Ozato, and Alison A McBride. The mitotic chromosome binding activity of the papillomavirus e2 protein correlates with interaction with the cellular chromosomal protein, brd4. *Journal of virology*, 79(8):4806–4818, 2005.

Melanie Beglin, Marta Melar-New, and Laimonis Laimins. Human papillomaviruses and the interferon response. *Journal of Interferon & Cytokine Research*, 29(9):629–635, 2009.

Monika Bergvall, Thomas Melendy, and Jacques Archambault. The e1 proteins. *Virology*, 445 (1-2):35–56, 2013.

Vivien Béziat, Jean-Laurent Casanova, and Emmanuelle Jouanguy. Human genetic and immunological dissection of papillomavirus-driven diseases: new insights into their pathogenesis. *Current Opinion in Virology*, 51:9–15, 2021.

Malgorzata Bienkowska-Haba, Wioleta Luszczek, Katarzyna Zwolinska, Rona S Scott, and Martin Sapp. Genome-wide transcriptome analysis of human papillomavirus 16-infected primary keratinocytes reveals subtle perturbations mostly due to e7 protein expression. *Journal of Virology*, 94(3):e01360–19, 2020.

Kerry L Blacker, Mary L Williams, and Marc Goldyne. Mitomycin c-treated 3 t 3 fibroblasts used as feeder layers for human keratinocyte culture retain the capacity to generate eicosanoids. *Journal of investigative dermatology*, 89(6):536–539, 1987.

Simon Blaine-Sauer, Myeong-Kyun Shin, Kristina A Matkowskyj, Ella Ward-Shaw, and Paul F Lambert. A novel model for papillomavirus-mediated anal disease and cancer using the mouse papillomavirus. *Mbio*, 12(4):e01611–21, 2021.

Francoise Breitburd, Reinhard Kirnbauer, Nancy L Hubbert, Bernadete Nonnenmacher, Carole Trin-Dinh-Desmarquet, Gerard Orth, John T Schiller, and Douglas R Lowy. Immunization with viruslike particles from cottontail rabbit papillomavirus (crpv) can protect against experimental crpv infection. *Journal of virology*, 69(6):3959–3963, 1995.

Sarah Brendle, Jingwei J Li, Nancy M Cladel, Debra A Shearer, Lynn R Budgeon, Karla K Balogh, Hannah Atkins, Marina Costa-Fujishima, Paul Lopez, Neil D Christensen, et al. Mouse papillomavirus l1 and l2 are dispensable for viral infection and persistence at both cutaneous and mucosal tissues. *Viruses*, 13(9):1824, 2021.

Molly L Bristol, Xu Wang, Nathan W Smith, Minkyeong P Son, Michael R Evans, and Iain M Morgan. Dna damage reduces the quality, but not the quantity of human papillomavirus 16 e1 and e2 dna replication. *Viruses*, 8(6):175, 2016.

Molly L Bristol, Dipon Das, and Iain M Morgan. Why human papillomaviruses activate the dna damage response (ddr) and how cellular and viral replication persists in the presence of ddr signaling. *Viruses*, 9(10):268, 2017.

Julia ML Brotherton. Human papillomavirus vaccination update: Nonavalent vaccine and the two-dose schedule. *Australian journal of general practice*, 47(7):417–421, 2018.

James E Brownell, Jianxin Zhou, Tamara Ranalli, Ryuji Kobayashi, Diane G Edmondson, Sharon Y Roth, and C David Allis. Tetrahymena histone acetyltransferase a: a homolog to yeast gcn5p linking histone acetylation to gene activation. *Cell*, 84(6):843–851, 1996.

Christopher B Buck, Naiqian Cheng, Cynthia D Thompson, Douglas R Lowy, Alasdair C Steven, John T Schiller, and Benes L Trus. Arrangement of l2 within the papillomavirus capsid. *Journal of virology*, 82(11):5190–5197, 2008.

Christopher B Buck, Patricia M Day, and Benes L Trus. The papillomavirus major capsid protein l1. *Virology*, 445(1-2):169–174, 2013.

Stanley Burnett, AC Ström, N Jareborg, A Alderborn, J Dillner, J Moreno-Lopez, U Pettersson, and U Kiessling. Induction of bovine papillomavirus e2 gene expression and early region transcription by cell growth arrest: correlation with viral dna amplification and evidence for differential promoter induction. *Journal of virology*, 64(11):5529–5541, 1990.

Dirksen E Bussiere, Xiangpeng Kong, David A Egan, Karl Walter, Thomas F Holzman, Frank Lindh, Terry Robins, and Vincent L Giranda. Structure of the e2 dna-binding domain from human papillomavirus serotype 31 at 2.4 å. *Acta Crystallographica Section D: Biological Crystallography*, 54(6):1367–1376, 1998.

Christine M Calton, Matthew P Bronnimann, Ariana R Manson, Shuaizhi Li, Janice A Chapman, Marcela Suarez-Berumen, Tatum R Williamson, Sudheer K Molugu, Ricardo A Bernal, and Samuel K Campos. Translocation of the papillomavirus l2/vdna complex across the limiting membrane requires the onset of mitosis. *PLoS pathogens*, 13(5):e1006200, 2017.

J-L Chang, Y-P Tsao, D-W Liu, S-J Huang, W-H Lee, and S-L Chen. The expression of hpv-16 e5 protein in squamous neoplastic changes in the uterine cervix. *Journal of biomedical science*, 8(2):206–213, 2001.

Sreejata Chatterjee, Sa Do Kang, Samina Alam, Anna C Salzberg, Janice Milici, Sjoerd H Van Der Burg, Willard Freeman, and Craig Meyers. Tissue-specific gene expression during productive human papillomavirus 16 infection of cervical, foreskin, and tonsil epithelium. *Journal of virology*, 93(17):e00915–19, 2019.

Anil K Chaturvedi, Eric A Engels, Ruth M Pfeiffer, Brenda Y Hernandez, Weihong Xiao, Esther Kim, Bo Jiang, Marc T Goodman, Maria Sibug-Saber, Wendy Cozen, et al. Human papillo-

mavirus and rising oropharyngeal cancer incidence in the united states. *Journal of clinical oncology*, 29(32):4294, 2011.

Cong Chen, Chao Ge, Zheng Liu, Liangyu Li, Fangyu Zhao, Hua Tian, Taoyang Chen, Hong Li, Ming Yao, and Jinjun Li. Atf3 inhibits the tumorigenesis and progression of hepatocellular carcinoma cells via upregulation of cyr61 expression. *Journal of Experimental & Clinical Cancer Research*, 37(1):1–16, 2018.

J Don Chen and Ronald M Evans. A transcriptional co-repressor that interacts with nuclear hormone receptors. *Nature*, 377(6548):454–457, 1995.

Xiaojiang S Chen, Robert L Garcea, Ilya Goldberg, Gregory Casini, and Stephen C Harrison. Structure of small virus-like particles assembled from the l1 protein of human papillomavirus 16. *Molecular cell*, 5(3):557–567, 2000.

Hanbyoul Cho, Joon-Yong Chung, Sunghoon Kim, Till Braunschweig, Tae Heung Kang, Jennie Kim, Eun Joo Chung, Stephen M Hewitt, and Jae-Hoon Kim. Mica/b and ulbp1 nkg2d ligands are independent predictors of good prognosis in cervical cancer. *BMC cancer*, 14:1–11, 2014.

Nicoletta Colombo, Coraline Dubot, Domenica Lorusso, M Valeria Caceres, Kosei Hasegawa, Ronnie Shapira-Frommer, Krishnansu S Tewari, Pamela Salman, Edwin Hoyos Usta, Eduardo Yañez, et al. Pembrolizumab for persistent, recurrent, or metastatic cervical cancer. *New England Journal of Medicine*, 385(20):1856–1867, 2021.

Gene Ontology Consortium. The gene ontology resource: enriching a gold mine. *Nucleic acids research*, 49(D1):D325–D334, 2021. URL 10.1093/nar/gkaa1113.

Pierre A Coulombe, M Elizabeth Hutton, Robert Vassar, and Elaine Fuchs. A function for keratins and a common thread among different types of epidermolysis bullosa simplex diseases. *The Journal of cell biology*, 115(6):1661–1674, 1991.

Fiona Cunningham, James E Allen, Jamie Allen, Jorge Alvarez-Jarreta, M Ridwan Amode, Irina M Armean, Olanrewaju Austine-Orimoloye, Andrey G Azov, If Barnes, Ruth Bennett, et al. Ensembl 2022. *Nucleic acids research*, 50(D1):D988–D995, 2022.

Fabio Dall'Olio and Marco Trinchera. Epigenetic bases of aberrant glycosylation in cancer. *International journal of molecular sciences*, 18(5):998, 2017.

Clare E Davy, Deborah J Jackson, Qian Wang, Kenneth Raj, Phillip J Masterson, Nicola F Fenner, Shirley Southern, Scott Cuthill, Jonathan BA Millar, and John Doorbar. Identification of a g2 arrest domain in the e1 e4 protein of human papillomavirus type 16. *Journal of virology*, 76(19):9806–9818, 2002.

Koen De Geest, Mary E Turyk, Margaret I Hosken, John B Hudson, Laimonis A Laimins, and George D Wilbanks. Growth and differentiation of human papillomavirus type 31b positive human cervical cell lines. *Gynecologic oncology*, 49(3):303–310, 1993.

Sarah Jill De Jong, Amandine Créquer, Irina Matos, David Hum, Vignesh Gunasekharan, Lazaro Lorenzo, Fabienne Jabot-Hanin, Elias Imahorn, Andres A Arias, Hassan Vahidnezhad, et al. The human cib1–ever1–ever2 complex governs keratinocyte-intrinsic immunity to β-papillomaviruses. *Journal of Experimental Medicine*, 215(9):2289–2310, 2018.

Catherine De Martel, Martyn Plummer, Jerome Vignat, and Silvia Franceschi. Worldwide burden of cancer attributable to hpv by site, country and hpv type. *International journal of cancer*, 141(4):664–670, 2017.

Cristina Mendes De Oliveira, José Humberto TG Fregnani, and Luisa Lina Villa. Hpv vaccine: updates and highlights. *Acta cytologica*, 63(2):159–168, 2019.

Michel Deschuyteneer, Abdelatif Elouahabi, Dominique Plainchamp, Michel Plisnier, Dominique Soete, Yvon Corazza, Laurence Lockman, Sandra Giannini, and Marguerite Deschamps. Molecular and structural characterization of the l1 virus-like particles that are used as vaccine antigens in cervarix™, the as04-adjuvanted hpv-16 and-18 cervical cancer vaccine. *Human vaccines*, 6(5):407–419, 2010.

Daniel DiMaio, Donna Guralski, and John T Schiller. Translation of open reading frame e5 of bovine papillomavirus is required for its transforming activity. *Proceedings of the National Academy of Sciences*, 83(6):1797–1801, 1986.

Kara Dolinski, S Dwight, J Eppig, M Harris, D Hill, L Issel-Tarver, A Kasarskis, S Lewis, JC Matese, JE Richardson, et al. Gene ontology: tool for the unification of biology. the gene ontology consortium. *Nat Genet*, 25(1):2529Attri, 2000.

John Doorbar. The e4 protein; structure, function and patterns of expression. *Virology*, 445 (1-2):80–98, 2013.

John Doorbar, S Ely, J Sterling, C McLean, and L Crawford. Specific interaction between hpv-16 e1–e4 and cytokeratins results in collapse of the epithelial cell intermediate filament network. *Nature*, 352(6338):824–827, 1991.

Koenraad Van Doorslaer, Zhiwen Li, Sandhya Xirasagar, Piet Maes, David Kaminsky, David Liou, Qiang Sun, Ramandeep Kaur, Yentram Huyen, and Alison A. McBride. The papillomavirus episteme: a major update to the papillomavirus sequence database. *Nucleic Acids Research*, 45(D1):D499–D506, oct 2016. doi: 10.1093/nar/gkw879.

Marcel Dreer, Jasmin Fertey, Saskia van de Poel, Elke Straub, Johannes Madlung, Boris Macek, Thomas Iftner, and Frank Stubenrauch. Interaction of ncor/smrt repressor com-

plexes with papillomavirus e8ˆ e2c proteins inhibits viral replication. *PLoS pathogens*, 12 (4):e1005556, 2016.

Marcel Dreer, Saskia van de Poel, and Frank Stubenrauch. Control of viral replication and transcription by the papillomavirus e8ˆ e2 protein. *Virus research*, 231:96–102, 2017.

Matthias Dürst, RT Dzarlieva-Petrusevska, P Boukamp, NE Fusenig, and L Gissmann. Molecular and cytogenetic analysis of immortalized human primary keratinocytes obtained after transfection with human papillomavirus type 16 dna. *Oncogene*, 1(3):251–256, 1987.

Nagayasu Egawa and John Doorbar. The low-risk papillomaviruses. *Virus Research*, 231: 119–127, mar 2017. doi: 10.1016/j.virusres.2016.12.017.

Nagayasu Egawa, Qian Wang, Heather M Griffin, Isao Murakami, Deborah Jackson, Radma Mahmood, and John Doorbar. Hpv16 and 18 genome amplification show different e4-dependence, with 16e4 enhancing e1 nuclear accumulation and replicative efficiency via its cell cycle arrest and kinase activation functions. *PLoS pathogens*, 13(3):e1006282, 2017.

Nagayasu Egawa, Aslam Shiraz, Robin Crawford, Taylor Saunders-Wood, Jeremy Yarwood, Marc Rogers, Ankur Sharma, Gary Eichenbaum, and John Doorbar. Dynamics of papillomavirus in vivo disease formation &amp susceptibility to high-level disinfection—implications for transmission in clinical settings. *EBioMedicine*, 63:103177, jan 2021. doi: 10.1016/j.ebiom.2020.103177.

Matthew J Emmett and Mitchell A Lazar. Integrative regulation of physiology by histone deacetylase 3. *Nature reviews Molecular cell biology*, 20(2):102–115, 2019.

Antonio Fabregat, Steven Jupe, Lisa Matthews, Konstantinos Sidiropoulos, Marc Gillespie, Phani Garapati, Robin Haw, Bijay Jassal, Florian Korninger, Bruce May, et al. The reactome pathway knowledgebase. *Nucleic acids research*, 46(D1):D649–D655, 2018.

Micaela P Fairman and Bruce Stillman. Cellular factors required for multiple stages of sv40 dna replication in vitro. *The EMBO journal*, 7(4):1211–1218, 1988.

L Fang, LR Budgeon, John Doorbar, ER Briggs, and MK Howett. The human papillomavirus type 11 e1ˆ e4 protein is not essential for viral genome amplification. *Virology*, 351(2):271–279, 2006.

Frauke Fehrmann, David J Klumpp, and Laimonis A Laimins. Human papillomavirus type 31 e5 protein supports cell cycle progression and activates late viral functions upon epithelial differentiation. *Journal of virology*, 77(5):2819–2831, 2003.

SP Flanagan. 'nude', a new hairless gene with pleiotropic effects in the mouse. *Genetics Research*, 8(3):295–309, 1966.

Mark G Frattini, Hock B Lim, and Laimonis A Laimins. In vitro synthesis of oncogenic human papillomaviruses requires episomal genomes for differentiation-dependent late expression. *Proceedings of the National Academy of Sciences*, 93(7):3062–3067, 1996.

Jerrold Fried, Amaury G Perez, and Bayard D Clarkson. Flow cytofluorometric analysis of cell cycle distributions using propidium iodide. properties of the method and mathematical analysis of the data. *The Journal of cell biology*, 71(1):172–181, 1976.

Claire F Friedman, Alexandra Snyder Charen, Qin Zhou, Michael A Carducci, Alexandre Buckley De Meritens, Bradley R Corr, Siqing Fu, Travis J Hollmann, Alexia Iasonos, Jason A Konner, et al. Phase ii study of atezolizumab in combination with bevacizumab in patients with advanced cervical cancer. *Journal for immunotherapy of cancer*, 8(2), 2020.

Elaine Fuchs and Howard Green. Changes in keratin gene expression during terminal differentiation of the keratinocyte. *Cell*, 19(4):1033–1042, 1980.

Sybil M Genther, Stephanie Sterling, Stefan Duensing, Karl Munger, Carol Sattler, and Paul F Lambert. Quantitative role of the human papillomavirus type 16 e5 gene during the productive stage of the viral life cycle. *Journal of virology*, 77(5):2832–2842, 2003.

Sybil M Genther Williams, Gary L Disbrow, Richard Schlegel, Daekee Lee, David W Threadgill, and Paul F Lambert. Requirement of epidermal growth factor receptor for hyperplasia induced by e5, a high-risk human papillomavirus oncogene. *Cancer research*, 65(15):6534–6542, 2005.

Goea Gey. Tissue culture studies of the proliferative capacity of cervical carcinoma and normal epithelium. *Cancer research*, 12:264–265, 1952.

Kenric A Gillespie, Kavi P Mehta, Laimonis A Laimins, and Cary A Moody. Human papillomaviruses recruit cellular dna repair and homologous recombination factors to viral replication centers. *Journal of virology*, 86(17):9520–9526, 2012.

Christopher K Glass and Michael G Rosenfeld. The coregulator exchange in transcriptional functions of nuclear receptors. *Genes & development*, 14(2):121–141, 2000.

Bernd Gloss and Hans-Ulrich Bernard. The e6/e7 promoter of human papillomavirus type 16 is activated in the absence of e2 proteins by a sequence-aberrant sp1 distal element. *Journal of Virology*, 64(11):5577–5584, 1990.

Daniel J Goetschius, Samantha R Hartmann, Suriyasri Subramanian, Carol M Bator, Neil D Christensen, and Susan L Hafenstein. High resolution cryo em analysis of hpv16 identifies minor structural protein l2 and describes capsid flexibility. *Scientific reports*, 11(1):1–15, 2021.

Miranda Grace and Karl Munger. Proteomic analysis of the gamma human papillomavirus type 197 e6 and e7 associated cellular proteins. *Virology*, 500:71–81, 2017.

Sheila V Graham. Papillomavirus 3'utr regulatory elements. *Frontiers in Bioscience-Landmark*, 13(15):5646–5663, 2008.

K Grassmann, B Rapp, H Maschek, KU Petry, and T Iftner. Identification of a differentiation-inducible promoter in the e7 open reading frame of human papillomavirus type 16 (hpv-16) in raft cultures of a new cell line containing high copy numbers of episomal hpv-16 dna. *Journal of virology*, 70(4):2339–2349, 1996.

Michael Grunstein. Histone acetylation in chromatin structure and transcription. *Nature*, 389 (6649):349–352, 1997.

Matthew G Guenther, William S Lane, Wolfgang Fischle, Eric Verdin, Mitchell A Lazar, and Ramin Shiekhattar. A core smrt corepressor complex containing hdac3 and tbl1, a wd40-repeat protein linked to deafness. *Genes & development*, 14(9):1048–1057, 2000.

Yu Feng Han, Yueh-Ming Loo, Kevin T Militello, and Thomas Melendy. Interactions of the papovavirus dna replication initiator proteins, bovine papillomavirus type 1 e1 and simian virus 40 large t antigen, with human replication protein a. *Journal of virology*, 73(6):4899–4907, 1999.

Douglas Hanahan and Robert A Weinberg. Hallmarks of cancer: the next generation. *cell*, 144 (5):646–674, 2011.

Alessandra Handisurya, Patricia M Day, Cynthia D Thompson, Michael Bonelli, Douglas R Lowy, and John T Schiller. Strain-specific properties and t cells regulate the susceptibility to papilloma induction by mus musculus papillomavirus 1. *PLoS pathogens*, 10(8):e1004314, 2014.

Rashmi S Hegde and Elliot J Androphy. Crystal structure of the e2 dna-binding domain from human papillomavirus type 16: implications for its dna binding-site selection mechanism. *Journal of molecular biology*, 284(5):1479–1489, 1998.

Shiyuan Hong and Laimonis A Laimins. Regulation of the life cycle of hpvs by differentiation and the dna damage response. *Future microbiology*, 8(12):1547–1557, 2013.

Felix Hoppe-Seyler and Karin Butz. Activation of human papillomavirus type 18 e6–e7 oncogene expression by transcription factor sp1. *Nucleic acids research*, 20(24):6701–6706, 1992.

Andreas J Hörlein, Anders M Näär, Thorsten Heinzel, Joseph Torchia, Bernd Gloss, Riki Kurokawa, Aimee Ryan, Yasutomi Kamei, Mats Söderström, Christopher K Glass, et al. Ligand-independent repression by the thyroid hormone receptor mediated by a nuclear receptor co-repressor. *Nature*, 377(6548):397–404, 1995.

Peter M Howley and Herbert J Pfister. Beta genus papillomaviruses and skin cancer. *Virology*, 479:290–296, 2015.

Ya-Chieh Hsu and Elaine Fuchs. Building and maintaining the skin. *Cold Spring Harbor perspectives in biology*, 14(7):a040840, 2022.

Hsi-Yuan Huang, Yang-Chi-Dung Lin, Shidong Cui, Yixian Huang, Yun Tang, Jiatong Xu, Jiayang Bao, Yulin Li, Jia Wen, Huali Zuo, et al. mirtarbase update 2022: an informative resource for experimentally validated mirna–target interactions. *Nucleic acids research*, 50 (D1):D222–D230, 2022.

Lee-Wen Huang, Shiouh-Lirng Chao, and Bor-Heng Lee. Integration of human papillomavirus type-16 and type-18 is a very early event in cervical carcinogenesis. *Journal of clinical pathology*, 61(5):627–631, 2008.

Mary Hummel, John B Hudson, and Laimonis A Laimins. Differentiation-induced and constitutive transcription of human papillomavirus type 31b in cell lines containing viral episomes. *Journal of virology*, 66(10):6070–6080, 1992.

Thomas Iftner, Juliane Haedicke-Jarboui, Shwu-Yuan Wu, and Cheng-Ming Chiang. Involvement of brd4 in different steps of the papillomavirus life cycle. *Virus research*, 231:76–82, 2017.

Naureen Ehsan Ilahi and Attya Bhatti. Impact of hpv e5 on viral life cycle via egfr signaling. *Microbial pathogenesis*, 139:103923, 2020.

A Ingle, S Ghim, J Joh, I Chepkoech, A Bennett Jenson, and JP Sundberg. Novel laboratory mouse papillomavirus (muspv) infection. *Veterinary pathology*, 48(2):500–505, 2011.

Erin Isaacson Wechsler, Qian Wang, Ian Roberts, Emilio Pagliarulo, Deborah Jackson, Christina Untersperger, Nick Coleman, Heather Griffin, and John Doorbar. Reconstruction of human papillomavirus type 16-mediated early-stage neoplasia implicates e6/e7 deregulation and the loss of contact inhibition in neoplastic progression. *Journal of virology*, 86(11): 6358–6364, 2012.

Sumiyasu Ishii. The role of histone deacetylase 3 complex in nuclear hormone receptor action. *International journal of molecular sciences*, 22(17):9138, 2021.

Lionel B Ivashkiv and Laura T Donlin. Regulation of type i interferon responses. *Nature Reviews Immunology*, 14(1):36–49, 2014.

John L. Jainchill, Stuart A. Aaronson, and George J. Todaro. Murine sarcoma and leukemia viruses: Assay using clonal lines of contact-inhibited mouse cells. *Journal of Virology*, 4(5): 549–553, nov 1969. doi: 10.1128/jvi.4.5.549-553.1969.

Claire D James, Dipon Das, Molly L Bristol, and Iain M Morgan. Activating the dna damage response and suppressing innate immunity: human papillomaviruses walk the line. *Pathogens*, 9(6):467, 2020.

Moon Kyoo Jang, Kui Shen, and Alison A McBride. Papillomavirus genomes associate with brd4 to replicate at fragile sites in the host genome. *PLoS pathogens*, 10(5):e1004117, 2014.

Rong Jia and Zhi-Ming Zheng. Regulation of bovine papillomavirus type 1 gene expression by rna processing. *Frontiers in bioscience: a journal and virtual library*, 14:1270, 2009.

Cecilia Johansson and Stefan Schwartz. Regulation of human papillomavirus gene expression by splicing and polyadenylation. *Nature reviews Microbiology*, 11(4):239–251, 2013.

Bogumil Kaczkowski, Maria Rossing, Ditte K Andersen, Anita Dreher, Marya Morevati, Melissa A Visser, Ole Winther, Finn Cilius Nielsen, and Bodil Norrild. Integrative analyses reveal novel strategies in hpv11,-16 and-45 early infection. *Scientific reports*, 2(1):515, 2012.

Meelis Kadaja, Toomas Silla, Ene Ustav, and Mart Ustav. Papillomavirus dna replication—from initiation to genomic instability. *Virology*, 384(2):360–368, 2009.

Minoru Kanehisa and Susumu Goto. Kegg: kyoto encyclopedia of genes and genomes. *Nucleic acids research*, 28(1):27–30, 2000.

Minoru Kanehisa, Miho Furumichi, Yoko Sato, Masayuki Kawashima, and Mari Ishiguro-Watanabe. Kegg for taxonomy-based analysis of pathways and genomes. *Nucleic Acids Research*, 51(D1):D587–D592, 2023.

Michael B Kastan and Jiri Bartek. Cell-cycle checkpoints and cancer. *Nature*, 432(7015): 316–323, 2004.

Barbara Kell, Richard J Jewers, John Cason, Farzin Pakarian, Jeremy N Kaye, and Jennifer M Best. Detection of e5 oncoprotein in human papillomavirus type 16-positive cervical scrapes using antibodies raised to synthetic peptides. *Journal of General Virology*, 75(9):2451–2456, 1994.

Simran Khurana, Tovah E Markowitz, Juraj Kabat, and Alison A McBride. Spatial and functional organization of human papillomavirus replication foci in the productive stage of infection. *Mbio*, 12(6):e02684–21, 2021.

Reinhard Kirnbauer, F Booy, N Cheng, DR Lowy, and JT50722 Schiller. Papillomavirus l1 major capsid protein self-assembles into virus-like particles that are highly immunogenic. *Proceedings of the National Academy of Sciences*, 89(24):12180–12184, 1992.

Reinhard Kirnbauer, J Taub, H Greenstone, R Roden, M Dürst, L Gissmann, D R Lowy, and J T Schiller. Efficient self-assembly of human papillomavirus type 16 l1 and l1-l2 into virus-like particles. *Journal of Virology*, 67(12):6929–6936, dec 1993. doi: 10.1128/jvi.67.12.6929-6936.1993.

David J Klumpp and Laimonis A Laimins. Differentiation-induced changes in promoter usage for transcripts encoding the human papillomavirus type 31 replication protein e1. *Virology*, 257(1):239–246, 1999.

Tetyana Klymenko, Q Gu, I Herbert, A Stevenson, V Iliev, G Watkins, C Pollock, Ramya Bhatia, Kate Cuschieri, P Herzyk, et al. Rna-seq analysis of differentiated keratinocytes reveals a massive response to late events during human papillomavirus 16 infection, including loss of epithelial barrier function. *Journal of virology*, 91(24):e01001–17, 2017.

Gillian L Knight, John R Grainger, Phillip H Gallimore, and Sally Roberts. Cooperation between different forms of the human papillomavirus type 1 e4 protein to block cell cycle progression and cellular dna synthesis. *Journal of virology*, 78(24):13920–13933, 2004.

Sebastian Köhler, Michael Gargano, Nicolas Matentzoglu, Leigh C Carmody, David Lewis-Smith, Nicole A Vasilevsky, Daniel Danis, Ganna Balagura, Gareth Baynam, Amy M Brower, et al. The human phenotype ontology in 2021. *Nucleic acids research*, 49(D1):D1207–D1217, 2021.

Abolfazl Kooti, Haniyeh Abuei, Ali Farhadi, Abbas Behzad-Behbahani, and Maryam Zarrabi. Activating transcription factor 3 mediates apoptotic functions through a p53-independent pathway in human papillomavirus 18 infected hela cells. *Virus Genes*, 58(2):88–97, 2022.

Katherine A Krause, Daniel Neelon, and Samantha L Butler. Koilocytosis. In *StatPearls [Internet]*. StatPearls Publishing, 2022.

Gert-Jan Kremers, Joachim Goedhart, Erik B van Munster, and Theodorus WJ Gadella. Cyan and yellow super fluorescent proteins with improved brightness, protein folding, and fret förster radius. *Biochemistry*, 45(21):6570–6580, 2006.

Franziska Kuehner and Frank Stubenrauch. Functions of papillomavirus proteins in tissue culture and in vivo. *Viruses*, 14(5):953, may 2022. doi: 10.3390/v14050953.

Franziska Kuehner, Elke Straub, Thomas Iftner, and Frank Stubenrauch. Deregulation of host gene expression by hpv16 knock-out genomes is due to increased productive replication. *Virology*, 581:39–47, 2023. doi: https://doi.org/10.1016/j.virol.2023.02.007.

Michael J. Lace, James R. Anson, Gregory S. Thomas, Lubomir P. Turek, and Thomas H. Haugen. The e8^e2 gene product of human papillomavirus type 16 represses early transcription and replication but is dispensable for viral plasmid persistence in keratinocytes. *Journal of Virology*, 82(21):10841–10853, November 2008. doi: 10.1128/jvi.01481-08.

Chunyan Lan, Jingxian Shen, Yin Wang, Jundong Li, Zhimin Liu, Mian He, Xinping Cao, Jiayu Ling, Jiaming Huang, Min Zheng, et al. Camrelizumab plus apatinib in patients with advanced cervical cancer (clap): a multicenter, open-label, single-arm, phase ii trial. *Journal of Clinical Oncology*, 38(34):4095, 2020.

Laura Lau, Elizabeth E Gray, Rebecca L Brunette, and Daniel B Stetson. Dna tumor virus oncogenes antagonize the cgas-sting dna-sensing pathway. *Science*, 350(6260):568–571, 2015.

Moyra Lawrence, Sylvain Daujat, and Robert Schneider. Lateral thinking: how histone modifications regulate gene expression. *Trends in Genetics*, 32(1):42–56, 2016.

Jiwen Li, Jin Wang, Jianxiang Wang, Zafar Nawaz, Johnson M Liu, Jun Qin, and Jiemin Wong. Both corepressor proteins smrt and n-cor exist in large protein complexes containing hdac3. *The EMBO journal*, 19(16):4342–4350, 2000.

Wei Li, Wei Wang, Mani Si, Linfei Han, Qinglei Gao, Aiyue Luo, Yan Li, Yunping Lu, Shixuan Wang, and Ding Ma. The physical state of hpv16 infection and its clinical significance in cancer precursor lesion and cervical carcinoma. *Journal of cancer research and clinical oncology*, 134:1355–1361, 2008.

VF Liu and DT Weaver. The ionizing radiation-induced replication protein a phosphorylation response differs between ataxia telangiectasia and normal human cells. *Molecular and cellular biology*, 13(12):7222–7231, 1993.

Yueh-Ming Loo and Thomas Melendy. Recruitment of replication protein a by the papillomavirus e1 protein and modulation by single-stranded dna. *Journal of virology*, 78(4):1605–1615, 2004.

Norman J Maitland, Sarah Conway, Nafisa S Wilkinson, Jane Ramsdale, Jo R Morris, Cyril M Sanders, Julie E Burns, Peter L Stern, and Michael Wells. Expression patterns of the human papillomavirus type 16 transcription factor e2 in low-and high-grade cervical intraepithelial neoplasia. *The Journal of Pathology: A Journal of the Pathological Society of Great Britain and Ireland*, 186(3):275–280, 1998.

Anna Manawapat-Klopfer. *Identifikation und Charakterisierung von potentiellen Biomarkern für die Persistenz und Progression einer HPV16-Infektion*. PhD thesis, Universität Tübingen, 2013.

Marvin Martens, Ammar Ammar, Anders Riutta, Andra Waagmeester, Denise N Slenter, Kristina Hanspers, Ryan A. Miller, Daniela Digles, Elisson N Lopes, Friederike Ehrhart, et al. Wikipathways: connecting communities. *Nucleic acids research*, 49(D1):D613–D621, 2021.

Mihaela Matovina, Ivan Sabol, Goran Grubišić, Nina Milutin Gašperov, and Magdalena Grce. Identification of human papillomavirus type 16 integration sites in high-grade precancerous cervical lesions. *Gynecologic oncology*, 113(1):120–127, 2009.

Volker Matys, Olga V Kel-Margoulis, Ellen Fricke, Ines Liebich, Sigrid Land, A Barre-Dirrie, Ingmar Reuter, D Chekmenev, Mathias Krull, Klaus Hornischer, et al. Transfac® and its module transcompel®: transcriptional gene regulation in eukaryotes. *Nucleic acids research*, 34(suppl_1):D108–D110, 2006.

John P Maufort, Anny Shai, Henry C Pitot, and Paul F Lambert. A role for hpv16 e5 in cervical carcinogenesishpv16 e5 in cervical cancer. *Cancer research*, 70(7):2924–2931, 2010.

Alison A McBride. The papillomavirus e2 proteins. *Virology*, 445(1-2):57–79, 2013.

Alison A. McBride. Mechanisms and strategies of papillomavirus replication. *Biological Chemistry*, 398(8):919–927, jul 2017. doi: 10.1515/hsz-2017-0113.

Maria G McPhillips, Keiko Ozato, and Alison A McBride. Interaction of bovine papillomavirus e2 protein with brd4 stabilizes its association with chromatin. *Journal of virology*, 79(14): 8920–8932, 2005.

Jordan M Meyers, Aayushi Uberoi, Miranda Grace, Paul F Lambert, and Karl Munger. Cutaneous hpv8 and mmupv1 e6 proteins target the notch and tgf-β tumor suppressors to inhibit differentiation and sustain keratinocyte proliferation. *PLoS Pathogens*, 13(1):e1006171, 2017.

Huaiyu Mi, Anushya Muruganujan, Dustin Ebert, Xiaosong Huang, and Paul D Thomas. Panther version 14: more genomes, a new panther go-slim and improvements in enrichment analysis tools. *Nucleic acids research*, 47(D1):D419–D426, 2019.

Snježana Mikuličić, Johannes Strunk, and Luise Florin. Hpv16 entry into epithelial cells: Running a gauntlet. *Viruses*, 13(12):2460, 2021.

Antoaneta Mincheva, Lutz Gissmann, and Harald Zur Hausen. Chromosomal integration sites of human papillomavirus dna in three cervical cancer cell lines mapped by in situ hybridization. *Medical microbiology and immunology*, 176:245–256, 1987.

Yorgo Modis, Benes L Trus, and Stephen C Harrison. Atomic model of the papillomavirus capsid. *The EMBO journal*, 21(18):4754–4762, 2002.

Yu-Keung Mok, Mark Bycroft, Gonzalo De Prat Gay, and P Jonathan Butler. Equilibrium dissociation and unfolding of the dimeric human papillomavirus strain-16 e2 dna-binding domain. *Protein science*, 5(2):310–319, 1996.

Cary A Moody. Mechanisms by which hpv induces a replication competent environment in differentiating keratinocytes. *Viruses*, 9(9):261, 2017.

Cary A Moody and Laimonis A Laimins. Human papillomaviruses activate the atm dna damage pathway for viral genome amplification upon differentiation. *PLoS pathogens*, 5(10): e1000605, 2009.

Cary A Moody and Laimonis A Laimins. Human papillomavirus oncoproteins: pathways to transformation. *Nature Reviews Cancer*, 10(8):550–560, 2010.

Harvey J Motulsky. Graphpad prism 9 statistics guide. URL `https://www.graphpad.com/guides/prism/latest/statistics/index.htm`. last accessed 28.02.2023.

Julia E. Myers, J. T. Guidry, M. L. Scott, K. Zwolinska, G. Raikhy, K. Prasai, M. Bienkowska-Haba, J. M. Bodily, M. J. Sapp, and R. S. Scott. Detecting episomal or integrated human papillomavirus 16 DNA using an exonuclease V-qPCR-based assay. *Virology*, 537:149–156, 2019. ISSN 0042-6822. doi: https://doi.org/10.1016/j.virol.2019.08.021.

Tomomi Nakahara, Akiko Nishimura, Masakazu Tanaka, Takaharu Ueno, Akinori Ishimoto, and Hiroyuki Sakai. Modulation of the cell division cycle by human papillomavirus type 18 e4. *Journal of virology*, 76(21):10914–10920, 2002.

Tomomi Nakahara, Woei Ling Peh, John Doorbar, Denis Lee, and Paul F Lambert. Human papillomavirus type 16 e1 e4 contributes to multiple facets of the papillomavirus life cycle. *Journal of virology*, 79(20):13150–13165, 2005.

Robert Wendel Naumann, Antoine Hollebecque, Tim Meyer, Michael-John Devlin, Ana Oaknin, Joseph Kerger, Jose M López-Picazo, Jean-Pascal Machiels, Jean-Pierre Delord, Thomas RJ Evans, et al. Safety and efficacy of nivolumab monotherapy in recurrent or metastatic cervical, vaginal, or vulvar carcinoma: results from the phase i/ii checkmate 358 trial. *Journal of Clinical Oncology*, 37(31):2825, 2019.

Huck Hui Ng and Adrian Bird. Histone deacetylases: silencers for hire. *Trends in biochemical sciences*, 25(3):121–126, 2000.

Tara J Nulton, Amy L Olex, Mikhail Dozmorov, Iain M Morgan, and Brad Windle. Analysis of the cancer genome atlas sequencing data reveals novel properties of the human papillomavirus 16 genome in head and neck squamous cell carcinoma. *Oncotarget*, 8(11):17684, 2017.

David M O'Malley, Ana Oaknin, Bradley J Monk, Frédéric Selle, Carlos Rojas, Laurence Gladieff, Dominique Berton, Alexandra Leary, Kathleen N Moore, Maria DP Estevez-Diz, et al. Phase ii study of the safety and efficacy of the anti-pd-1 antibody balstilimab in patients with recurrent and/or metastatic cervical cancer. *Gynecologic Oncology*, 163(2):274–280, 2021.

Peter Ordentlich, Michael Downes, Wen Xie, Anna Genin, Nancy B Spinner, and Ronald M Evans. Unique forms of human and mouse nuclear receptor corepressor smrt. *Proceedings of the National Academy of Sciences*, 96(6):2639–2644, 1999.

Gérard Orth. Genetics of epidermodysplasia verruciformis: insights into host defense against papillomaviruses. In *Seminars in immunology*, volume 18, pages 362–374. Elsevier, 2006.

EM Pantelouris. Absence of thymus in a mouse mutant. *Nature*, 217:370–371, 1968.

Eun-Ju Park, Daniel J Schroen, Maozhou Yang, Hui Li, Li Li, and J Don Chen. Smrte, a silencing mediator for retinoid and thyroid hormone receptors-extended isoform that is more related to the nuclear receptor corepressor. *Proceedings of the National Academy of Sciences*, 96 (7):3519–3524, 1999.

Roland A Pattillo, RO Hussa, MT Story, ACF Ruckert, MR Shalaby, and RF Mattingly. Tumor antigen and human chorionic gonadotropin in caski cells: a new epidermoid cervical cancer cell line. *Science*, 196(4297):1456–1458, 1977.

Kerri J Penrose and Alison A McBride. Proteasome-mediated degradation of the papillomavirus e2-ta protein is regulated by phosphorylation and can modulate viral genome copy number. *Journal of virology*, 74(13):6031–6038, 2000.

Michael W Pfaffl. A new mathematical model for relative quantification in real-time rt–pcr. *Nucleic acids research*, 29(9):e45–e45, 2001.

Maria LC Powell, Jennifer A Smith, Mathew E Sowa, J Wade Harper, Thomas Iftner, Frank Stubenrauch, and Peter M Howley. Ncor1 mediates papillomavirus e8^ e2c transcriptional repression. *Journal of virology*, 84(9):4451–4460, 2010.

Todd R Pray and Laimonis A Laimins. Differentiation-dependent expression of e1^ e4 proteins in cell lines maintaining episomes of human papillomavirus type 31b. *Virology*, 206(1):679–685, 1995.

Mikk Puustusmaa and Aare Abroi. Conservation of the e8 cds of the e8^ e2 protein among mammalian papillomaviruses. *Journal of General Virology*, 97(9):2333–2345, 2016.

Kenneth Raj, Samuel Berguerand, Shirley Southern, John Doorbar, and Peter Beard. E1 e4 protein of human papillomavirus type 16 associates with mitochondria. *Journal of virology*, 78(13):7199–7207, 2004.

Uku Raudvere, Liis Kolberg, Ivan Kuzmin, Tambet Arak, Priit Adler, Hedi Peterson, and Jaak Vilo. g: Profiler: a web server for functional enrichment analysis and conversions of gene lists (2019 update). *Nucleic acids research*, 47(W1):W191–W198, 2019.

Tina M Rehm, Elke Straub, Stephan Forchhammer, Ulrike Leiter, Thomas Iftner, and Frank Stubenrauch. Transcription properties of beta-hpv8 and hpv38 genomes in human keratinocytes. *Journal of Virology*, pages e01498–22, 2022a.

Tina M Rehm, Elke Straub, Thomas Iftner, and Frank Stubenrauch. Restriction of viral gene expression and replication prevents immortalization of human keratinocytes by a beta-human papillomavirus. *Proceedings of the National Academy of Sciences*, 119(11):e2118930119, 2022b.

Danny Rischin, Marta Gil-Martin, Antonio González-Martin, Irene Braña, June Y Hou, Daniel Cho, Gerald S Falchook, Silvia Formenti, Salma Jabbour, Kathleen Moore, et al. Pd-1 blockade in recurrent or metastatic cervical cancer: Data from cemiplimab phase i expansion cohorts and characterization of pd-l1 expression in cervical cancer. *Gynecologic oncology*, 159(2):322–328, 2020.

Sally Roberts, Ian Ashmole, Loretta J Gibson, Susan M Rookes, Geoff J Barton, and Phillip H Gallimore. Mutational analysis of human papillomavirus e4 proteins: identification of structural features important in the formation of cytoplasmic e4/cytokeratin networks in epithelial cells. *Journal of virology*, 68(10):6432–6445, 1994.

Sally Roberts, Ian Ashmole, Susan M Rookes, and Phillip H Gallimore. Mutational analysis of the human papillomavirus type 16 e1–e4 protein shows that the c terminus is dispensable for keratin cytoskeleton association but is involved in inducing disruption of the keratin filaments. *Journal of virology*, 71(5):3554–3562, 1997.

Richard Roden and Peter L Stern. Opportunities and challenges for human papillomavirus vaccination in cancer. *Nature Reviews Cancer*, 18(4):240–254, 2018.

Lucienne V Ronco, Alla Y Karpova, Marc Vidal, and Peter M Howley. Human papillomavirus 16 e6 oncoprotein binds to interferon regulatory factor-3 and inhibits its transcriptional activity. *Genes & development*, 12(13):2061–2072, 1998.

Maria Rusan, Yvonne Y Li, and Peter S Hammerman. Genomic landscape of human papillomavirus–associated cancersgenomics of hpv-associated cancers. *Clinical cancer research*, 21(9):2009–2019, 2015.

Ziad Sahab, Sawali R Sudarshan, Xuefeng Liu, YiYu Zhang, Alexander Kirilyuk, Christopher M Kamonjoh, Vera Simic, Yuhai Dai, Stephen W Byers, John Doorbar, et al. Quantitative measurement of human papillomavirus type 16 e5 oncoprotein levels in epithelial cell lines by mass spectrometry. *Journal of virology*, 86(17):9465–9473, 2012.

Nozomi Sakakibara, Dan Chen, Moon Kyoo Jang, Dong Wook Kang, Hans F Luecke, Shwu-Yuan Wu, Cheng-Ming Chiang, and Alison A McBride. Brd4 is displaced from hpv replication factories as they expand and amplify viral dna. *PLoS pathogens*, 9(11):e1003777, 2013.

Aziz Sancar, Laura A Lindsey-Boltz, Keziban Ünsal-Kaçmaz, and Stuart Linn. Molecular mechanisms of mammalian dna repair and the dna damage checkpoints. *Annual review of biochemistry*, 73(1):39–85, 2004.

Cyril M Sanders and Norman J Maitland. Kinetic and equilibrium binding studies of the human papillomavirus type-16 transcription regulatory protein e2 interacting with core enhancer elements. *Nucleic acids research*, 22(23):4890–4897, 1994.

Taylor Saunders-Wood, Nagayasu Egawa, Ke Zheng, Alberto Giaretta, Heather M Griffin, and John Doorbar. Role of e6 in maintaining the basal cell reservoir during productive papillomavirus infection. *Journal of Virology*, 96(5):e01181–21, 2022.

Martin Scheffner, Karl Münger, Janet C Byrne, and Peter M Howley. The state of the p53 and retinoblastoma genes in human cervical carcinoma cell lines. *Proceedings of the National Academy of Sciences*, 88(13):5523–5527, 1991.

Mark Schiffman, Philip E Castle, Jose Jeronimo, Ana C Rodriguez, and Sholom Wacholder. Human papillomavirus and cervical cancer. *The lancet*, 370(9590):890–907, 2007.

Dominik Schmiedel and Ofer Mandelboim. Nkg2d ligands–critical targets for cancer immune escape and therapy. *Frontiers in immunology*, 9:2040, 2018.

Markus Schmitt and Michael Pawlita. The hpv transcriptome in hpv16 positive cell lines. *Molecular and cellular probes*, 25(2-3):108–113, 2011.

Markus Schneider, M Müller, Aylin Yigitliler, J Xi, Claudia Simon, T Feger, H-J Rziha, Frank Stubenrauch, H-G Rammensee, Thomas Iftner, et al. Orf virus-based therapeutic vaccine for treatment of papillomavirus-induced tumors. *Journal of Virology*, 94(15):e00398–20, 2020.

John W Schoggins. Interferon-stimulated genes: roles in viral pathogenesis. *Current opinion in virology*, 6:40–46, 2014.

John W Schoggins, Donna A MacDuff, Naoko Imanaka, Maria D Gainey, Bimmi Shrestha, Jennifer L Eitson, Katrina B Mar, R Blake Richardson, Alexander V Ratushny, Vladimir Litvak, et al. Pan-viral specificity of ifn-induced genes reveals new roles for cgas in innate immunity. *Nature*, 505(7485):691–695, 2014.

Hiromasa Sekine, Akira Fuse, Noriyuki Inaba, Hiroyoshi Takamizawa, and Bunsiti Simizu. Detection of the human papillomavirus 6b e2 gene product in genital condyloma and laryngeal papilloma tissues. *Virology*, 170(1):92–98, 1989.

Arlene H Sharpe and Kristen E Pauken. The diverse functions of the pd1 inhibitory pathway. *Nature Reviews Immunology*, 18(3):153–167, 2018.

Joseph G Skeate, Andrew W Woodham, Mark H Einstein, Diane M Da Silva, and W Martin Kast. Current therapeutic vaccination and immunotherapy strategies for hpv-related diseases. *Human vaccines & immunotherapeutics*, 12(6):1418–1429, 2016.

Chelsey C Spriggs and Laimonis A Laimins. Human papillomavirus and the dna damage response: exploiting host repair pathways for viral replication. *Viruses*, 9(8):232, 2017.

Megan E Spurgeon and Paul F Lambert. Mus musculus papillomavirus 1: a new frontier in animal models of papillomavirus pathogenesis. *Journal of Virology*, 94(9):e00002–20, 2020.

Megan E Spurgeon, Aayushi Uberoi, Stephanie M McGregor, Tao Wei, Ella Ward-Shaw, and Paul F Lambert. A novel in vivo infection model to study papillomavirus-mediated disease of the female reproductive tract. *MBio*, 10(2):e00180–19, 2019.

Dominik Stelzle, Luana F Tanaka, Kuan Ken Lee, Ahmadaye Ibrahim Khalil, Iacopo Baussano, Anoop SV Shah, David A McAllister, Sami L Gottlieb, Stefanie J Klug, Andrea S Winkler, et al. Estimates of the global burden of cervical cancer associated with hiv. *The Lancet Global Health*, 9(2):e161–e169, 2021.

Jane C Sterling, Jeremy N Skepper, and Margaret A Stanley. Immunoelectron microscopical localization of human papillomavirus type 16 l1 and e4 proteins in cervical keratinocytes cultured in vivo. *Journal of investigative dermatology*, 100(2):154–158, 1993.

David E Sterner and Shelley L Berger. Acetylation of histones and transcription-related factors. *Microbiology and molecular biology reviews*, 64(2):435–459, 2000.

STIKO. Epidemiologisches bulletin 2007-12, empfehlungen der ständigen impfkommission (stiko) am robert koch-institut. (12):97–106, 2007.

STIKO. Epidemiologisches bulletin 2018-26, empfehlungen der ständigen impfkommission (stiko) am robert koch-institut. (26):233–254, 2018a.

STIKO. Epidemiologisches bulletin 2018-34, empfehlungen der ständigen impfkommission (stiko) am robert koch-institut. (34):335–382, 2018b. doi: 10.17886/EpiBull-2018-042.5.

Melissa Conrad Stöppler, Samuel W Straight, Grace Tsao, Richard Schlegel, and Dennis J Mccance. The e5 gene of hpv-16 enhances keratinocyte immortalization by full-length dna. *Virology*, 223(1):251–254, 1996.

Elke Straub, Marcel Dreer, Jasmin Fertey, Thomas Iftner, and Frank Stubenrauch. The viral e8^e2 c repressor limits productive replication of human papillomavirus 16. *Journal of Virology*, 88(2):937–947, January 2014. doi: 10.1128/jvi.02296-13.

Elke Straub, Jasmin Fertey, Marcel Dreer, Thomas Iftner, and Frank Stubenrauch. Characterization of the human papillomavirus 16 e8 promoter. *Journal of virology*, 89(14):7304–7313, 2015.

Frank Stubenrauch, Mary Hummel, Thomas Iftner, and Laimonis A Laimins. The e8ˆ e2 c protein, a negative regulator of viral transcription and replication, is required for extrachromosomal maintenance of human papillomavirus type 31 in keratinocytes. *Journal of virology*, 74(3):1178–1186, 2000.

Frank Stubenrauch, Thomas Zobel, and Thomas Iftner. The e8 domain confers a novel long-distance transcriptional repression activity on the e8^ e2c protein of high-risk human papillomavirus type 31. *Journal of virology*, 75(9):4139–4149, 2001.

Frank Stubenrauch, Elke Straub, Katrin Klein, Daniela Kramer, Thomas Iftner, Margaret Wong, and Richard BS Roden. Expression of e8^ e2 is required for wart formation by mouse papillomavirus 1 in vivo. *Journal of virology*, 95(8):e01930–20, 2021.

X Sun, A Yang, B Wu, L Zhou, and Z Liu. Kegg (kyoto encyclopedia of genes and genomes) assignment of unigenes in the mantle transcriptome of p. yessoensis. *PLoS One*, 2015.

Hyuna Sung, Jacques Ferlay, Rebecca L Siegel, Mathieu Laversanne, Isabelle Soerjomataram, Ahmedin Jemal, and Freddie Bray. Global cancer statistics 2020: Globocan estimates of incidence and mortality worldwide for 36 cancers in 185 countries. *CA: a cancer journal for clinicians*, 71(3):209–249, 2021.

JoAnn A Suzich, Shin-Je Ghim, Frances J Palmer-Hill, Wendy I White, James K Tamura, Judith A Bell, Joseph A Newsome, A Bennett Jenson, and Richard Schlegel. Systemic immunization with papillomavirus l1 protein completely prevents the development of viral mucosal papillomas. *Proceedings of the National Academy of Sciences*, 92(25):11553–11557, 1995.

Miren Taberna, Montserrat Torres, María Alejo, Marisa Mena, Sara Tous, Sandra Marquez, Miquel A Pavón, Xavier León, Jacinto García, Marta Guix, et al. The use of hpv16-e5, egfr, and pegfr as prognostic biomarkers for oropharyngeal cancer patients. *Frontiers in Oncology*, 8:589, 2018.

Jack Taunton, Christian A Hassig, and Stuart L Schreiber. A mammalian histone deacetylase related to the yeast transcriptional regulator rpd3p. *Science*, 272(5260):408–411, 1996.

Krishnansu S Tewari, BJ Monk, I Vergote, A Miller, AC De Melo, HS Kim, YM Kim, A Lisyanskaya, V Samouëlian, D Lorusso, et al. Vp4-2021: Empower-cervical 1/gog-3016/engot-cx9: Interim analysis of phase iii trial of cemiplimab vs. investigator's choice (ic) chemotherapy (chemo) in recurrent/metastatic (r/m) cervical carcinoma. *Annals of Oncology*, 32(7):940–941, 2021.

Françoise Thierry. Transcriptional regulation of the papillomavirus oncogenes by cellular and viral transcription factors in cervical carcinoma. *Virology*, 384(2):375–379, 2009.

Françoise Thierry, Giannis Spyrou, M Yaniv, and P Howley. Two ap1 sites binding junb are essential for human papillomavirus type 18 transcription in keratinocytes. *Journal of virology*, 66(6):3740–3748, 1992.

Massimo Tommasino. The biology of beta human papillomaviruses. *Virus research*, 231:128–138, 2017. doi: 10.1016/j.virusres.2016.11.013.

Joseph E Tota, Ana F Best, Zachary S Zumsteg, Maura L Gillison, Philip S Rosenberg, and Anil K Chaturvedi. Evolution of the oropharynx cancer epidemic in the united states: moderation of increasing incidence in younger individuals and shift in the burden to older individuals. *Journal of Clinical Oncology*, 37(18):1538, 2019.

Dimitris Tsakogiannis, Zaharoula Kyriakopoulou, Irina Georgia Anna Ruether, Grigoris D Amoutzias, Tilemachos G Dimitriou, Valentina Diamantidou, Constantin Kotsovassilis, and Panayotis Markoulatos. Determination of human papillomavirus 16 physical status through e1/e6 and e2/e6 ratio analysis. *Journal of medical microbiology*, 63(12):1716–1723, 2014.

Dimitris Tsakogiannis, P Gortsilas, Z Kyriakopoulou, IGA Ruether, TG Dimitriou, Georges Orfanoudakis, and P Markoulatos. Sites of disruption within e1 and e2 genes of hpv16 and association with cervical dysplasia. *Journal of medical virology*, 87(11):1973–1980, 2015.

George Tsitsiridis, Ralph Steinkamp, Madalina Giurgiu, Barbara Brauner, Gisela Fobo, Goar Frishman, Corinna Montrone, and Andreas Ruepp. Corum: the comprehensive resource of mammalian protein complexes–2022. *Nucleic Acids Research*, 51(D1):D539–D545, 2023.

Aayushi Uberoi, Satoshi Yoshida, Ian H Frazer, Henry C Pitot, and Paul F Lambert. Role of ultraviolet radiation in papillomavirus-induced disease. *PLoS pathogens*, 12(5):e1005664, 2016.

Mathias Uhlén, Linn Fagerberg, Björn M Hallström, Cecilia Lindskog, Per Oksvold, Adil Mardinoglu, Åsa Sivertsson, Caroline Kampf, Evelina Sjöstedt, Anna Asplund, et al. Tissue-based map of the human proteome. *Science*, 347(6220):1260419, 2015. URL `proteinatlas.org`.

Sung Ho Um, Neil Mundi, John Yoo, David A Palma, Kevin Fung, Danielle MacNeil, Bret Wehrli, Joe S Mymryk, John W Barrett, and Anthony C Nichols. Variable expression of the forgotten oncogene e5 in hpv-positive oropharyngeal cancer. *Journal of Clinical Virology*, 61(1):94–100, 2014.

Harsh Jayesh Vaidya, Alberto Briones Leon, and C Clare Blackburn. Foxn1 in thymus organogenesis and development. *European journal of immunology*, 46(8):1826–1837, 2016.

Koenraad Van Doorslaer, Zhiwen Li, Sandhya Xirasagar, Piet Maes, David Kaminsky, David Liou, Qiang Sun, Ramandeep Kaur, Yentram Huyen, and Alison A McBride. The papillomavirus episteme: a major update to the papillomavirus sequence database. *Nucleic acids research*, 45(D1):D499–D506, 2017.

Elizabeth A Van Dyne, S Jane Henley, Mona Saraiya, Cheryll C Thomas, Lauri E Markowitz, and Vicki B Benard. Trends in human papillomavirus–associated cancers—united states, 1999–2015. *Morbidity and Mortality Weekly Report*, 67(33):918, 2018.

Eric Verdin and Melanie Ott. 50 years of protein acetylation: from gene regulation to epigenetics, metabolism and beyond. *Nature reviews Molecular cell biology*, 16(4):258–264, 2015.

Cornelia Wähner, Johannes Hübner, Dörte Meisel, Jörg Schelling, Rebecca Zingel, Sarah Mihm, Regine Wölle, and Miriam Reuschenbach. Uptake of hpv vaccination among boys after the introduction of gender-neutral hpv vaccination in germany before and during the covid-19 pandemic. *Infection*, pages 1–12, 2023.

Hsu-Kun Wang, Aaron A Duffy, Thomas R Broker, and Louise T Chow. Robust production and passaging of infectious hpv in squamous epithelium of primary human keratinocytes. *Genes & development*, 23(2):181–194, 2009.

Jingang Wang, Dan Zhou, Anjali Prabhu, Richard Schlegel, and Hang Yuan. The canine papillomavirus and gamma hpv e7 proteins use an alternative domain to bind and destabilize the retinoblastoma protein. *PLoS pathogens*, 6(9):e1001089, 2010.

Joshua W Wang and Richard BS Roden. L2, the minor capsid protein of papillomavirus. *Virology*, 445(1-2):175–186, 2013.

Joshua W Wang, Rosie Jiang, Shiwen Peng, Yung-Nien Chang, Chien-Fu Hung, and Richard BS Roden. Immunologic control of mus musculus papillomavirus type 1. *PLoS pathogens*, 11(10):e1005243, 2015.

Qian Wang, Heather Griffin, Shirley Southern, Deborah Jackson, Ana Martin, Pauline McIntosh, Clare Davy, Phillip J Masterson, Philip A Walker, Peter Laskey, et al. Functional analysis of the human papillomavirus type 16 e1 e4 protein provides a mechanism for in vivo and in vitro keratin filament reorganization. *Journal of virology*, 78(2):821–833, 2004.

Xiaohong Wang, Craig Meyers, Hsu-Kun Wang, Louise T Chow, and Zhi-Ming Zheng. Construction of a full transcription map of human papillomavirus type 18 during productive viral infection. *Journal of virology*, 85(16):8080–8092, 2011.

Peter J Watson, Louise Fairall, and John WR Schwabe. Nuclear hormone receptor corepressors: structure and function. *Molecular and cellular endocrinology*, 348(2):440–449, 2012.

Tao Wei, Darya Buehler, Ella Ward-Shaw, and Paul F Lambert. An infection-based murine model for papillomavirus-associated head and neck cancer. *MBio*, 11(3):e00908–20, 2020.

Tao Wei, Miranda Grace, Aayushi Uberoi, James C Romero-Masters, Denis Lee, Paul F Lambert, and Karl Munger. The mus musculus papillomavirus type 1 e7 protein binds to the retinoblastoma tumor suppressor: implications for viral pathogenesis. *Mbio*, 12(4):e02277–21, 2021.

Nicolas Wentzensen, Svetlana Vinokurova, and Magnus von Knebel Doeberitz. Systematic review of genomic integration sites of human papillomavirus genomes in epithelial dysplasia and invasive cancer of the female lower genital tract. *Cancer research*, 64(11):3878–3884, 2004.

Andreas Wieland, Mihir R. Patel, Maria A. Cardenas, Christiane S. Eberhardt, William H. Hudson, Rebecca C. Obeng, Christopher C. Griffith, Xu Wang, Zhuo G. Chen, Haydn T. Kissick, Nabil F. Saba, and Rafi Ahmed. Defining HPV-specific b cell responses in patients with head and neck cancer. *Nature*, 597(7875):274–278, nov 2020. doi: 10.1038/s41586-020-2931-3.

Regina Wilson, Frauke Fehrmann, and Laimonis A Laimins. Role of the e1 e4 protein in the differentiation-dependent life cycle of human papillomavirus type 31. *Journal of virology*, 79 (11):6732–6740, 2005.

Regina Wilson, Gordon B Ryan, Gillian L Knight, Laimonis A Laimins, and Sally Roberts. The full-length e1^ e4 protein of human papillomavirus type 18 modulates differentiation-dependent viral dna amplification and late gene expression. *Virology*, 362(2):453–460, 2007.

C Richard Wobbe, Lawrence Weissbach, James A Borowiec, Frank B Dean, Yasufumi Murakami, Peter Bullock, and Jerard Hurwitz. Replication of simian virus 40 origin-containing dna in vitro with purified proteins. *Proceedings of the National Academy of Sciences*, 84(7): 1834–1838, 1987.

Marc S Wold and Thomas Kelly. Purification and characterization of replication protein a, a cellular protein required for in vitro replication of simian virus 40 dna. *Proceedings of the National Academy of Sciences*, 85(8):2523–2527, 1988.

CD Woodworth, J Doniger, and JA DiPaolo. Immortalization of human foreskin keratinocytes by various human papillomavirus dnas corresponds to their association with cervical carcinoma. *Journal of Virology*, 63(1):159–164, 1989.

Chengjun Wu, Naoko Kajitani, and Stefan Schwartz. Splicing and polyadenylation of human papillomavirus type 16 mrnas. *International journal of molecular sciences*, 18(2):366, 2017.

Bo Xu, Sasithorn Chotewutmontri, Stephan Wolf, Ursula Klos, Martina Schmitz, Matthias Dürst, and Elisabeth Schwarz. Multiplex identification of human papillomavirus 16 dna integration sites in cervical carcinomas. *PloS one*, 8(6):e66693, 2013.

Xiang-Yang Xue, Vladimir Majerciak, Aayushi Uberoi, Bong-Hyun Kim, Deanna Gotte, Xiongfong Chen, Maggie Cam, Paul F Lambert, and Zhi-Ming Zheng. The full transcription map of mouse papillomavirus type 1 (mmupv1) in mouse wart tissues. *PLoS Pathogens*, 13(11): e1006715, 2017.

Yuezhen Xue, Sophie Bellanger, Wenying Zhang, Diana Lim, Jeffrey Low, Declan Lunny, and Françoise Thierry. HPV16 e2 is an immediate early marker of viral infection, preceding e7

expression in precursor structures of cervical carcinoma. *Cancer Research*, 70(13):5316–5325, jun 2010. doi: 10.1158/0008-5472.can-09-3789.

Yuezhen Xue, Diana Lim, Liang Zhi, Pingping He, Jean-Pierre Abastado, and Françoise Thierry. Loss of hpv16 e2 protein expression without disruption of the e2 orf correlates with carcinogenic progression. *The open virology journal*, 6:163, 2012.

Carole Yee, Indira Krishnan-Hewlett, CC Baker, R Schlegel, and PM Howley. Presence and expression of human papillomavirus sequences in human cervical carcinoma cell lines. *The American journal of pathology*, 119(3):361, 1985.

Ho-Geun Yoon, Doug W Chan, Zhi-Qing Huang, Jiwen Li, Joseph D Fondell, Jun Qin, and Jiemin Wong. Purification and functional characterization of the human n-cor complex: the roles of hdac3, tbl1 and tblr1. *The EMBO journal*, 22(6):1336–1346, 2003.

Jianxin You, Jennie L Croyle, Akiko Nishimura, Keiko Ozato, and Peter M Howley. Interaction of the bovine papillomavirus e2 protein with brd4 tethers the viral dna to host mitotic chromosomes. *Cell*, 117(3):349–360, 2004.

Jinsong Zhang, Markus Kalkum, Brian T Chait, and Robert G Roeder. The n-cor-hdac3 nuclear receptor corepressor complex inhibits the jnk pathway through the integral subunit gps2. *Molecular cell*, 9(3):611–623, 2002.

Yunji Zheng, Xiaoxu Cui, Kersti Nilsson, Haoran Yu, Lijing Gong, Chengjun Wu, and Stefan Schwartz. Efficient production of hpv16 e2 protein from hpv16 late mrnas spliced from sd880 to sa2709. *Virus research*, 285:198004, 2020.

Bin-Bing S Zhou and Stephen J Elledge. The dna damage response: putting checkpoints in perspective. *Nature*, 408(6811):433–439, 2000.

Thomas Zobel, Thomas Iftner, and Frank Stubenrauch. The papillomavirus e8 e2c protein represses dna replication from extrachromosomal origins. *Molecular and cellular biology*, 23 (22):8352–8362, 2003.

Harald zur Hausen. Papillomaviruses and cancer: from basic studies to clinical application. *Nature reviews cancer*, 2(5):342–350, 2002.

Harald zur Hausen. Papillomaviruses in the causation of human cancers—a brief historical account. *Virology*, 384(2):260–265, 2009.

11 Appendix

11.1 Publications

Parts of this work have been published as follows:

Franziska Kuehner and Frank Stubenrauch (2022). Functions of Papillomavirus E8^E2 Proteins in Tissue Culture and In Vivo. *Viruses*, 14(5), 953. https://doi.org/10.3390/v14050953

Franziska Kuehner, Elke Straub, Thomas Iftner, and Frank Stubenrauch (2023). Deregulation of host gene expression by HPV16 E8^E2 knock-out genomes is due to increased productive replication. *Virology*, https://doi.org/10.1016/j.virol.2023.02.007

Accepted publication:

Franziska Kuehner, Margaret Wong, Elke Straub, John Doorbar, Thomas Iftner, Richard BS Roden, Frank Stubenrauch (2023). *Mus musculus* papillomavirus 1 E8^E2 represses expression of late protein E4 in basal-like keratinocytes via NCoR/SMRT-HDAC3 co-repressor complexes to enable wart formation *in vivo*. mBio, accepted 22.05.2023

11.2 Location of Suppliers

Table 30: Location of Suppliers

Supplier	Location
Abcam	Cambridge, UK
Agilent Technologies	Santa Clara, US
Analytik Jena	Jena, Germany
AppliChem GmbH	Darmstad, Germany
B. Braun SE	Melsungen, Germany
Bandelin electronic GmbH Co. KG	Berlin, Germany
Becton Dickinson	East Rutherford, New Jersey, US
Berthold Technologies GmbH Co. KG	Bad Wildbad, Germany
Bio-Rad Laboratories, Inc.	Hercules, US
Biozym Scientific GmbH	Hessisch Oldendorf, Germany
Carl Roth GmbH Co. KG	Karlsruhe, Germany
Carl Zeiss	Oberkochen, Germany
Cell Signaling Technology	Danvers, US
Clontech Laboratories Inc.	Mountain View, US
Corning	New York, US
Cytiva Europe GmbH	Freiburg, Germany
Davids Biotechnology	Regensburg, Germany
Dharmacon	Lafayette, US
ENVIGO	Indianapolis, US
Eppendorf SE	Hamburg, Germany
Eurofins Scientific SE/ GATC Biotech AG	Luxemburg
Fermentas	Waltham, US
GE Healthcare	Chicago, US
Genscript	Piscataway Township, USA
Gilson Inc.	Middleton, US
Glaswarenfabrik Karl Hecht GmbH Co. KG	Sondheim vor der Rhön, Germany
Greiner Bio-One GmbH	Frickenhausen, Germany
Heathrow Scientific	Vernon Hills, US
Heidolph Instruments GmbH Co. KG	Schwabach, Germany
Heraeus	Hanau, Germany
Hirschmann Laborgeräte GmbH Co. KG	Eberstadt, Germany
Honeywell Specialty Chemicals GmbH	Seelze, Germany
Intas Science Imaging Instruments GmbH	Göttingen, Germany
INTEGRA Biosciences AG	Zizers, Switzerland
KERN + SOHN GmbH	Balingen, Germany

Supplier	**Location**
Konrad Benda Laborgeräte	Wiesloch, Germany
LaboTect	Rosdorf, Germany
Leica Camera AG	Wetzlar, Germany
LI-COR Biosciences	Lincoln, US
Life Technologies	Carlsbad, US
Lonza Group AG	Basel, Switzerland
Medac GmbH	Wedel, Germany
Memmert GmbH Co. KG	Schwabach, Germany
Merck KGaA	Darmstad, Germany
Miltenyi Biotec	Bergisch Gladbach, Germany
NanoEnTek	Soul, Korea
New England BioLabs	Ipswich, US
Paul Marienfeld GmbH Co. KG	Lauda-Königshofen, Germany
Pechiney, Plastic Packaging	Chicago, US
PerkinElmer Inc.	Waltham, US
PJK GmbH	Kleinblittersdorf, Germany
Promega	Madison, US
Qiagen	Hilden, Germany
Roche Holding	Basel, Schwitzerland
Santa Cruz Biotechnology	Dallas, US
Sarstedt AG Co. KG	Nümbrecht, Germany
Takara Bio Inc.	Kusatsu, Japan
Thermo Fisher Scientific	Waltham, US
VWR International	Radnor, US
Whatman plc	Maidstone , UK
Xylem Inc.	Washington, D.C., US
ZIRBUS technology GmbH	Bad Grund, Germany
Zymo Research	Irvine, US

12 Acknowledgements

First of all, I want to thank Prof. Dr. Frank Stubenrauch for the support and guidance throughout my PhD and many scientific discussions.

Furthermore, I want to thank Prof. Dr. Thomas Iftner who gave me the opportunity to do my PhD in the Institute of Medical Virology and Epidemiology of Viral Diseases Tübingen.

Thank you Prof. Dr. Weber for agreeing to be my first examiner on behalf of the Faculty of Mathematics and Natural Sciences Tübingen!

I would like to thank Andreas Wieland for providing the HPV16 E2 antibody and Nagayasu Egawa and John Doorbar for the MmuPV1 E4 antibody.
Thanks Margaret Wong and Richard Roden for doing the mouse *in vivo* experiments.
Furthermore, I'm grateful for Ferdinand Kollotzek providing me with mice tails for keratinocyte isolation.

Elke, you deserve an award for your angelic patience and overall great help. The lab would not be the same without you, I will miss you a lot!
Thank you to my fellow PhD students Tina, Meret and Janis for dealing with me and my (bad) jokes, and for sometimes pretending to find them funny, even though they were not just to make me happy.

Some people were there for a shorter period of time, thank you nevertheless: Katrin, Aylin, Markus, Alisha, Barbara, Chrissy, Rhumsha, Lukas, Francesca and anyone I might have forgotten. I would also like to thank all the people at the Institute of Virology Tübingen, who were a big help, especially Carlos. A special thanks to Nora and Wen for taking me on my protein purification adventure and for being incredibly patient with me.

Cheers to my little sister Stefanie for your emotional support, tolerating my frequent venting and your help with Latex. Für meine Eltern, Großeltern, meinenen Lieblingsonkel und meine große Schwester auf deutsch: Danke für eure Unterstützung und dass ihr immer an mich geglaubt habt, auch wenn ich es selbst nicht immer getan habe.

Now is the time to thank the love of my life: coffee. You kiss me awake in the morning and pick me up whenever I need it. Thank you for always being there for me, I couldn't have done it without your support. Words cannot espresso how much you bean to me!

13 Statutory Declaration

I hereby declare that I am the sole author of this Ph.D. thesis.
I only made use of the cited sources and permitted resources, and marked literal or paraphrased passages as such.
I declare that I abided by the guidelines for safeguarding good scientific practice (Richtlinien zur Sicherung guter wissenschaftlicher Praxis) at the University of Tübingen (conclusion of the Academic Senate of 25 May 2000).
I hereby make an affirmation in lieu of an oath (Eidesstattliche Versicherung) that all of the above-stated declarations are true and that I did not withhold or conceal anything.
I am well aware that false affidavits are punishable by a prison sentence up to three years or by a monetary penalty under German law.
Currently, I am not accepted or registered at another university as a doctoral student.
There are no former interrupted or terminated Ph.D. procedures or corresponding examinations.
The presented Ph.D. thesis, as a whole or in parts, has not yet been published as a Dissertation. The Ph.D. thesis has not yet been handed in, completely or partially, to the Dean's office as part of a different examination.
I declare, that I did not take part in any commercially arranged agreements with regard to my Ph.D. project. I especially did not contact any organizations, which engage in the active search for supervisors for Ph.D. theses and receive money for their services. I furthermore state that I did not use such organizations, which adopt the applicant's obligations and take care of the academic requirements partially or entirely. Furthermore, I state that I am aware of the legal consequences of using a commercial thesis-writing agency (disqualification as a doctoral student, elimination of acceptance to the doctoral qualification process, termination of the Ph.D. examination procedure, and annulment of the degree in accordance with §21).
I have no penal convictions, disciplinary measures, pending criminal- and disciplinary proceedings to declare.
I hereby declare that the printed version and the electronic version of my dissertation are identical. I agree to the screening of my dissertation for plagiarized parts or passages.
I am aware that I am only entitled to hold the doctorate title from the very day I receive the official doctorate certificate. I am also aware that all of the rights I acquired throughout the examination procedure expire if, after successfully passing the oral exam, I do not hand in in the required amount of copies of my published dissertation within 2 years.
I hereby declare that at least one of the two reviewers is not a co-author of a joint publication containing results of my dissertation.

Tübingen, 2023